Cape Peninsula
University of Technology

THE INTEGRATION OF A WIND FARM THROUGH IEC 61850 STANDARD-BASED PROTECTION IN SMART GRIDS

by

Yongama Gcelu

Thesis submitted in partial fulfilment of the requirements for the degree.

Master of Engineering: Electrical Engineering (Smart Grid)

in the Faculty of Engineering and the Built Environment

at the Cape Peninsula University of Technology

Supervisor: Dr. M.E.S Mnguni

Bellville
November 2025

DECLARATION

I, Yongama Gcelu, declare that the contents of this dissertation/thesis represent my own unaided work, and that the dissertation/thesis has not previously been submitted for academic examination towards any qualification. Furthermore, it represents my own opinions and not necessarily those of the Cape Peninsula University of Technology.

11th November 2025

Signed **Date**

ABSTRACT

The increasing integration of renewable power plants (RPPs), particularly wind power plants (WPPs), into electrical grids requires advanced protection schemes to maintain grid reliability, stability, and selectivity. This thesis presents the design, implementation, and validation of a coordinated protection system for high-voltage (HV) transformers used in the integration of a large-scale wind farm (LSWF) within a smart grid environment. The proposed protection scheme is IEC 61850 standard-based. It uses high-speed communication among Intelligent Electronic Devices (IEDs) via Generic Object-Oriented Substation Event (GOOSE) messaging to ensure reliable fault coordination.

A modified IEEE 9-bus power system integrated with a large-scale wind farm (LSWF) made of eighteen Vestas V117-4.2 MW wind turbine generator units (WTGUs) is used as the test network. The transformer differential protection is implemented as the main using the SEL-487E Station Phasor Measurement Unit. The backup to this main is done using the SEL-751A Feeder Protection Relay. The system is modeled using the Real-Time Digital Simulator (RTDS) in conjunction with its software, Real-time Simulation Computer Aided Design (RSCAD) FX. Hardware-in-the-loop (HIL) testing is conducted to validate the protection logic and communication performance under various fault conditions.

The results confirm that the IEC 61850 standard-based protection scheme improves the speed of detection of the fault, the latency of communication, and the accuracy of coordination. GOOSE messaging enables a timely and selective response, with trip and blocking signals successfully exchanged between IEDs. The developed protection scheme demonstrates robust performance under both internal and external fault conditions. This supports reliable and efficient integration of LSWFs into modern smart grids.

Keywords: Generic object-oriented substation event (GOOSE), hardware-in-the-loop (HIL), IEC 61850 standard, large-scale wind farm (LSWF), point of common coupling (PCC), real-time digital simulator (RTDS), smart grid, transformer differential protection system, wind turbine generator units (WTGUs).

ACKNOWLEDGEMENTS

I would like to extend my sincere gratitude to the following individuals, whose support and contribution were instrumental in the successful completion of my Master's degree:

- Dr. M.E.S. Mnguni, my supervisor, for his invaluable guidance, expert advice, and mentorship throughout my academic journey.
- Mr. S. Nomandela, for his technical expertise and unwavering dedication, which greatly motivated me to complete this research output.
- Mrs. S. Thuthu-Gcelu, my wife, for her unwavering support, encouragement, and strength, which sustained me throughout this journey.
- Iminathi Dopholo, my son, for his understanding and patience during the periods I was fully engaged in research, providing me with the motivation to persevere.
- Mr. T. S. Nontsele, my business partner, for his exceptional leadership and management of our business during my academic absence. His support and encouragement ensured continuity and success, allowing me to focus on my studies.

DEDICATION

This thesis is dedicated to my son, Nkwenkwezi Lingcwele Gcelu, who came into my life during the pursuit of my Master’s degree, and to my company, YG Solutions, which provided strength and motivation throughout this academic journey. Both Nkwenkwezi and YG Solutions have been the driving forces behind my renewed determination and perseverance during my second return to postgraduate studies.

TABLE OF CONTENTS

LIST OF FIGURES

LIST OF TABLES

GLOSSARY

Circuit breaker (CB): A mechanical switching device that interrupts fault current and isolates faulty sections in a power system.

Configured IED Description (CID): A file that defines the configuration of an Intelligent Electronic Device (IED) for IEC 61850 standard communication.

Current transformer (CT): An instrument transformer used to measure high currents and provide scaled-down values for metering or protection.

Distributed energy resource (DER): A small-scale electricity generation or storage technology that is connected to the distribution grid.

Distributed generation (DG): The generation of electricity from decentralized energy sources, often close to the load.

Global positioning system (GPS): A satellite-based system providing precise time synchronization and location for electrical power grid operations.

Generic Object-Oriented Substation Event (GOOSE): The latest type of control model defined under the IEC 61850 standard, which is responsible for high-speed exchange of analogue and digital signals between IEDs.

Hardware-In-the-Loop (HIL): A simulation method that supports the interface of physical devices for testing.

Intelligent Electronic Device (IED): A microprocessor-based control, monitoring, or protection device used in substations.

Local Area Network (LAN): A communication network that connects devices within a limited geographical area, for instance, a substation.

Large-scale wind power plant (LSWPP/LSWF): A utility-scale wind power generation facility that feeds power into the transmission electrical power grid.

Point of common coupling (PCC): The point in the modern power grid where the wind farm or distributed energy resource (DER) is integrated.

Precision Time Protocol (PTP): A protocol used to synchronize clocks in automation systems.

Real-time digital simulator (RTDS): A computer-like device used as a platform for modeling and simulation of power systems and other control circuits in real-time.

Substation Configuration Description (SCD): A file containing the complete configuration of IEDs in a substation as per IEC 61850.

Schweitzer Engineering Laboratories (SEL): A manufacturer of protection, automation, and control products for electric power systems.

Transmission Control Protocol/Internet Protocol (TCP/IP): A set of communication protocols used for networking and Internet data transfer.

Voltage transformer (VT): A special type of transformer used to scale down high voltage signals to lower levels suitable for protection or measurement devices.

ABBREVIATIONS/ACRONYMS

AR	Auto reclose
CB	Circuit breaker
CID	Configured IED Description
CT	Current transformer
DER	Distributed energy resource
DG	Distributed generation
EMS	Energy management system
FACTS	Flexible alternating current transmission system
GOOSE	Generic object-oriented substation event
HIL	Hardware-in-the-loop
IED	Intelligent Electronic Device
LAN	Local Area Network
LSWPP/LSWF	Large-scale wind power plant or large-scale wind farm
MMS	Manufacturing message specification
PCC	Point of common coupling
PTP	Precision Time Protocol
REF	Restricted earth fault
ROCOF	Rate of change of frequency
RTDS	Real-time digital simulator
SA	Substation automation
SCADA	Supervisory control and data acquisition
SCD	Substation Configuration Description
SEL	Schweitzer Engineering Laboratories
SV	Sampled values
TCP/IP	Transmission control protocol/internet protocol
VT	Voltage transformer
WT	Wind turbine
WTG	Wind turbine generator
WTGU	Wind turbine generator unit

CHAPTER ONE
INTRODUCTION

1.1 Background of the Study

The integration of renewable power plants (RPPs) into the electrical power grids has been a leading task in the field of power systems since the beginning of the global transition towards smart and sustainable energy systems. This integration forms smart grids, which are an enabler of distributed energy resources (DERs) such as wind farms (WFs) operating in grid-connected mode, while at the same time maintaining the reliability, flexibility, and efficiency of electrical power grids (Anees, 2012; Song et al., 2012).

Wind farm integration has demonstrated excellent growth in the past decade due to its environmental friendliness and cost decline. As a result, many large-scale wind farms (LSWFs) are now operated in grid-connected mode and are mostly integrated at the transmission level. This, in turn, requires advanced forms of protection schemes due to the complexity and sensitivity of electrical disturbances experienced by these resultant interconnected systems or smart grids (Han et al., 2010; Ibrahim et al., 2011).

The reliability of protection schemes is key at the interconnection point between the LSWFs and the main electrical power grid. Power transformers at high voltage (HV) level are expensive and sensitive, and therefore require fast and accurate protection schemes (George & Ashok, 2018; Gao et al., 2014).

The IEC 61850 standard has been drafted to standardize the communication that enables high-speed, interoperable, and flexible substation automation. The standard enables improved speed of detection of electrical faults and allows coordination between protection devices. The generic object-oriented substation event (GOOSE) and hardware-in-the-loop (HIL) testing method is key to achieving these features (Ahmed & Kim, 2014; Cardenas et al., 2010).

1.2 Problem Statement

One of the most expensive power components in both conventional and smart grids is HV power transformers. It is therefore significant that these transformers get protected with high-standard forms of protection schemes, such as dedicated transformer differential protection schemes (Saad et al., 2015; Medeiros et al., 2016).

However, the existing literature has limits in attention given to the protection of HV power transformers in smart grid contexts. The little literature that exists barely addresses any incorporation when it comes to the IEC 61850 standard as the enabler of communication between coordinated protection devices.

IEC 61850 standard is a global standard for communication in substations based on an Ethernet network. It enables strong support for the integration of measurement, protection, and control functions in substations (Camachi et al., 2017). Nonetheless, maintaining high levels of power system reliability remains a critical requirement.

1.3 Research Aim and Objectives

1.3.1 Aim

This study aims to design and implement an IEC 61850 standard-based protection scheme that prioritizes the reliability of fault detection and coordination for HV transformers within a large-scale wind farm integrated into the power grid.

1.3.2 Objectives

The following objectives have been followed to achieve the aim mentioned in 1.3.1:

1. Analyze existing protection schemes used in smart grids with wind farm integration.
2. Investigate reliability concerns of HV transformers under dynamic wind conditions.
3. Develop a multi-layered protection scheme incorporating differential and overcurrent protection.
4. Model the smart grid integrated with a wind farm using RTDS and RSCAD FX.
5. Implement and test IEC 61850 communication using GOOSE messaging.
6. Validate the system through hardware-in-the-loop (HIL) simulations.
7. Evaluate protection performance during various fault scenarios.

1.4 Research Question and Hypothesis

Research question: Can an IEC 61850-based multi-layered protection scheme significantly enhance the fault detection, coordination, and reliability of smart grid systems connected with LSWFs?

Hypothesis: The application of an IEC 61850-based protection scheme that combines differential and backup protection schemes will improve high-voltage transformer security, minimize fault clearance times, and increase overall system stability compared to conventional protection methods.

1.5 Scope and Limitations

Scope:

- The focus is on high-voltage (HV) transformer protection at the point of connection between LSWFs and the grid.
- The system is modeled using a pre-established IEEE 9-bus power system and LSWF configuration.
- IEC 61850 standard communication is implemented using the GOOSE control model.

Limitations: The smart grid system is modeled and simulated using the Real-Time Digital Simulator (RTDS) along with Real-time Simulation Computer-Aided Design (RSCAD) FX. The hardware-in-the-loop (HIL) tests are restricted to the available Intelligent Electronic Devices (IEDs), such as SEL-487E Station Phasor Measurement Unit and SEL-751A Feeder Protection Relay, whose injection currents are generated using the Omicron CMS 356 and CMS 156 amplifiers.

1.6 Significance of the Study

This study contributes to the advancement of protection schemes for smart grid systems integrated with LSWFs by: developing a real-time, multi-layered protection framework for HV step-up transformers; utilizing the IEC 61850 standard to achieve seamless communication among devices; demonstrating the role of HIL validation in bridging the gap between simulation and real-world deployment; and supporting the renewable integration goals of South Africa by improving grid stability and fault response under wind variability.

1.7 Thesis Structure

This thesis consists of six chapters and is structured as follows:

- **Chapter 1:** Introduces the background, research problem, and objectives.
- **Chapter 2:** Reviews existing literature on wind farm integration and protection schemes.
- **Chapter 3:** Describes the methodology, tools, and test framework used.
- **Chapter 4:** Details the modeling and implementation of the smart grid and IEC 61850-based protection.
- **Chapter 5:** Presents and discusses results from simulations and HIL testing.
- **Chapter 6:** Concludes the study and provides recommendations.

This study involved no human or animal participants and adhered to CPUT's research ethics framework for engineering studies.

CHAPTER TWO
LITERATURE REVIEW

2.1 Smart Grid Architecture and Functions

A smart grid is an electrical supply network that improves its sustainability, efficiency, and reliability in power delivery through communication and information technology (Anees, 2012; Song et al., 2012). A smart grid consists of distinct operational zones, namely generation, transmission, distribution, and consumption. Each zone consists of Intelligent Electronic Devices (IEDs) for control, monitoring, and protection in real-time (George & Ashok, 2018). The IEDs in a smart grid provide automation and responsiveness.

Smart grids require multi-layered protection schemes due to the complexity of bidirectional power flows introduced by DERs. To ensure reliability and selectivity in the isolation of electrical faults in smart grids, each zone must be protected with a modified protection scheme (Ma et al., 2018; Gao et al., 2014).

2.2 Wind Farm Integration in Power Systems

Wind farms that are operated in grid-connected mode pose distinct operational and electrical characteristics. For instance, when made of doubly-fed induction generators (DFIGs), they operate efficiently over a wide range of wind speeds. However, this operation causes fluctuations in voltage and frequency. This results in complications of coordination and fault detection of protection schemes (Zheng et al., 2011; Cai & Su, 2011).

Wind farms often produce low or delayed fault current magnitudes. This again poses some challenges for traditional protection schemes. It should be remembered that traditional or conventional protection schemes rely solely on clear and consistent fault current magnitudes (Song et al., 2012; Han et al., 2010).

Moreover, worldwide, grid codes require low-voltage ride-through (LVRT) capability of WFs to remain connected to the electrical grid during voltage fluctuations. This improves electrical power grid stability; however, it affects the coordination and responsiveness of conventional protection schemes towards fault detection (Ibrahim et al., 2011; George & Ashok, 2018).

2.3 Protection Requirements for Wind Farms

The protection schemes for smart grid systems integrated with WFs have at least five key requirements:

- Ability to detect and protect the system against internal faults within HV transformers.
- Differential protection function with high sensitivity and high-speed clearance.
- A backup protection function which includes overcurrent and (maybe) voltage-based elements.
- An adaptive protection function that can handle variations caused by the intermittency of wind.
- A coordination of protection devices throughout voltage levels and respective zones.

An emphasis has already been made that conventional protection schemes, such as impedance (distance) protection, are often not suitable for LSWFs due to the inconsistent fault impedance, harmonic distortion, and dynamic response of the doubly-fed induction generator (DFIG) (Ma et al., 2018; George & Ashok, 2018).

2.4 Overview of IEC 61850 Standard

The IEC 61850 standard was designed primarily for automation of electrical substations, and it enables high-speed communication among devices of different or the same manufacturers.

The standard consists of key components listed below:

- **Generic Object-Oriented Substation Event (GOOSE):** This is a control model that enables high-speed (≤4 ms) communication of status signals and control commands.
- **Manufacturing Message Specification (MMS):** This is used for client-server communication and configuration.

The IEC 61850 standard works with Logical Nodes (LNs) that represent functional modules of physical Intelligent Electronic Devices (IEDs). It also uses the Substation Configuration Language (SCL) to enable system configuration and integration across different manufacturers.

A demonstration of IEC 61850 standard benefits in the reduction of wiring, enhancement of data exchange, as well as the flexibility across protection IEDs has been made in the studies by the authors (Cardenas et al., 2010) and (Ahmed et al., 2014). However, there is still a limited demonstration on the adoption of the standard and its hardware-in-the-loop (HIL) validation in HV transformer protection schemes.

2.5 Related Work and Research Gaps

2.5.1 Thematic summary of existing work

Different research studies have looked at protection challenges experienced in WF-integrated smart grids, and the role played by the IEC 61850 standard in the enhancement of coordination and reliability of protection schemes.

An emphasis on the reliability and protection challenges of smart grids integrated with WFs has been made in the studies by the authors (Anees, 2012) and (Ibrahim et al., 2011). The authors (Song et al., 2012) and (Han et al., 2010) stated that there are limitations introduced by DFIG-based WFs in conventional protection schemes due to their low-fault current contributions and dynamic response under fault conditions.

Moreover, the authors (Ma et al., 2018) and (Li et al., 2023) proposed some improvements on the impedance protection schemes using adaptive quadrilateral characteristics and dynamic frequency estimation. Also, an adaptive dual-slope power transformer differential protection scheme that accounts for fluctuating operating conditions for transformers in WF environments has been proposed by the authors (George & Ashok, 2018).

The authors (Alizadeh & Ozansoy, 2016) discussed the significant role played by the IEC 61850 standard and the IEC 61400 standard in achieving real-time coordination and interoperability between protection IEDs. Additionally, (Ustun et al., 2012) examined the successful application of IEC 61850 in substation protection, although predominantly at the medium-voltage (MV) level.

Regarding system validation, (Barra et al., 2021) and (Member et al., 2010) highlighted the importance of real-time testing using RTDS and hardware-in-the-loop (HIL) platforms. These techniques allow evaluation of protection system responses under dynamic grid conditions. However, their application in high-voltage (HV) wind integration remains limited.

2.5.2 Identified gaps and limitations

Despite significant progress, several gaps remain in the current literature, as discussed below:

- **Lack of Integrated Multi-Layered Protection Schemes:** Most studies propose protection methods in isolation, such as distance or differential protection, but do not address coordination across multiple protection layers (primary, backup, and auxiliary) within wind farm-connected smart grids (Alasali et al., 2024).
- **Underutilization of IEC 61850 in HV Transformer Protection:** While IEC 61850 has been widely adopted for MV substation automation, its deployment in high-voltage transformer protection, especially under wind farm integration, is rare. Few studies explore the configuration, data modeling, or performance of IEC 61850-based protection applied specifically to HV transformer zones (Ustun et al., 2012).

- **Limited Use of Real-Time HIL Validation:** Many proposed protection schemes rely on simulation tools without undergoing validation in real-time environments using HIL platforms. Such validation is essential for assessing practical implementation feasibility, communication latency, and IED response accuracy (Barra et al., 2021).

2.5.3 Research gap and motivation

From the above review, it is evident that current research lacks a comprehensive, real-time, validated protection framework for smart grids integrating large-scale wind farms. Specifically, there is a need for:

A coordinated, multi-layered protection scheme tailored for HV transformers, utilizing IEC 61850 for communication and validated in real-time using RTDS and HIL environments.

This thesis addresses this gap by designing, implementing, and validating such a scheme, offering a novel contribution to the development of protection systems in renewable-rich smart grids.

2.6 Conclusions

This chapter provided a structured and critical review of literature relevant to the protection of smart grids integrated with wind farms. Beginning with an overview of smart grid architecture and wind farm operational behavior, the chapter discusses the challenges posed by renewable energy sources, particularly wind farms using Doubly-Fed Induction Generators (DFIGs), on traditional protection systems.

A focused discussion on protection requirements revealed the inadequacy of conventional protection methods in the face of wind variability, low fault current levels, and LVRT obligations. IEC 61850 standard emerged as a modern, standardized solution offering fast, interoperable, and flexible communication for protection systems, though its deployment in high-voltage transformer protection remains limited.

A thematic analysis of recent research identified key contributions, including adaptive protection strategies, improvements in distance and differential protection, and the role of IEC 61850 in substation automation. However, the review also revealed significant limitations in the literature, as discussed below:

- Most protection studies remain focused on isolated schemes, lacking coordination across multiple layers (primary, backup, and auxiliary).
- The application of IEC 61850 is mostly restricted to medium-voltage systems, with minimal attention to HV transformer zones under wind farm integration.
- Real-time validation using RTDS and HIL remains uncommon, limiting practical deployment and verification of proposed schemes.

The identified research gap thus lies in the lack of a coordinated, IEC 61850-based multi-layered protection framework that is specifically designed for high-voltage transformers in wind-integrated smart grids and validated through real-time HIL techniques.

This thesis addresses this gap by designing and implementing a protection architecture that brings together differential and backup protection elements within an IEC 61850 communication framework, tested in a realistic real-time simulation environment.

In summary, although numerous studies have explored IEC 61850-based protection schemes, their application has largely been confined to medium-voltage systems and substation automation environments. Limited attention has been given to high-voltage transformer zones within wind-integrated smart grids, where coordination and communication delays remain critical challenges. Furthermore, only a few investigations have validated such protection strategies through real-time or hardware-in-the-loop (HIL) testing, leaving uncertainties regarding their practical implementation performance.

These identified limitations directly motivated the design and experimental validation presented in this study. Chapters 3 and 4, therefore, focus on developing a coordinated, multi-layered protection framework using the IEC 61850 standard, combining transformer differential and overcurrent backup relays, and verifying its performance through RTDS-based real-time simulation and HIL testing. This approach ensures that the proposed system addresses both the technical and practical gaps highlighted in the reviewed literature.

The next chapter details the methodology used in developing and validating this protection scheme.

CHAPTER THREE
METHODOLOGY

3.1 Research Design

This study employs a simulation-based experimental design, validated with hardware-in-the-loop (HIL) testing to ensure real-world applicability. The methodology integrates theoretical research, real-time digital modeling, and experimental validation of a multi-layered protection scheme for HV transformers in smart grids connected with large-scale wind farms (LSWFs).

The research is divided into the following phases:

1. Literature review and theoretical analysis of smart grids, wind energy systems, and protection standards.
2. Modeling of a hybrid smart grid system incorporating a wind farm.
3. Design and development of an IEC 61850-based protection scheme using Real-Time Digital Simulator (RTDS).
4. Testing and validation through real-time simulation and HIL configuration.

3.2 System Configuration

The test system used in this study is a modified IEEE 9-bus power system integrated with a LSWF consisting of eighteen wind turbine generator units (WTGUs) grouped into three clusters, each connected via a medium-voltage collector system to a high-voltage (HV) step-up transformer.

Key elements of the system:

- Wind turbine specifications: Vestas V117-4.2 MW units.
- Integration point: Bus2 of the IEEE 9-bus power system.
- Smart grid zones: WTGU, collector cable (feeder), HV transformer, and transmission line.

Each zone is simulated with appropriate electrical parameters and control devices within the RTDS environment.

3.3 IEC 61850 Protection Scheme Design

The protection scheme is designed to be multi-layered, combining:

- **Differential protection:** Main protection for transformer zone faults.
- **Overcurrent protection:** To provide backup in case of transformer zone protection failure.

The SEL-487E IED is used to implement and coordinate the protection logic. Communication among devices is achieved using the IEC 61850 standard, particularly through GOOSE messaging for high-speed communication and control signals. This supports interoperability and fast coordination.

Logical Node mapping: Logical nodes such as D87UPDIF1 and D87RPDIF1 for differential protection are configured. Data models and mappings conform to IEC 61850-7-4 standards.

Tripping logic: IED tripping decisions are based on current thresholds, combined with fault logic. Inter-device messaging ensures selective tripping and coordination.

3.4 Tools and Software

The following software and hardware tools were used throughout the study:

- **Modeling and Simulation Tools:** Real-Time Digital Simulator (RTDS): Used for real-time power system modeling.
- **Real-Time Simulation Computer-Aided Design (RSCAD):** This is the proprietary software for integrating circuit building and control modeling with RTDS.
- **GOOSE Inspector:** For real-time monitoring and validation of GOOSE messages.

IED Configuration and Communication Tools:

- **AcSELerator QuickSet:** Used to configure and program protection IEDs.
- **AcSELerator Architect:** For setting up IEC 61850 logical nodes and communication architecture.
- **Test Universe and CMC 356:** For functional element testing of relays.
- **SEL SynchroWAVE Event Viewer:** For analyzing waveform and fault records.

3.5 Test Scenarios and Validation Approach

The proposed protection scheme is validated through three levels of testing:

1. **Real-Time Simulation:**
   - Performed using RTDS and RSCAD.
   - Simulates internal three-phase fault conditions (e.g., transformer zone faults).
   - Monitors the response of the protection logic and IED action.

The summary of the steps followed during the study is presented in the flowchart shown in Figure 3.1.

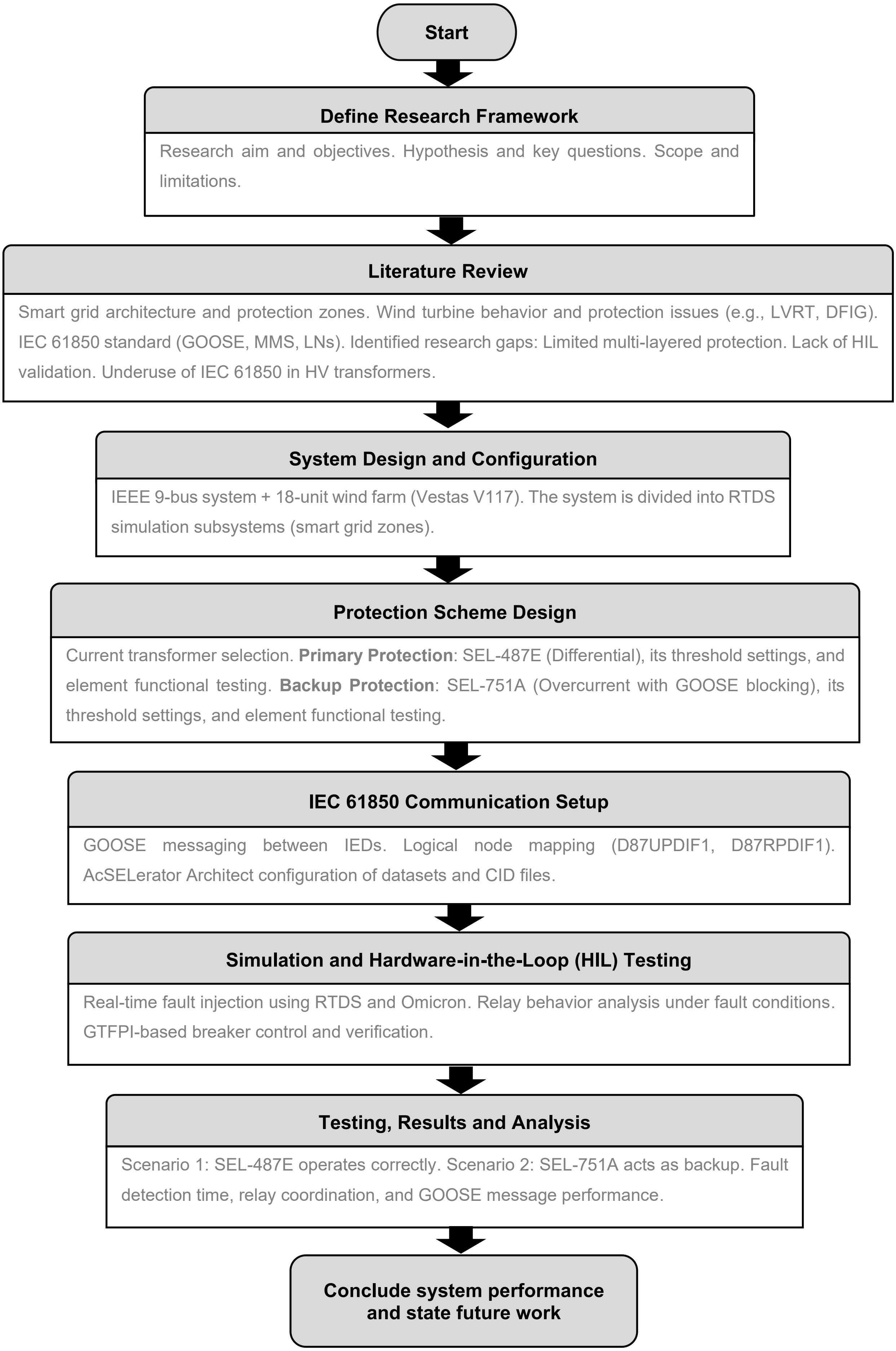

Figure 3.1: A flowchart followed during the study

2. **Hardware-in-the-Loop (HIL) Testing:**
   - Current signals (amperes) from RTDS are amplified using Omicron CMS amplifiers and made available for physical protection IEDs such as SEL-487E and SEL-751A.
   - Relay outputs are captured and analyzed under varying fault types.
   - GOOSE message communication is tested under real-time conditions.

3. **Performance Metrics:**
   - Fault detection and clearing time.
   - Relay coordination accuracy.
   - GOOSE message transmission.

This validation ensures that the system meets real-time operational requirements, consistent with IEC 61850 substation protection principles.

3.6 Conclusions

This chapter has discussed the methodology used in the design, implementation, and validation of the IEC 61850 standard-based protection scheme for a HV transformer of a smart grid system integrated with a large-scale wind farm (LSWF). The approach combines theoretical research, system modeling, real-time simulation, and hardware-in-the-loop (HIL) testing to ensure the practical applicability and robustness of the proposed protection system. The practical modeling and implementation of the smart grid system integrated with the LSWF, and the design and implementation of the proposed protection scheme, are done in the next chapter.

CHAPTER FOUR
SYSTEM MODELING AND IMPLEMENTATION

4.1 Wind Farm Modeling and Simulation

This study considered a large-scale wind farm (LSWF) made up of eighteen Vestas V117-4.2 MW wind turbine generator units (WTGUs). These WTGUs are organized into three collector groups, with each group consisting of six WTGUs connected to a 24 kV collector bus. The collector groups are integrated into a 230 kV high-voltage (HV) transmission network via HV step-up transformers and a shared busbar.

Key Characteristics of the Wind Turbines:

- Rated power per turbine: 4.2 MW
- Cut-in speed: 3 m/s
- Nominal wind speed: 14 m/s
- Generator type: Squirrel-cage induction generator (SCIG)
- Control Strategy: Fixed-speed operation with simplified pitch control

This study uses a smart grid system that has already been developed in the study by the author (Nomandela et al., 2025). The study by these authors focuses on developing a point of common coupling (PCC) protection scheme for a smart grid system. The authors combined an IEEE 9-bus power system and a large-scale wind farm (LSWF) to model a smart grid system.

In 1) and 2) below, the approach used by the authors mentioned above in the development of the smart grid system is described:

1) **IEEE 9-bus power system:** The study evaluated voltage instability points by increasing the overall system loading until the critical busbar was identified. In the study by the authors, the critical busbar is the one that reached the point of collapse quickly than the other busbars. At this point, the authors believed that alternative means to integrate additional electric power sources in the system were necessary to improve the affordability of load demand. This was when the authors modeled an LSWF to compensate for the shortage of electrical power that led to voltage instability in one of the busbars.

2) **The large-scale wind farm:** The LSWF, whose modelling was driven by the shortage of electrical power explained in 1) above, was modeled from the data gathered from the two sources (with some assumptions): Vestas Wind Turbine

Brochure and Power Conversion of Wind Energy Systems, Appendix B, referenced (Vestas, 2017) and (Wu et al., 2011). The LSWF, in total, has eighteen WTGUs grouped into three, with six WTGUs per group.

The integration of the LSWF at Bus2 of the IEEE 9-bus power system formed the smart grid, which this study opted for in testing the proposed and developed IEC 61850 standard-based protection scheme of the high-voltage step-up power transformer. The following subsections present how the modeling and simulation of the smart grid system were performed.

4.1.1 Smart grid modeling on RSCAD FX

RSCAD FX has the draft and the runtime modules. The draft enables gathering of components for an electrical power system (smart grid in this case), control, automation, or control model. The simulations of the model in the draft module are performed in real time using the runtime module, whose computations are done on the Real-Time Digital Simulator (RTDS) devices.

The electrical power system model in the draft module can be split among subsystems, which in real-time simulations would be performed in multiple RTDS devices known as racks, Rack 1, Rack 2, Rack 3, up to Rack n, according to the software RSCAD FX. These racks present subsystems.

The IEEE 9-bus power system was distributed into two subsystems, Rack 1 and Rack 2, and the LSWF occupied the three subsystems, Rack 3, Rack 4, and Rack 5, where each subsystem had one group of six WTGUs of a LSWF. Five subsystems in total were used for the smart grid system model.

This study focuses strictly on proposing and developing the protection scheme for the high-voltage (HV) step-up transformer involved in interconnecting LSWF with the electrical system; therefore, only the already interconnected system is presented. Figure 4.1 is an illustration of the modified and simplified smart grid system, whose abbreviations are listed in Table 4.1 along with their full names (Nomandela et al., 2025).

The parameters of the combined systems, the IEEE 9-bus power system, and the LSWF, are listed in Tables 4.2 to 4.8.

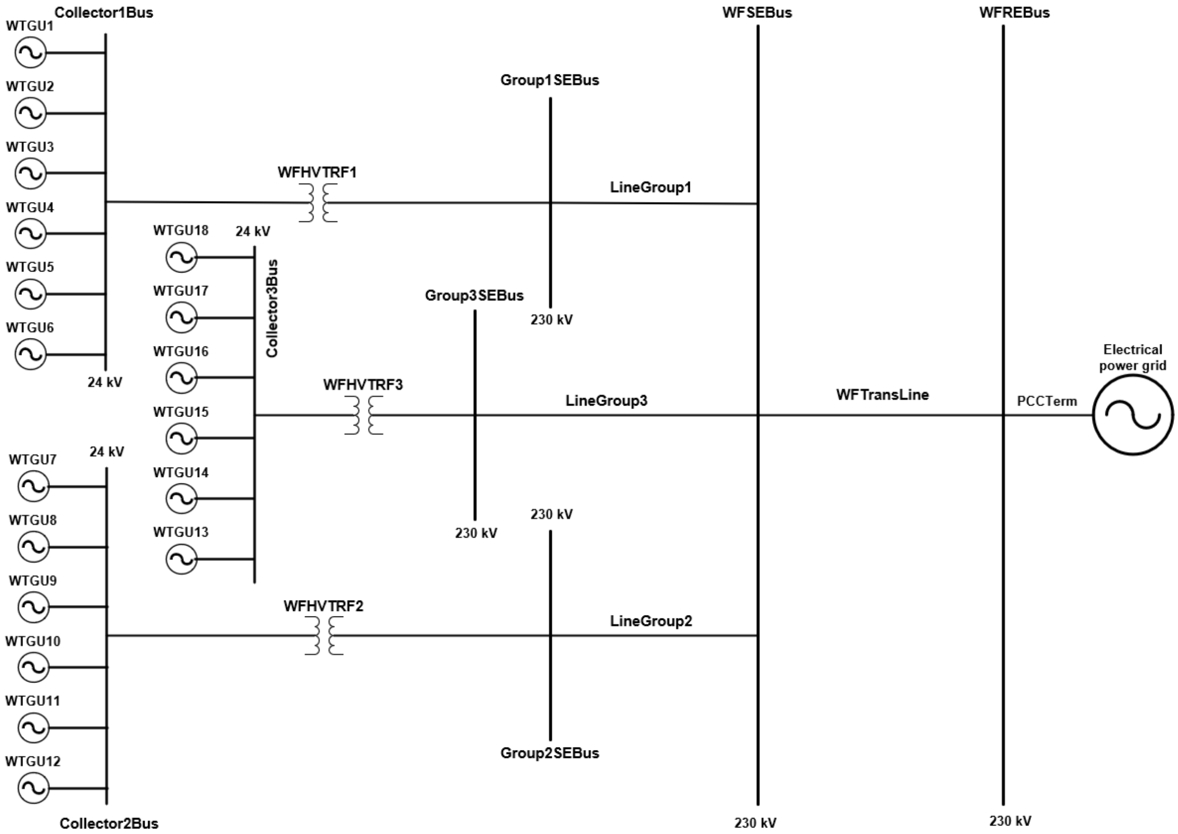

Figure 4.1: Single-line representation of the resultant smart grid system (Nomandela et al., 2025)

Table 4.1: Abbreviations used in the smart grid system in Figure 4.1

Abbreviation	Meaning
WTGU	Wind turbine generator unit
WFHVTRF1	Wind farm high-voltage transformer
WFSEBus	Wind farm sending-end busbar
WFREBus	Wind farm receiving-end busbar
WFTransLine	Wind farm transmission line (possible grid connection point)
PCCTerm	Point of common coupling terminal

The component labeled “Electrical power grid” in the smart grid system in Figure 4.1 represents the IEEE 9-bus power system.

Table 4.2: IEEE 9-bus power system line parameters with some values calculated on a 100 MVA base apparent power

Lines	The busbar to which the line is connected	Length (km)	Resistance (PU)	Reactance (PU)	Susceptance (PU)
Line12	Bus1/Bus2	89.93	0.01	0.085	0.176
Line13	Bus1/Bus3	97.34	0.017	0.092	0.158
Line24	Bus2/Bus4	170.34	0.032	0.161	0.306

Line36	Bus3/Bus6	179.86	0.039	0.17	0.358
Line45	Bus4/Bus5	76.18	0.0085	0.072	0.149
Line56	Bus5/Bus6	106.65	0.0119	0.1008	0.209

Table 4.3: Wind farm line parameters with some values calculated on a 100 MVA base apparent power

Lines	The busbar to which the line is connected	Length (km)	Resistance (PU)	Reactance (PU)	Susceptance (PU)
LineGroup1	Group1SEBus/WFSEBus	15	-	-	-
LineGroup2	Group2SEBus/WFSEBus	15	-	-	-
LineGroup3	Group3SEBus/WFSEBus	15	-	-	-
WFTransLine	WFSEBus/WFREBus	15	-	-	-

Table 4.4: Smart grid transformer parameters with some values calculated on a 100 MVA base apparent power

Transformer	The busbar to which the power transformer is connected	Voltage rating (kV)	Resistance (PU)	Inductive reactance (PU)	Capacity (MVA)
TRF1	G1Bus/Bus1	16.5/230	0.0	0.0576	100
TRF2	G2Bus/Bus4	18/230	0.0	0.0625	100
TRF3	G3Bus/Bus6	13.8/230	0.0	0.0586	100
WTGU1Trans	WTG1Terminal/Collector1Bus	4/24	-	-	5
Group1Trans	Collector1Bus/Group1SEBus	24/230	-	-	30
Group2Trans	Collector2Bus/Group2SEBus	24/230	-	-	30
Group3Trans	Collector3Bus/Group3SEBus	24/230	-	-	30

The transformer (WTGU1Trans) parameters are identical to those of WTGU2Trans and all other subsequent transformers up to WTGU18Trans for the other WTGUs.

Table 4.5: Wind farm, wind turbine generator units V117-4.2 MW wind turbine data

	Parameter	Value
Rotor data	Rotor diameter (D_R)	117 m
	Swept area (A_S)	10.751 m^2
	Minimum turbine angular speed, ω_{TRMin}	2.10 rpm = 0.22 rad/sec
	Nominal turbine angular speed, ω_{TRN}	9.9 rpm = 1.035 rad/sec
	Maximum turbine angular speed, ω_{TRMax}	17.7 rpm = 1.85 rad/sec
Operating data	Nominal power (P_N)	4 MW/4.2 MW
	Cut-in-speed (v_{CI})	3 m/s
	Nominal speed (v_N)	14 m/s
	Cut-out-speed (v_{CO})	25 m/s
	Re-cut-in-speed (V_{R-CI})	23 m/s
	Wind class	EC IB-T/IEC IIA-T/IEC S-T
	Standard operating temperatures	-20 ℃ to 45 ℃ with de-rating above 30 ℃ at 4 MW
	Nominal power (P_N)	4 MW/4.2 MW

	Cut-in-speed (v_{CI})	3 m/s
	Nominal speed (v_N)	14 m/s

Table 4.6: Wind farm wind turbine generator units squirrel-cage induction generator parameters, with some values calculated on a 100 MVA base apparent power

Parameter	Real value	Per unit value (on 100 MVA base value)
Rated output power	4 MW	-
Rated mechanical power	4.0606 MW	
Rated apparent power	4.842 MVA	
Rated line-to-line voltage	4 kV (rms)	
Rated phase voltage = Base voltage	2 309.4 V (RMS)	
Rated stator current = Base current	698.88 A (RMS)	
Rated stator frequency	50 Hz	
Rated power factor	0.8261	
Rated rotor speed	1 510.5 rpm	
Rated mechanical torque	25.6710 kN.m	
Rated stator flux linkage	7.3917 Wb (rms)	
Rated rotor flux linkage	6.7114 Wb (rms)	
Stator winding resistance	22.1040 mΩ	0.0067
Rotor winding resistance	23.1515 mΩ	0.0069
Stator leakage inductance	1.6980 mH	
Stator leakage reactance	j0.53344 Ω	j0.1615
Rotor leakage inductance	1.6980 mH	
Rotor leakage reactance	j0.53344 Ω	j0.1615
Magnetizing inductance	33.5970 mH	
Magnetizing reactance	j10.5548 Ω	j3.1946
Base flux linkage	7.3511 Wb (rms)	
Base impedance	3.3044 Ω	
Base inductance	10.518 mH	
Base capacitance	963.29 uF	

Table 4.7: IEEE 9-bus power system generator parameters with some values calculated on a 100 MVA base apparent power

Generator	The busbar to which the generator is connected	Xa (PU)	Xd (PU)	Xd' (PU)	Xd"	Xq	Xq'	Xq"
Gen1	G1Bus	0.0146	0.1460	0.0608	0.06	0.1	0.0969	0.06
Gen2	G2Bus	0.0896	0.8958	0.1198	0.11	0.8645	0.1969	0.11
Gen3	G3Bus	0.1313	1.3125	0.1813	0.18	1.2578	0.25	0.18

Table 4.8: IEEE 9-bus power system generator parameters (forceful data) with some values calculated on a 100 MVA base apparent power

Generator	The busbar to which the generator is connected	Ra (PU)	Tdo'	Tdo"	Tqo'	Tqo"	H	D (PU)
Gen1	G1Bus	0.00013	8.96	0.01	0.31	0.01	23.64	0

Gen2	G2Bus	0.00013	6	0.01	0.535	0.01	6.4	0
Gen3	G3Bus	0.00013	5.89	0.01	0.6	0.01	3.01	0

4.1.2 Smart grid simulation on RSCAD FX

The simulations of the smart grid system in this section were done under conditions and assumptions listed in Tables 4.9 and 4.10.

Table 4.9: Conditions and assumptions on the large-scale wind farm side

	Value	Reason where applicable
Temperature (℃)	25	The wind turbines in this smart grid system operate within a temperature range of -20 °C to 45 °C. When the temperature remains within this range, the turbines can be tuned to deliver a power output close to their rated capacity.
Humidity (%)	30	-
Air pressure (mbar)	1415	-
Wind speed (m/s)	14	WTs are expected to generate the rated output power at this speed.
Pitch angle (°)	32	-
Number of wind turbine generator units (WTGUs) operating at the same time	18 (all)	

It is important to note that not all WTGUs in a wind farm operate simultaneously. Their operation typically depends on the load demand, which is managed through control methods that determine which units should run at any given time. However, no control system was implemented to regulate the number of operating WTGUs in the original study, where the smart grid system was adopted. Additionally, the load demand was modeled based on a worst-case scenario.

Table 4.10: Conditions and assumptions on the IEEE 9-bus power system side

		Value/statement	Reason where applicable
Load demand (MVA)	DLoad1	172.5	-
	DLoad2	131.9	-
	DLoad3	143.1	-
Number of traditional generators operating at a time		3 (all)	-

Using the conditions listed in Tables 4.9 and 4.10, the load flow simulation on steady-state conditions of the smart grid system was performed in this study to check if the busbar voltages were in the acceptable range of 0.95 to 1.05 per unit for traditional electrical power grids and 0.9 to 1.0985 per unit for LSWFs as per the grid code specifications. Table 4.11 shows the apparent power on loads and corresponding busbar voltages.

Table 4.11: Apparent power on loads and busbar voltages on steady-state simulation of the smart grid system

Loads/busbars	Load apparent power (MVA)	Busbar voltage (PU)
Bus1	-	0.9981
DLoad1|Bus2	172.5	0.9558
DLoad2|Bus3	131.9	0.9707
Bus4	-	0.9975
DLoad3|Bus5	143.1	0.9801
Bus6	-	1.004
Coll1Bus	-	0.9458
Coll2Bus	-	0.9458
Coll3Bus	-	0.9458
WF1SEBus	-	0.9548
WF1REBus	-	0.9561

The value of the voltages recorded in Table 4.11 is satisfactory in terms of being within the specified ranges.

Developing the differential protection scheme for a power transformer requires that steady-state currents flowing in the protected power transformer be known. These currents are used for instrument transformer selection and differential protection relay elements threshold setting values. While the steady-state simulations of the smart grid system were performed, currents through the power transformers connecting the LSWF to the electrical power grid were also monitored, as recorded in Table 4.12.

Table 4.12: Currents recorded from the primary and secondary sides of the medium voltage to high step-up transformers for each group of wind turbine generator units

Large-scale wind farm side high-voltage step-up power transformers	Medium voltage side currents (kA)	High-voltage side currents (kA)
Group1Trans	0.5942	0.0623
Group2Trans	0.5942	0.0623
Group3Trans	0.5942	0.0623

However, it should be noted that the protection scheme will be tested only in the transformer Group1Trans.

The fundamental simulations that were performed above were to validate the accuracy of its data at steady-state conditions. During the simulations, the voltages and currents were monitored and recorded. As part of the requirements stated in the book Electric Power Systems (Weedy et al., 2012), such as ensuring that the busbar voltages are within the acceptable operating ranges for electrical power systems before using them for various studies, and that the voltage results obtained from the interconnected system studied above are satisfactory. The currents simulated and recorded in Table 4.12 were used in the next sections to develop the proposed protection scheme.

4.2 Smart Grid Model with IEC 61850 Standard Integration

The smart grid model used in this study was developed by integrating the modeled large-scale wind farm (LSWF) into the IEEE 9-bus power system using RSCAD FX on the RTDS platform. The LSWF is connected to Bus2, which was previously identified as a weak busbar in terms of voltage judgment. Bus2 was then selected as the connection point and was called the point of common coupling (PCC).

4.2.1 System configuration

- **IEEE 9-bus system:** Comprises three generators, nine buses, and six transmission lines, forming a classical benchmark network for power system analysis.
- **Wind farm integration point:** Bus2 at the 230 kV level was selected due to its sensitivity under high load conditions.
- **High-voltage (HV) transformer:** Each wind farm collector group connects to a transformer that steps up the voltage from 24 kV (medium voltage) to 230 kV (transmission level) for grid integration.
- **Load flow verification:** A steady-state load flow simulation was performed to confirm voltage profile compliance and overall system adequacy under the integrated wind farm condition.

This configuration forms the foundation for simulating both electrical and communication aspects of the smart grid, facilitating protection testing under various operating and fault conditions.

4.2.2 IEC 61850 standard communication architecture

- **Publisher/subscriber model:** Implemented for device communication using GOOSE messaging.
- **Client/server communication:** Used for configuration and data queries via MMS.
- **Substation zones:** Modeled to include wind turbine units, collector feeder, HV transformer, transmission line, and PCC.

This structure ensures both electrical and communication aspects of the smart grid are matched for protection testing.

4.3 Protection Configuration

The protection scheme focuses on the HV step-up transformer, where multiple types of faults could occur. The design ensures a successful integration of the primary and backup protection layers to prevent mal-operation or missed trips.

Relay settings:

- **Differential protection (Primary):** Detects faults in the protected transformer zone.
- **Overcurrent protection (Backup):** Responds to faults when the main protection fails.

The SEL-487E Station Phasor Measurement Unit IED is configured for coordination logic, using restraint and operating curves, slope-based differential thresholds, and harmonic blocking to handle CT saturation conditions. Another relay, the SEL-751A Feeder Protection Relay, is also configured for backup protection in case of the main protection relay failure.

These GTAO cards in the RSCAD draft are assigned to the current transformers (CTs). Therefore, selecting the appropriate instrument transformers in RSCAD was a necessary step before configuring the GTAOs.

4.3.1 Current transformer selection on RSCAD

The full-load currents, derived from a transformer rated at 30 MVA with voltage levels of 24 kV/230 kV, were 0.7217 kA on the primary (MV) side and 0.0753 kA on the secondary (HV) side. These values were used to determine the appropriate current transformer (CT) ratings. In line with the IEEE Guide for Selecting Protection CTs (IEEE, 2008), the recommended primary CT current ratio should range from 120% to 150% of the full-load current.

Accordingly, the CT ratios were chosen based on the upper limit of 150% to establish the medium voltage current transformer ratio (MVCTCR) and the high voltage current transformer ratio (HVCTCR).

The MV current transformer ratio:

$$\mathbf{MVCT_{CR} = 150\% \times I_{MV}} \quad \ldots \ldots \ldots \ldots \ldots \ldots \ldots \ldots \ldots \ldots \ldots \ldots \ldots \ldots \ldots \ldots \ldots \ldots \ldots \ldots \ldots \ldots \ldots \ldots .. \mathbf{(4.1)}$$

$$\mathbf{MVCT_{CR} = 150\% \times 0.7217\ kA}$$

$$\mathbf{MVCT_{CR} = 1082.55\ A}$$

The HV current transformer ratio:

$$\mathbf{HVCT_{CR} = 150\% \times I_{HV}} \ldots \ldots \ldots \ldots \ldots \ldots \ldots \ldots \ldots \ldots \ldots \ldots \ldots \ldots \ldots \ldots \ldots \ldots \ldots \ldots \ldots \ldots \ldots \ldots \ldots \ldots \ldots \ldots .. (\mathbf{4.2})$$

$$\mathbf{HVCT_{CR} = 150\% \times 0.0753\ kA}$$

$$\mathbf{HVCT_{CR} = 112.9599\ A}$$

Based on the IEEE Guide for selecting protection current transformers (CTs), the closest standard CT ratios were chosen, resulting in the selection of 1200:5 for $MVCT_{CR}$ and 200:5 for $HVCT_{CR}$, respectively.

4.3.2 Configuration of SEL-487E Station Phasor Measurement Unit IED

The SEL-487E IED serves as the primary protection device, employing both restrained and unrestrained differential protection elements. This section outlines how the relay settings were configured based on calculated thresholds and how these configurations were implemented using the AcSELerator QuickSet software.

Restrained differential pickup settings (O87P). The restrained differential pickup threshold, denoted as O87P, was determined using the following formula:

$$\mathbf{O87P \geq 10\% \left(\frac{I_{Nominal}}{TAPS}\right)} \ldots \ldots \ldots \ldots \ldots \ldots \ldots \ldots \ldots \ldots \ldots \ldots \ldots \ldots \ldots \ldots \ldots \ldots \ldots \ldots \ldots \ldots \ldots \ldots \ldots \ldots (\mathbf{4.3})$$

Assuming a nominal current $I_{Nominal}$ = 1 A and TAPS = 3.01 A (tap value for selected CT secondary):

$$\mathbf{O87P \geq 10\% \left(\frac{1\ A}{3.01\ A}\right)}$$

$$\mathbf{O87P \geq 0.0332}$$

This setting ensures that the relay only operates for faults exceeding 3.32% of the selected tap input, thereby avoiding nuisance tripping.

Unrestrained differential pickup settings (U87P). The unrestrained pickup threshold U87P is configured as follows:

$$\mathbf{U87P = 167\%\left(\frac{I_{FullLoad}\left(\frac{I_{SecR}}{I_{PrimR}}\right)}{TAPS}\right)} \ldots\ldots\ldots\ldots\ldots\ldots\ldots\ldots\ldots\ldots\ldots\ldots\ldots\ldots\ldots\ldots\ldots\ldots\ldots\ldots.. \mathbf{(4.4)}$$

Where:

- $I_{Nomal\ Load}$ = 0.7217 kA
- I_{SecR} = 5 A
- I_{PrimR} = 1200 A
- TAPS = 3.01 A

$$\mathbf{U87P = 167\%\left(\frac{0.7217\ kA\left(\frac{5}{1\ 200}\right)}{3.01\ A}\right)}$$

$$\mathbf{U87P = 0.999}$$

The above calculations were done based on the medium-voltage (MV) side of the protected transformer Group1Trans. They ensure that during severe internal faults, the relay responds instantly without requiring restraint calculation.

Relay configuration in AcSELerator QuickSet. The relay was configured using AcSELerator QuickSet software, and snapshots of key configuration panels are shown in the figures below:

- Figure 4.2: SEL-487E settings interface showing device model and active protection elements.
- Figure 4.3: Current transformer (CT) settings panel, indicating MV and HV input side configurations.
- Figure 4.4: Differential protection element settings and pickup thresholds.
- Figure 4.5 and Figure 4.6: Slope settings.
- Figure 4.7: Breaker trip logic and mapping of the differential element to the digital output contacts.

- Figure 4.8: Relay status monitoring screen showing real-time values and fault indicators.

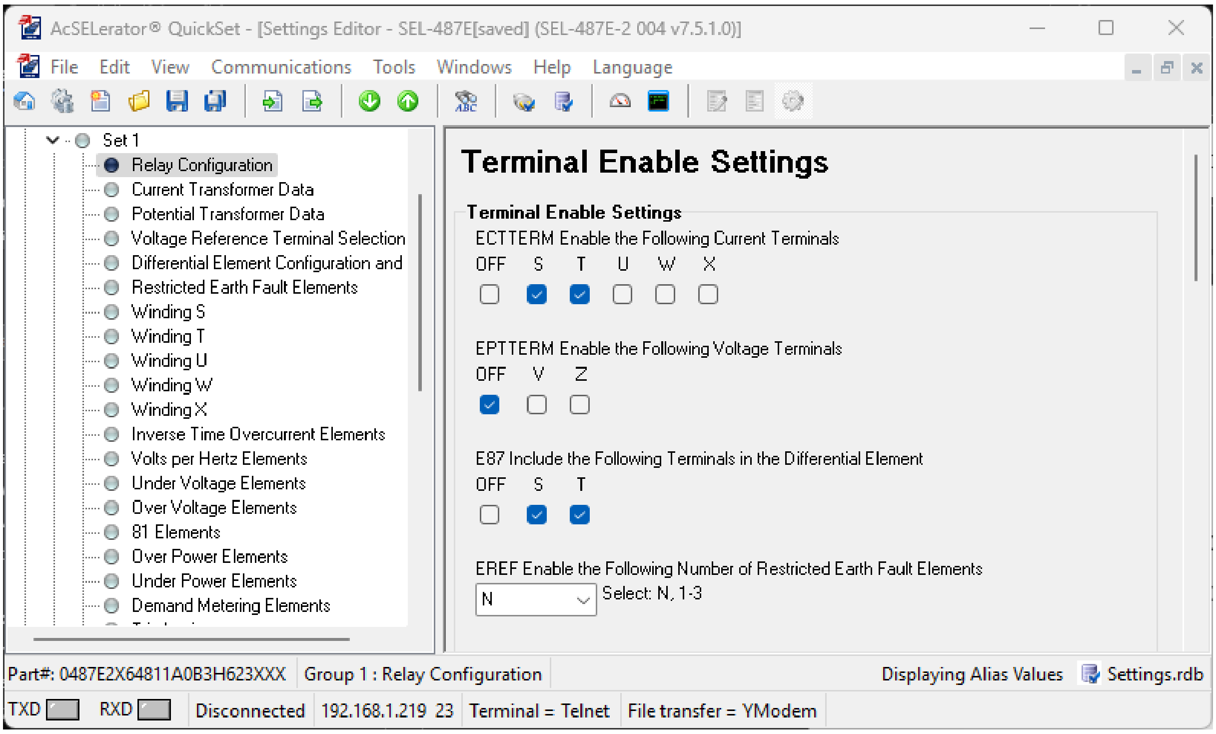

Figure 4.2: **SEL-487E settings interface showing device model and active protection elements**

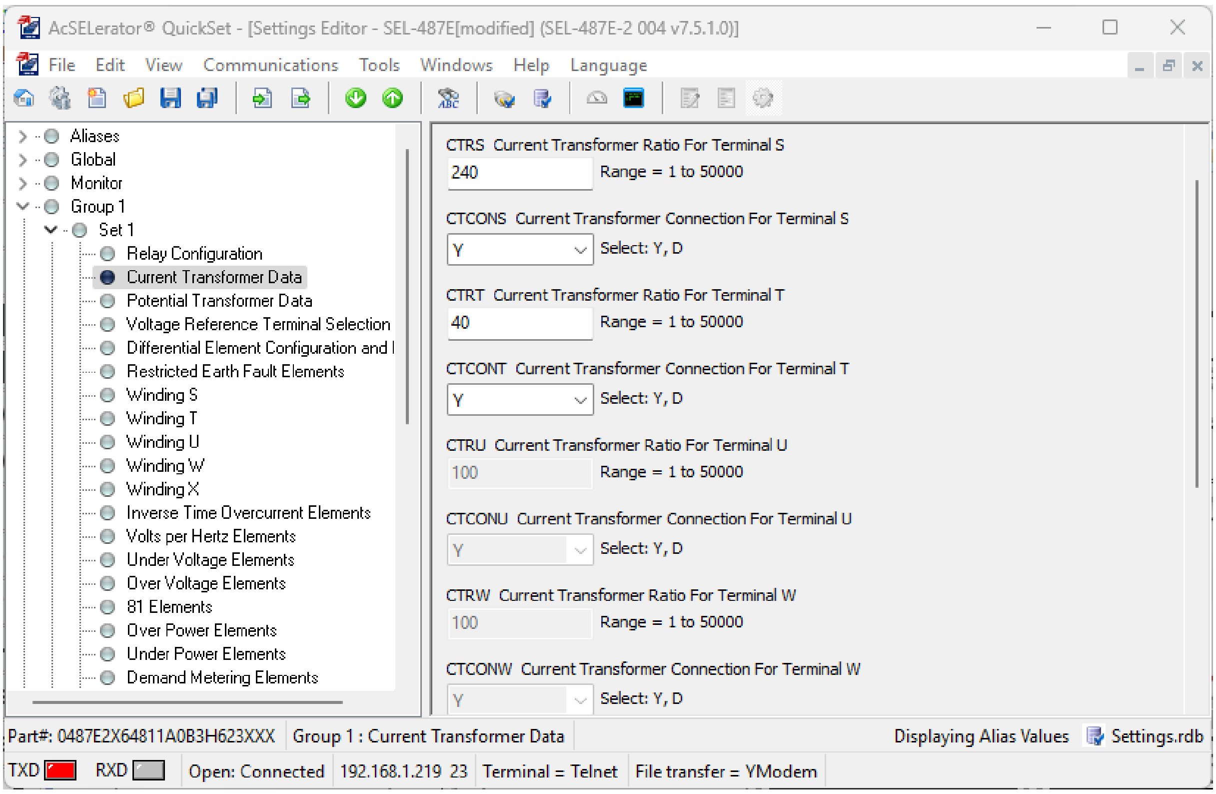

Figure 4.3: **Current transformer (CT) settings panel, indicating MV and HV input side configurations**

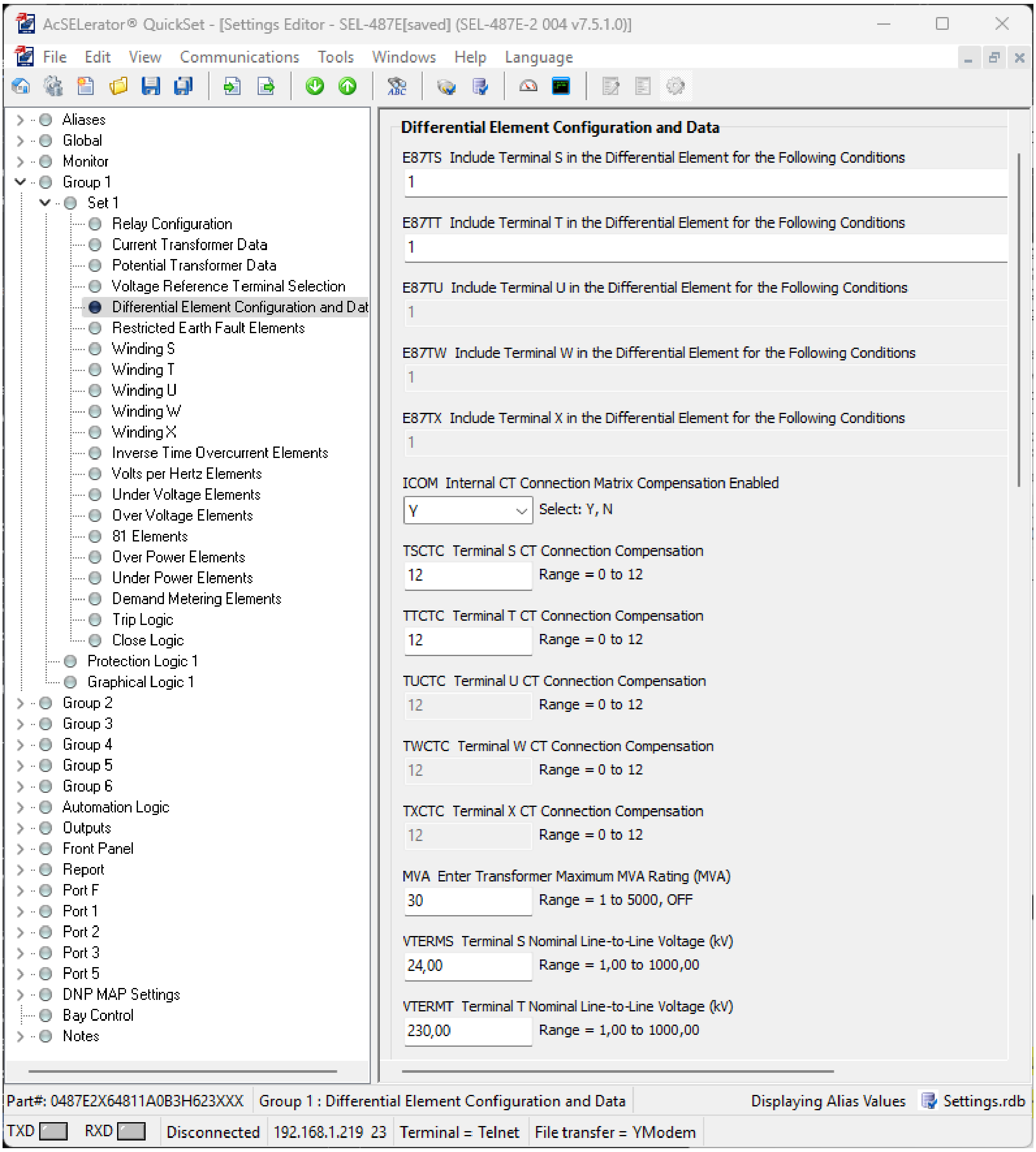

Figure 4.4: Differential protection element settings

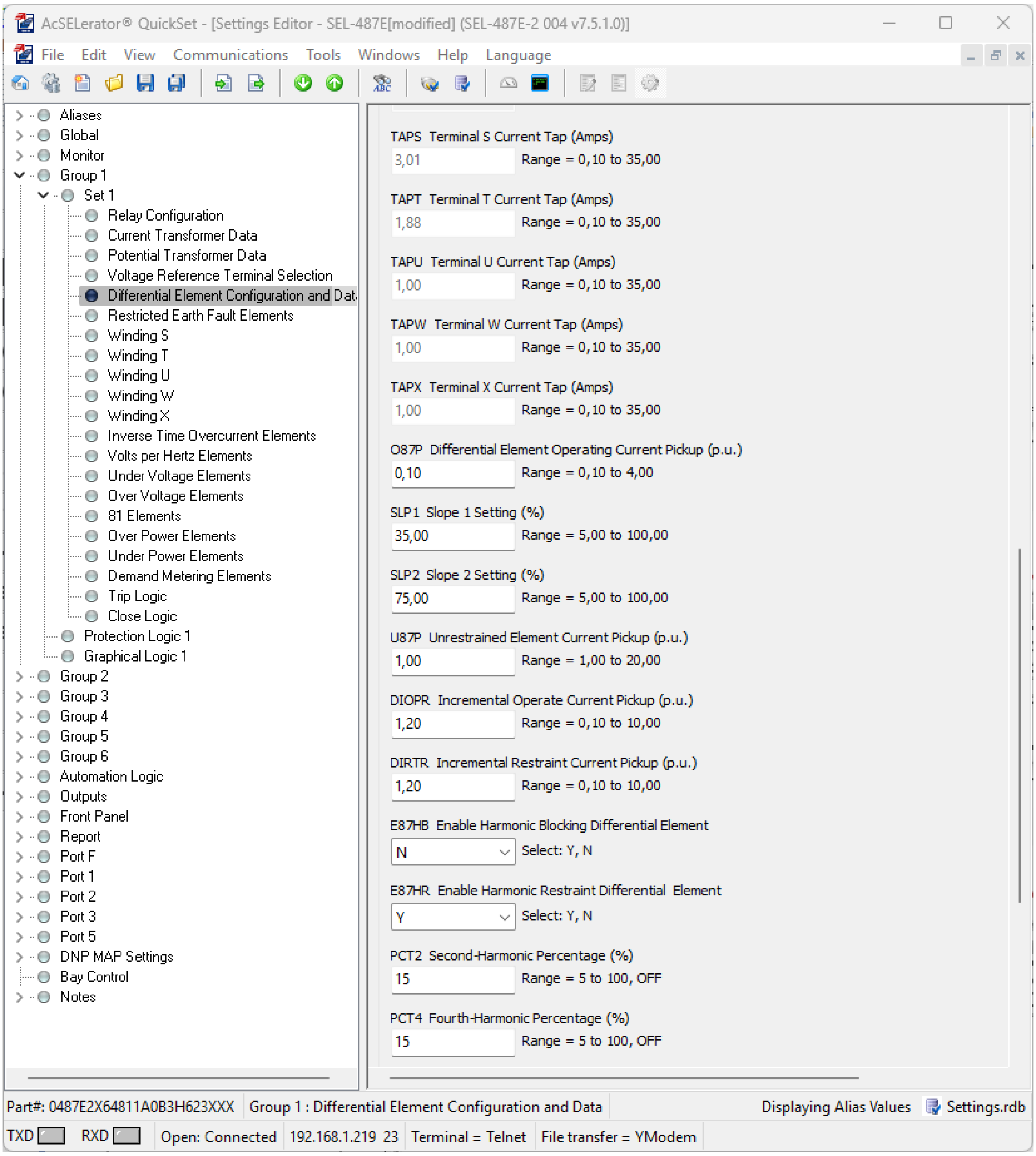

Figure 4.5: Slope settings configuration 1

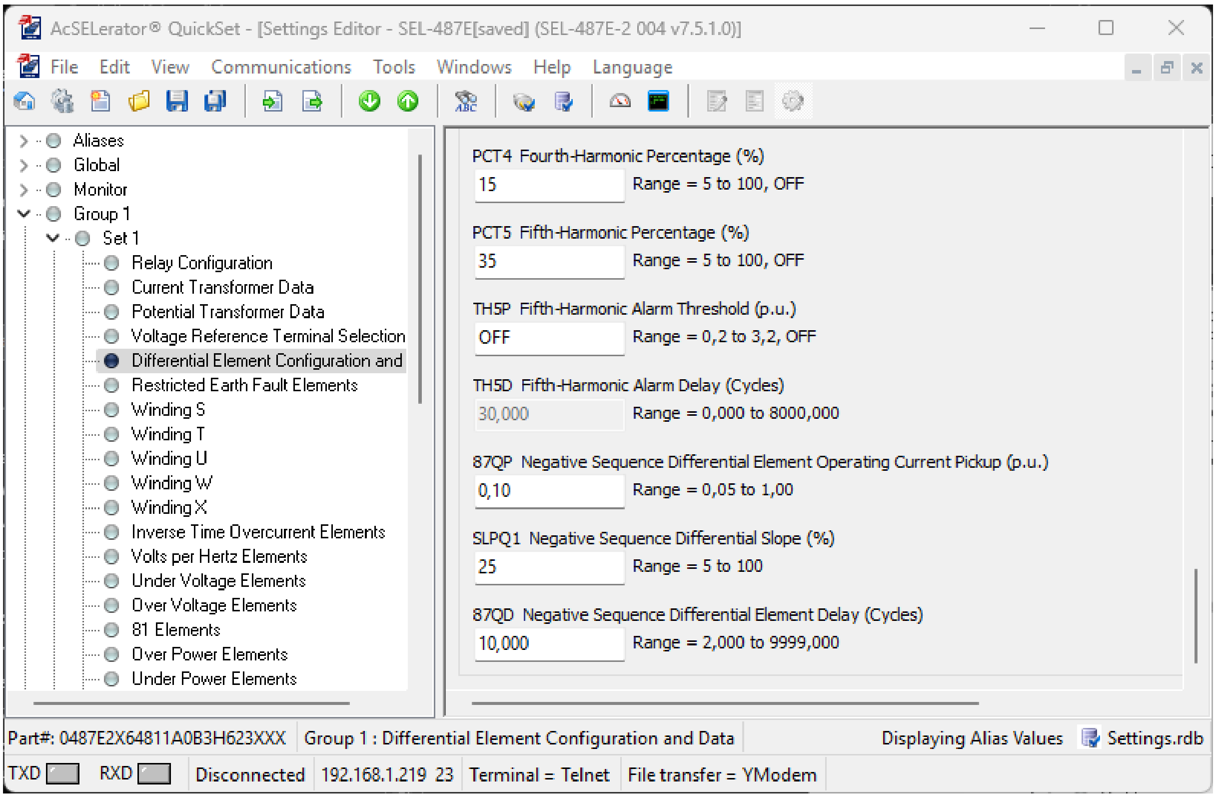

Figure 4.6: Slope settings configuration 2

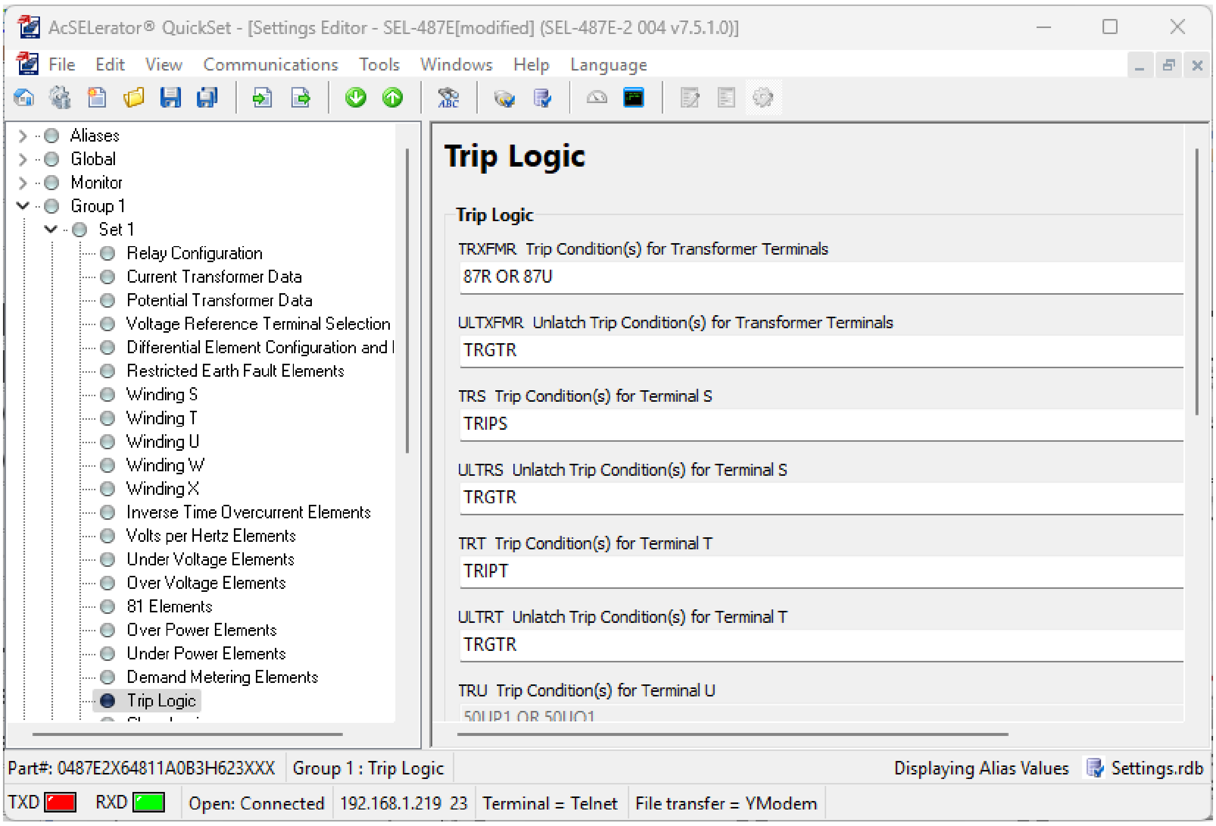

Figure 4.7: Relay trip logic settings

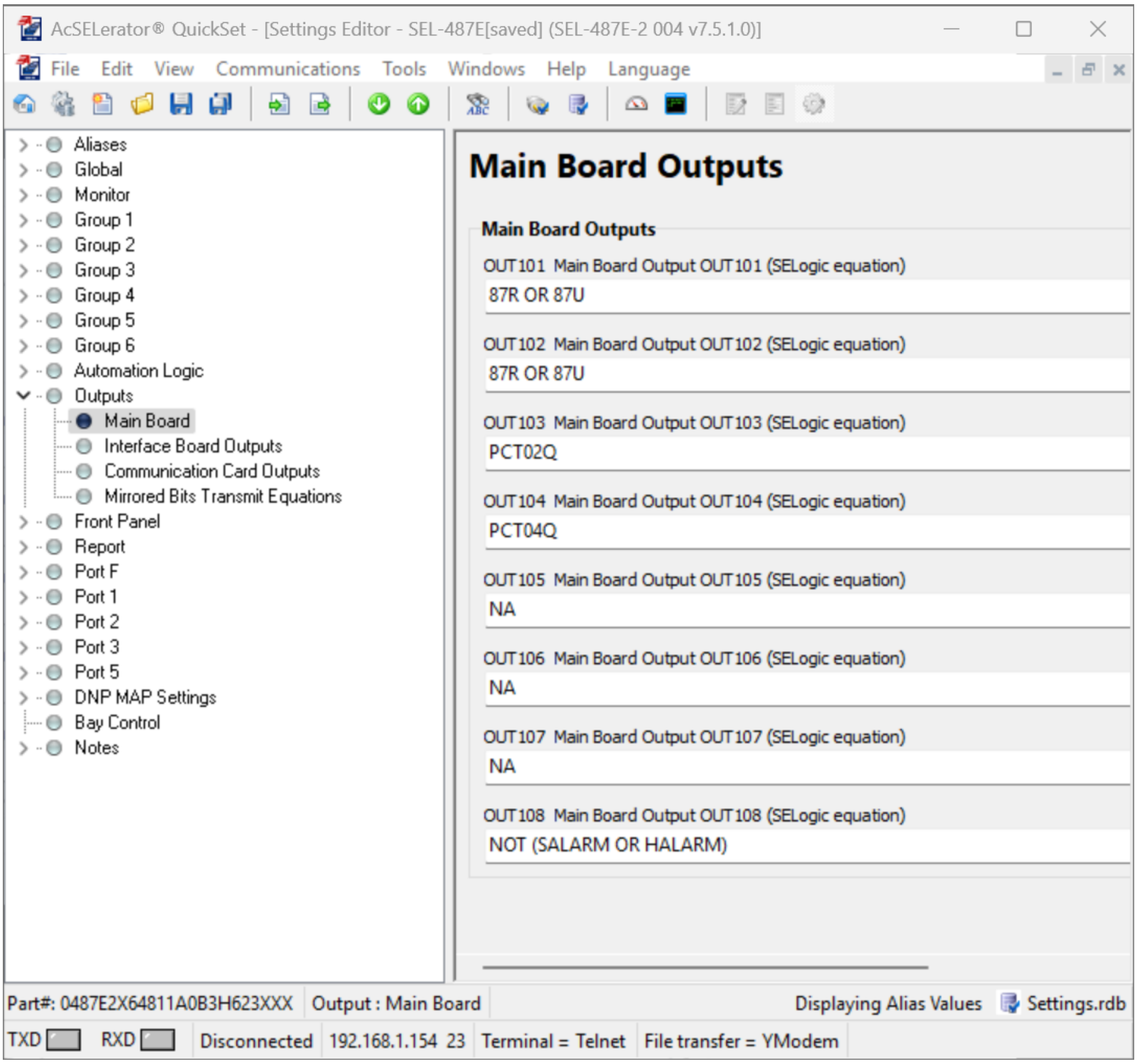

Figure 4.8: Breaker trip logic and mapping of the differential element to the digital output

These configurations collectively ensure the secure and dependable operation of the SEL-487E IED under various system conditions.

4.3.3 Configuration of backup protection device SEL-751A IED

The SEL-751A IED is configured to operate as a backup protection device, primarily using time-overcurrent (51P1P) elements. This configuration complements the primary differential protection provided by the SEL-487E relay, ensuring that faults are cleared in case the primary protection fails or is unavailable.

Overcurrent pickup setting (51P1P). The pickup current setting I_{Set} was calculated using the measured load current on the MV side of the protected transformer Group1Trans, which was 0.5942 kA. The relay uses a nominal current I_{Nom} = 5 A, and the CT ratio is 1200:5. The overcurrent pickup percentage (PS) is calculated as follows:

$$\left(\frac{I_{Prime}}{CT_{PTurns}}\right) = (90\%)(I_{Set}) = (90\%)(PS)(I_{Nom})$$

$$PS = \frac{I_{Prime}\left(\frac{I_{SecR}}{I_{PrimeR}}\right)}{(90\%)(I_{Nom})}$$

$$PS = \frac{0.5942\ kA\left(\frac{5\ A}{1\ 200\ A}\right)}{(90\%)(5\ A)}$$

$$\mathbf{PS = 55.0185\%}$$

From this percentage, the pickup current is:

$$I_{Set} = I_{51P1P} = 55.0185\% \times 5\ A$$

$$\mathbf{I_{51P1P} = 2.7509\ A}$$

However, due to software constraints in the pickup settings block (which limits the input range to 0.10 A to 3.20 A), a rounded-down value of 2.5 A was selected for setting 51P1P.

Time delay setting. The time delay for this overcurrent element was configured using a standard inverse time characteristic with a time multiplier setting (TMS) of 1. This delay ensures coordination with the SEL-487E relay, allowing primary protection a chance to clear faults before backup operation.

Table 4.13: SEL-751A settings

ANSI	Description	Setting current (A)	Time		Characteristic
			Delay (s)	Dial	
51P1P	Level 1 Maximum Phase Time-Overcurrent Element Pickup	2.5	N/A	1	$TMS\left(\frac{0.14}{(M)^{0.02}-1}\right)$

Torque control and logic implementation. To coordinate with the SEL-487E and prevent redundant tripping, GOOSE-based torque blocking was implemented using virtual bits VB001 (87R) and VB002 (87U). When either bit is received, the torque control logic blocks the overcurrent element.

The logic also includes:

- Pushbutton 1 (PB01) and Pushbutton 2 (PB02): Manual pushbuttons for latch and block control.

- Target LED 6 (T06_LED): A visual indicator on the front panel, which lights up upon GOOSE receipt, confirming the activation of torque blocking.

Relay setup in AcSELerator QuickSet. The following figures illustrate the key configuration interfaces:

- Figure 4.9: Current transformer ratio configuration
- Figure 4.10: Overcurrent pickup setting panel in AcSELerator QuickSet, showing 51P1P configured at 2.5 A and torque control logic tied to GOOSE-based virtual bits and latch reset. Manual latch release configuration, including PB01 and PB02 assignment.
- Figure 4.11: Trip logic configuration
- Figure 4.12: Trip logic mapping panel showing how relay outputs are linked to digital contacts and coordinated with breaker operation.

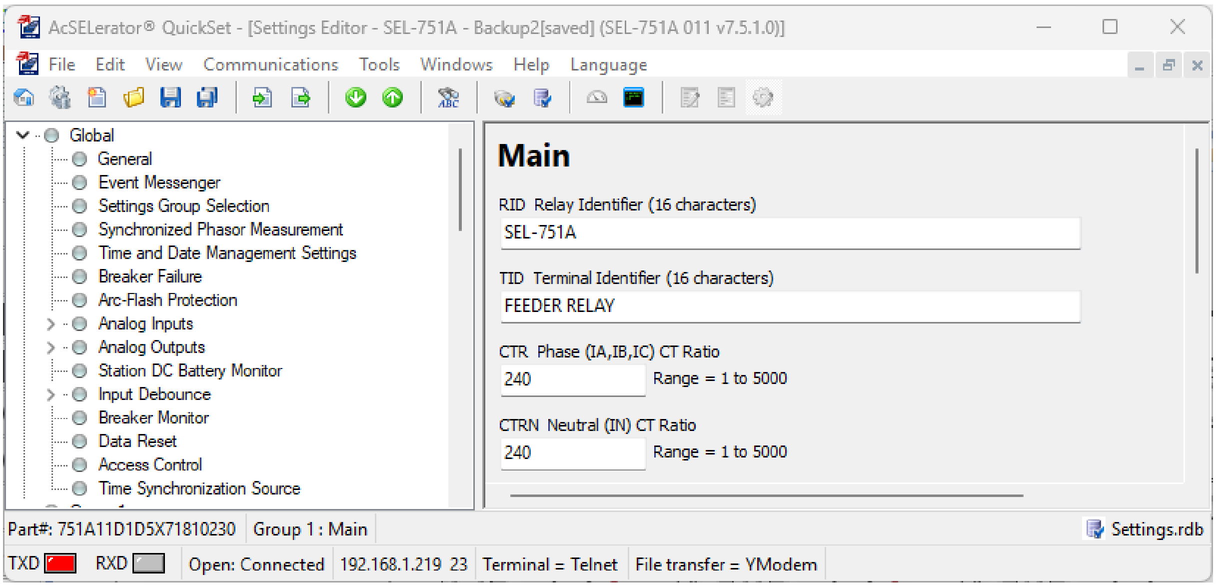

Figure 4.9: Current transformer ratio configuration

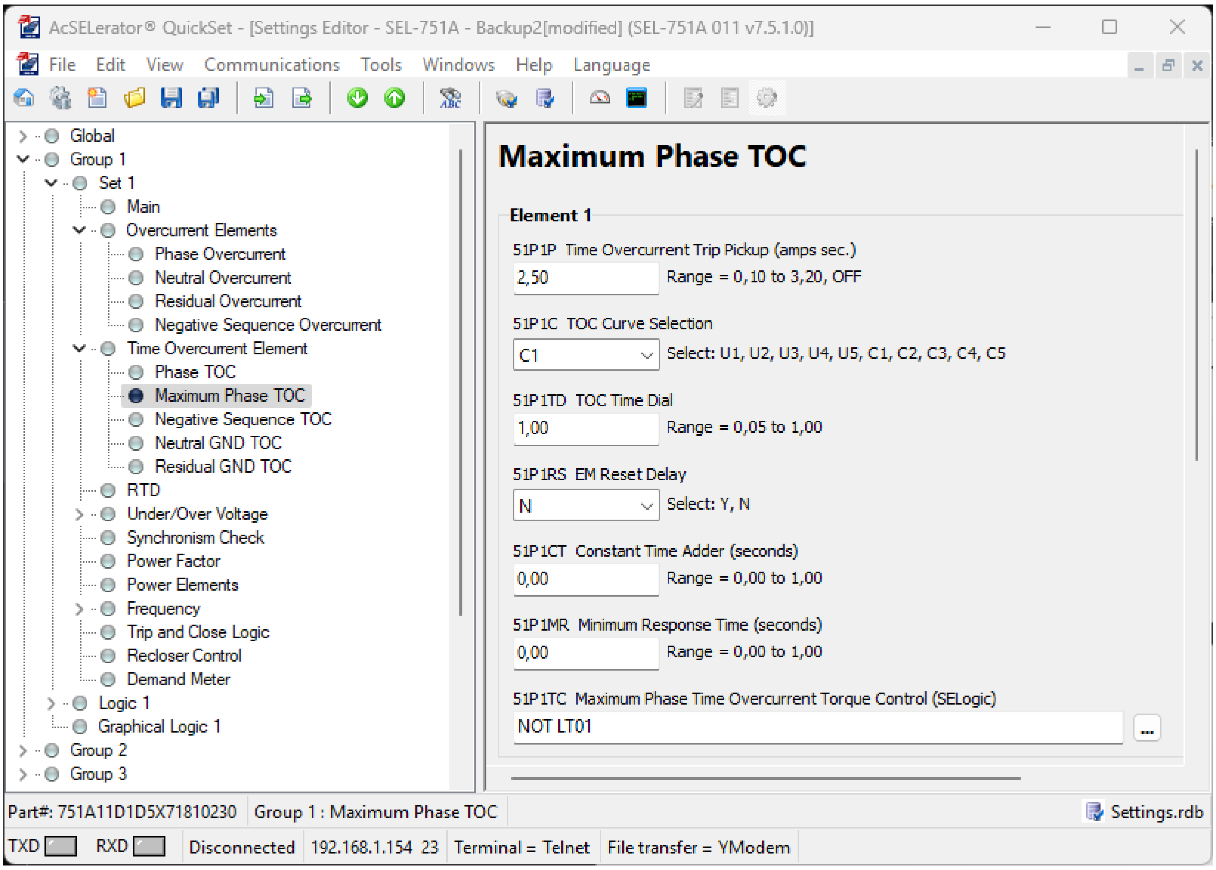

Figure 4.10: Overcurrent pickup setting panel in AcSELerator QuickSet, showing 51P1P configured at 2.5 A. Torque control logic tied to GOOSE-based virtual bits and latch reset

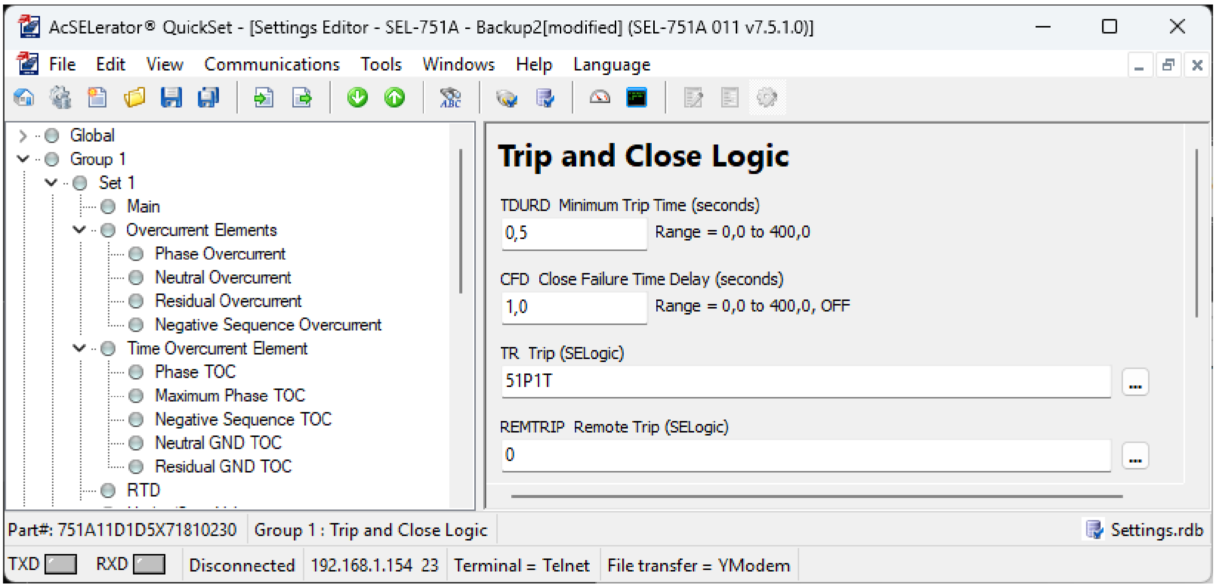

Figure 4.11: Trip logic configuration

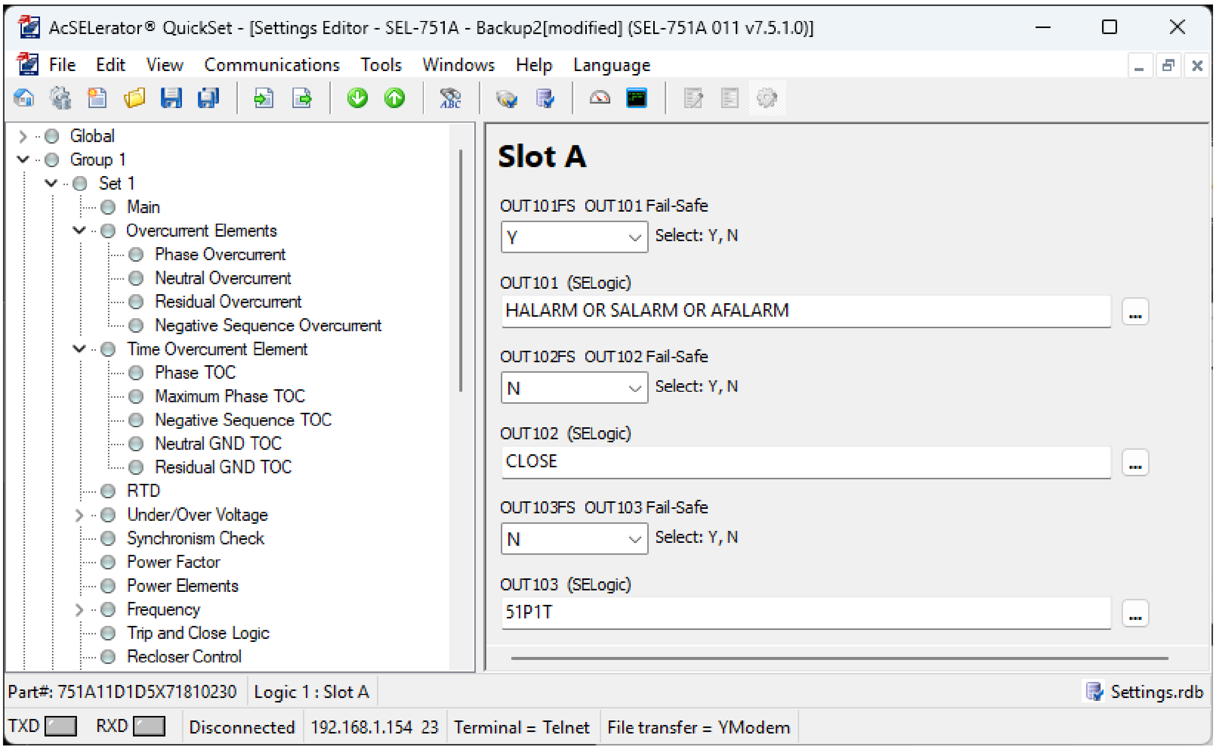

Figure 4.12: Trip logic mapping panel showing how relay outputs are linked to digital contacts and coordinated with breaker operation

These settings ensure that the SEL-751A operates reliably as a backup device and only trips when the SEL-487E either fails to detect or is unable to act on a fault.

4.4 Hardware-In-the-Loop Simulation Test Setup on RSCAD FX

This section describes how analog signals representing current transformer (CT) outputs are generated by the RTDS and sent to the SEL-487E and SEL-751A IEDs through giga-transceiver analog output (GTAO) modules. CT signals for CT0, CT1, and CT2 were carefully configured with primary winding turns ratios and secondary winding series resistances, aligning with the selected CT parameters (e.g., 180:1 turns ratio). The burden resistance and signal scaling for each CT were configured to ensure successful replication of the realistic conditions, particularly for accurate differential current calculation. This setup ensures that the relay receives accurate and phase-coherent analog inputs, crucial for precise protection operation, especially for detecting differential and restraint current magnitudes.

Figure 4.13 shows the main data parameter settings for CT0, which is mapped to the *Group1BRKIR*, *Group1BRKIY*, and *Group1BRKIB* signals, representing the three-phase current measurements from the medium-voltage side circuit breaker associated with the protected transformer. These values serve as the analog input signals from CT0 and are critical for simulating the MV breaker currents.

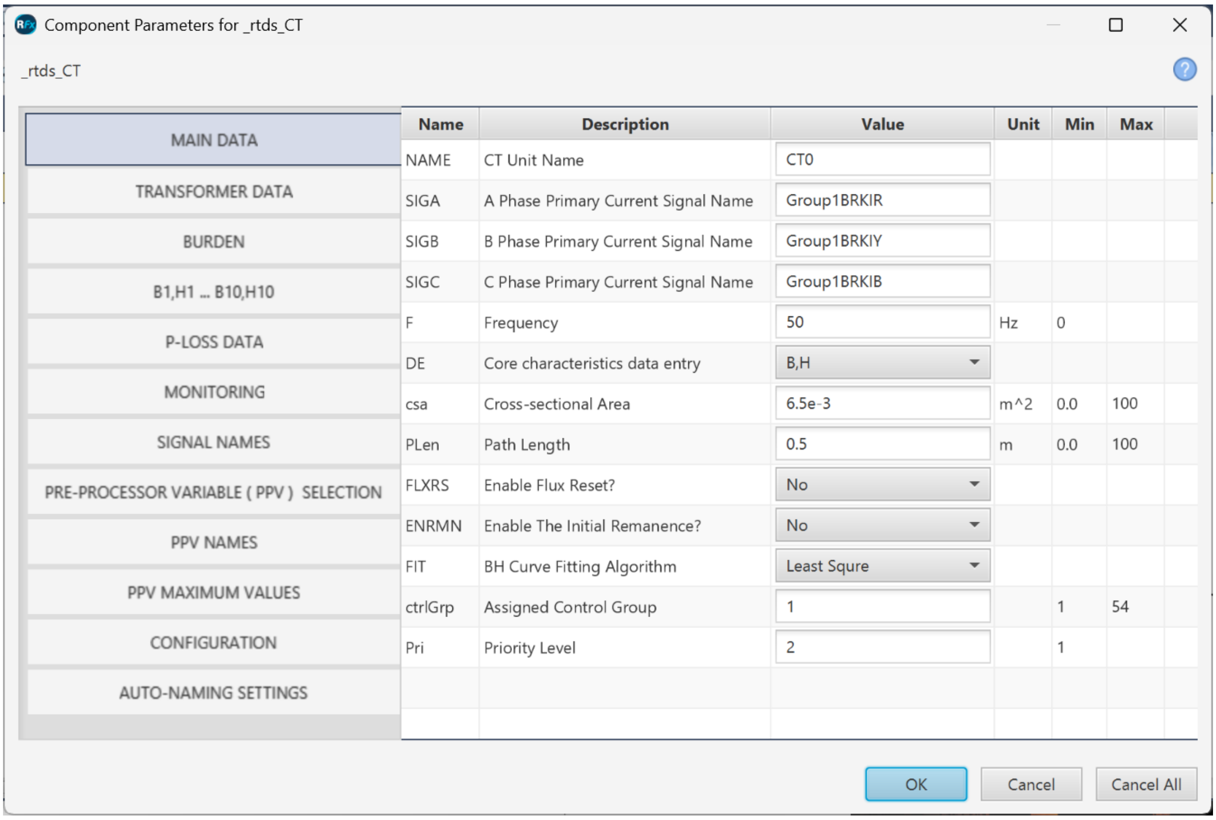

Figure 4.13: **Main data parameter settings for CT0. *Group1BRKIR*, *Group1BRKIY*, and *Group1BRKIB* are CT0 primary terminal current signals mapped from the medium-voltage circuit of the protected transformer**

Figure 4.14 illustrates the physical characteristics of CT0, including the primary winding turns ratio and the series resistance of the secondary winding. These parameters directly influence the magnitude and accuracy of the analog signals fed into the relay. Proper tuning ensures linear performance under both normal and fault conditions, avoiding issues like CT saturation.

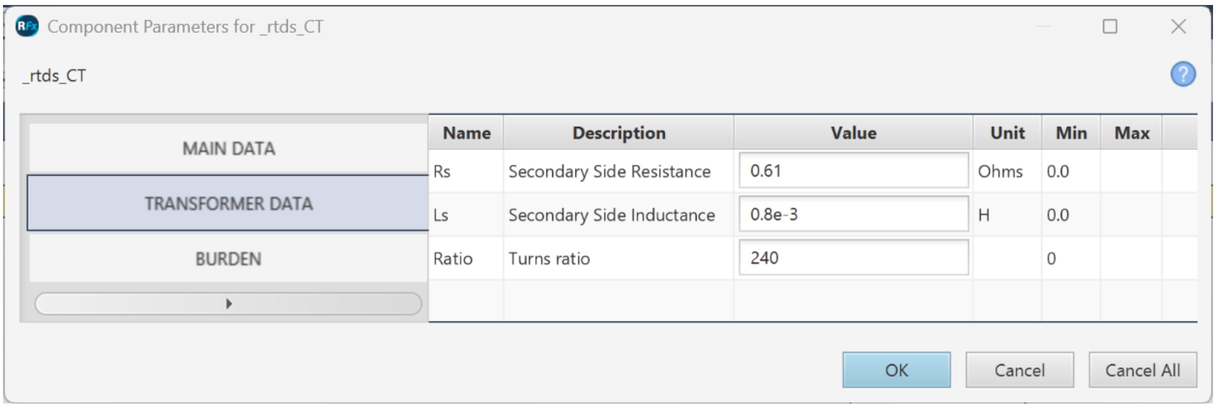

Figure 4.14: **Secondary winding series resistance and the primary winding turns ratio settings for CT0**

Figure 4.15 provides the signal monitoring interface in RSCAD FX, used to validate the real-time performance of CT0. The currents injected into the relay were monitored to confirm phase accuracy and correct magnitude scaling relative to the simulated grid conditions.

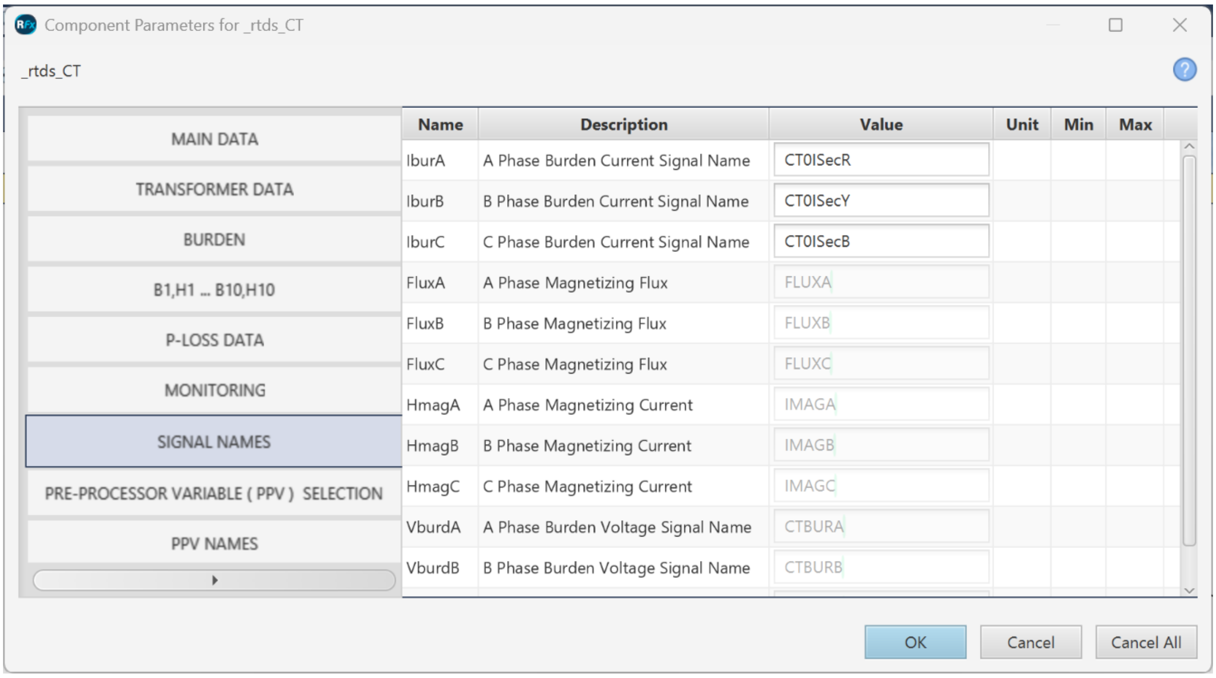

Figure 4.15: Signal monitoring settings for CT0. *CT0ISecR*, *CT0ISecY,* and *CT0ISecB* are CT0 secondary terminal current signals that will be accessible to the SEL-751A IED through the Omicron CMS 356S amplifier

Similar configuration steps were applied to CT1 and CT2. CT1 was mapped to the *Group1TransIPrIR*, *Group1TransIPrIY*, and *Group1TransIPrIB* signals, capturing the transformer's primary winding current inputs. CT2 was linked to the *Group1TransISecIR*, *Group1TransISecIY*, and *Group1TransISecIB* signals, which represent the high-voltage side secondary winding outputs of the protected transformer. Figures 4.16 to 4.21 display the configuration and monitoring settings for CT1 and CT2, including their winding ratios, series resistances, and output validation.

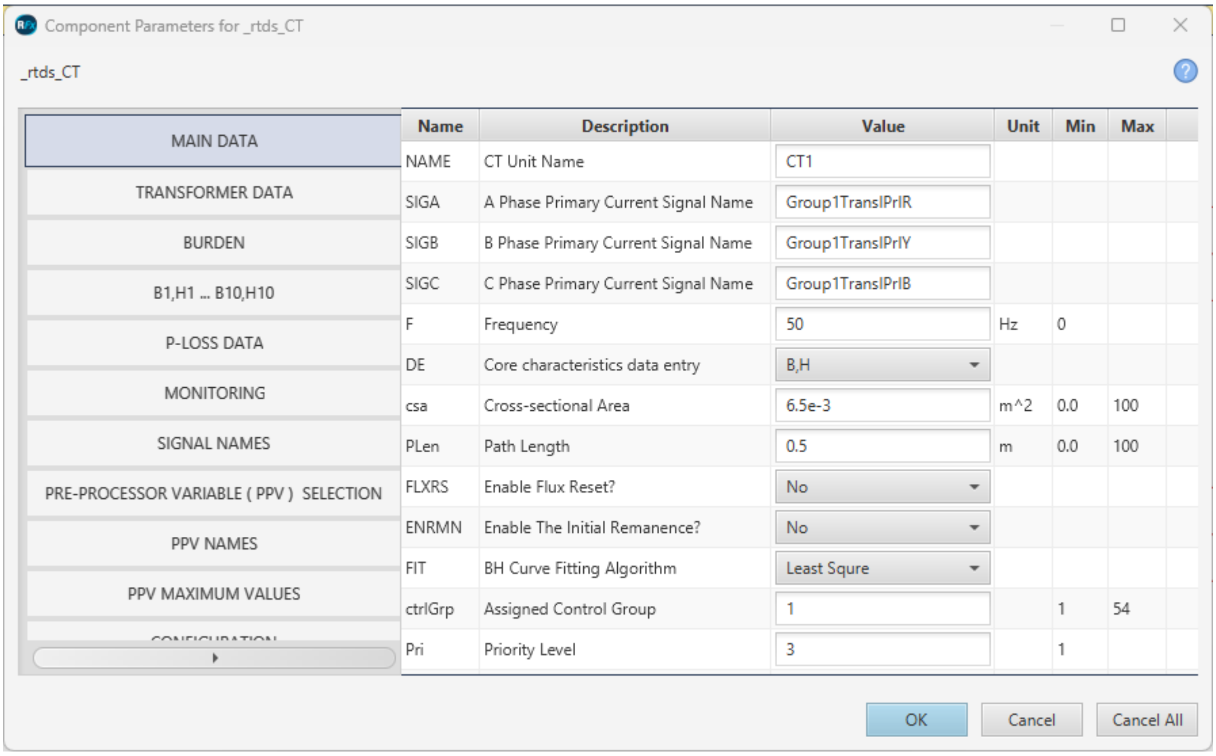

Figure 4.16: Main data parameter settings for CT1. *Group1TransIPrIR*, *Group1TransIPrIY*, and *Group1TransIPrIB* are CT1 primary terminal current signals mapped from the medium-voltage side of the protected transformer

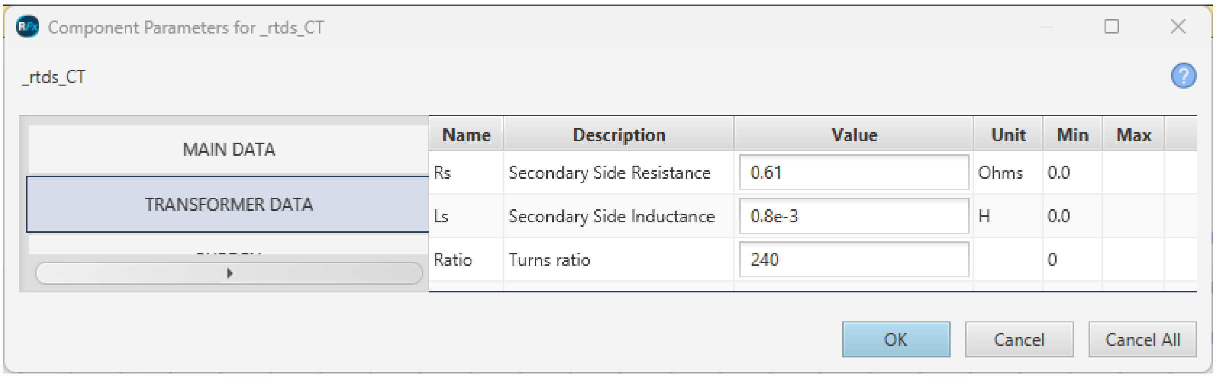

Figure 4.17: Series resistance of the secondary winding and the number of primary turns of CT1

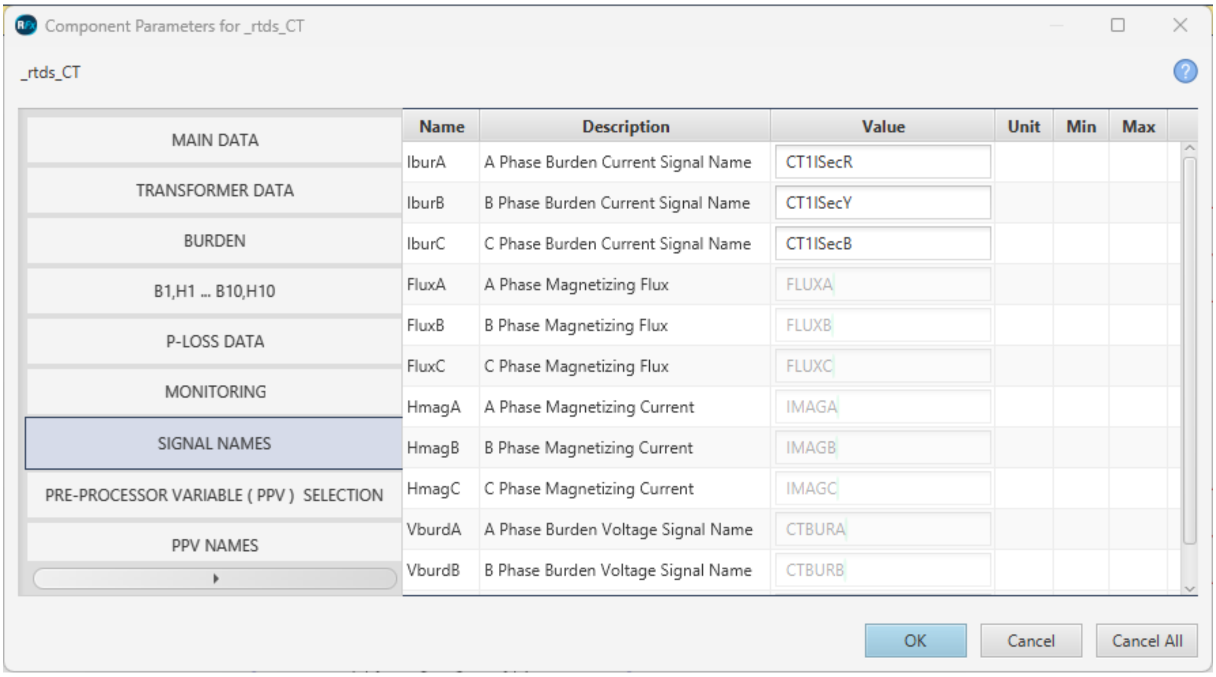

Figure 4.18: Signal monitoring settings for CT1. *CT1ISecR*, *CT1ISecY,* and *CT1ISecB* are CT1 secondary terminal current signals that will be accessible to terminal S of the SEL-487E IED through the Omicron CMS 156 amplifier 1

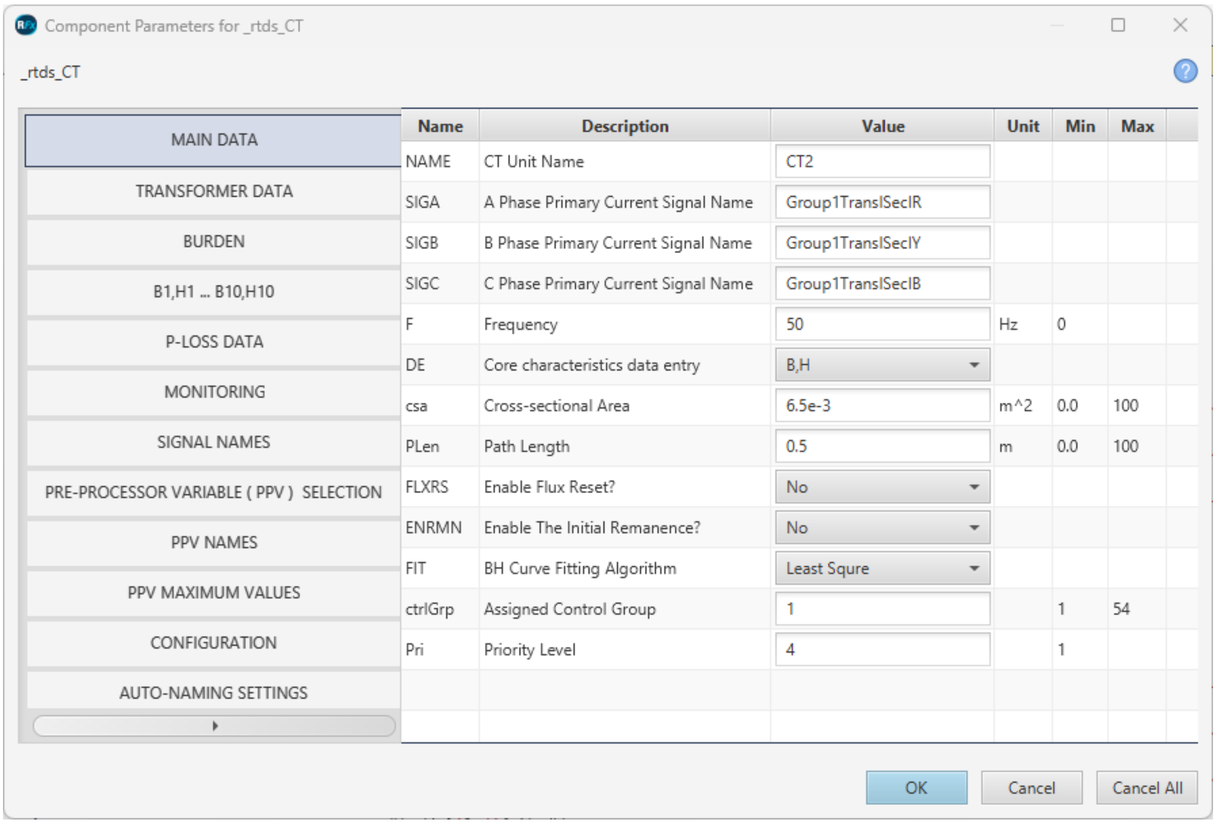

Figure 4.19: Main data parameter settings for CT2. *Group1TransISecIR*, *Group1TransISecIY*, and *Group1TransISecIB* are CT2 primary terminal current signals mapped from the high-voltage side of the protected transformer

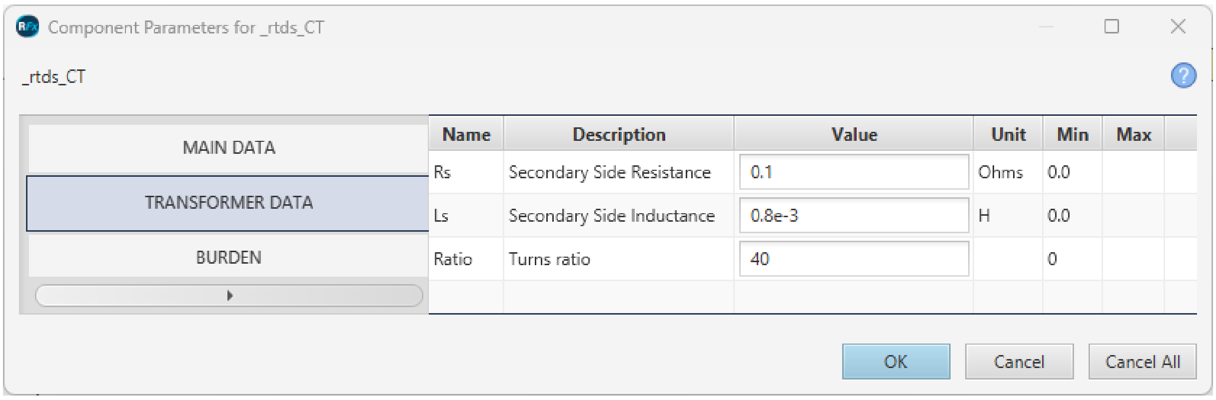

Figure 4.20: **Series resistance of the secondary winding and the number of primary turns of CT2**

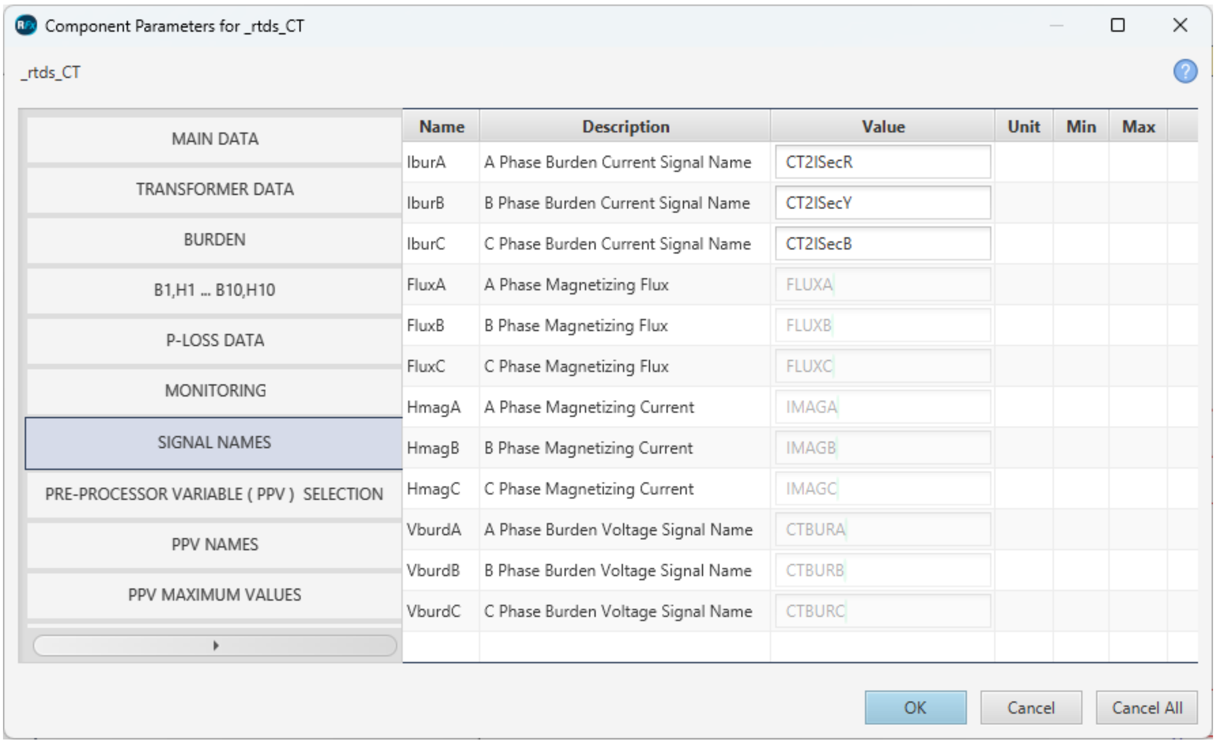

Figure 4.21: **Signal monitoring settings for CT2. *CT2ISecR*, *CT2ISecY,* and *CT2ISecB* are CT1 secondary terminal current signals that will be accessible to terminal T of the SEL-487E IED through the Omicron CMS 156 amplifier 2**

All CTs were assigned to dedicated GTAO channels, as shown in Figure 4.22. These modules interface the RTDS with the physical SEL-487E and SEL-751A IEDs by converting simulated current signals into analog voltages of +/-10 Volt DC. Each channel was calibrated to match the full-load current levels of the transformer, scaled to fit the 5 A nominal secondary input of the relay based on the CT ratios (e.g., 1200:5 for the MV side, 200:5 for the HV side).

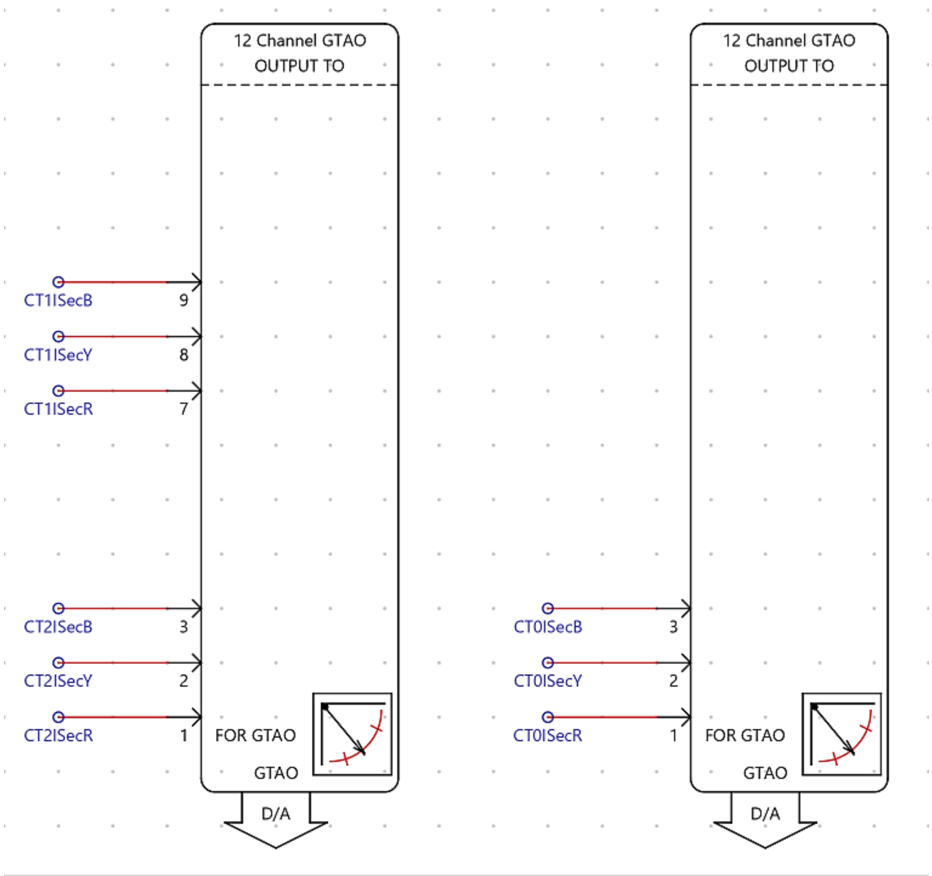

Figure 4.22: **GTAOs for the sampling of CT0, CT1, and CT2 signals. The input signals to the GTAO are connected from the secondary sides of the CTs**

The GTAO outputs were verified using real-time meters in RSCAD to ensure waveform integrity, phase alignment, and amplitude fidelity. These verifications were crucial to confirm that the injected currents reflected the simulated electrical behavior of the system under various faults and normal conditions.

Furthermore, the CT configurations adhered to IEEE Std C57.13 guidelines for CT selection and saturation avoidance, supporting the dependable operation of the differential protection logic. Accurate current replication was vital for the SEL-487E relay to correctly compute the differential and restraint currents needed to trigger its internal logic for restrained (87R) or unrestrained (87U) tripping.

Within the overall setup, the analog simulation environment and relay behavior formed a closed-loop protection system. This is so that when the fault is simulated, the analogue currents get injected into the physical relays SEL-487E and SEL-751A. When one of these relays identifies this as the fault, it will issue a trip signal to trigger a virtual circuit breaker (CB) within the RTDS/RSCAD FX.

The CB interface is achieved through the configuration of the Giga-Transceiver Front Panel Interface (GTFPI) module, which supports high-speed digital I/O communication between RTDS and external hardware.

In the RSCAD FX, these virtual CB components were placed on the medium-voltage (MV) and high-voltage (HV) sides of the protected transformer (Group1Trans). These CBs represent actual switching devices that would disconnect faulty equipment in a real-world substation. Their logical operation in the simulation is controlled by digital trip signals received from the SEL protection relays.

The trip signals were sent from the relay digital output contacts configured in AcSELerator QuickSet. Specifically:

- OUT101 and OUT102 of the SEL-487E relay were used to control the trip command for the MV and HV breakers of the protected transformer.
- OUT103 from the SEL-751A relay was configured as the backup trip signal, operating only when the primary relay (SEL-487E) failed to clear the fault.

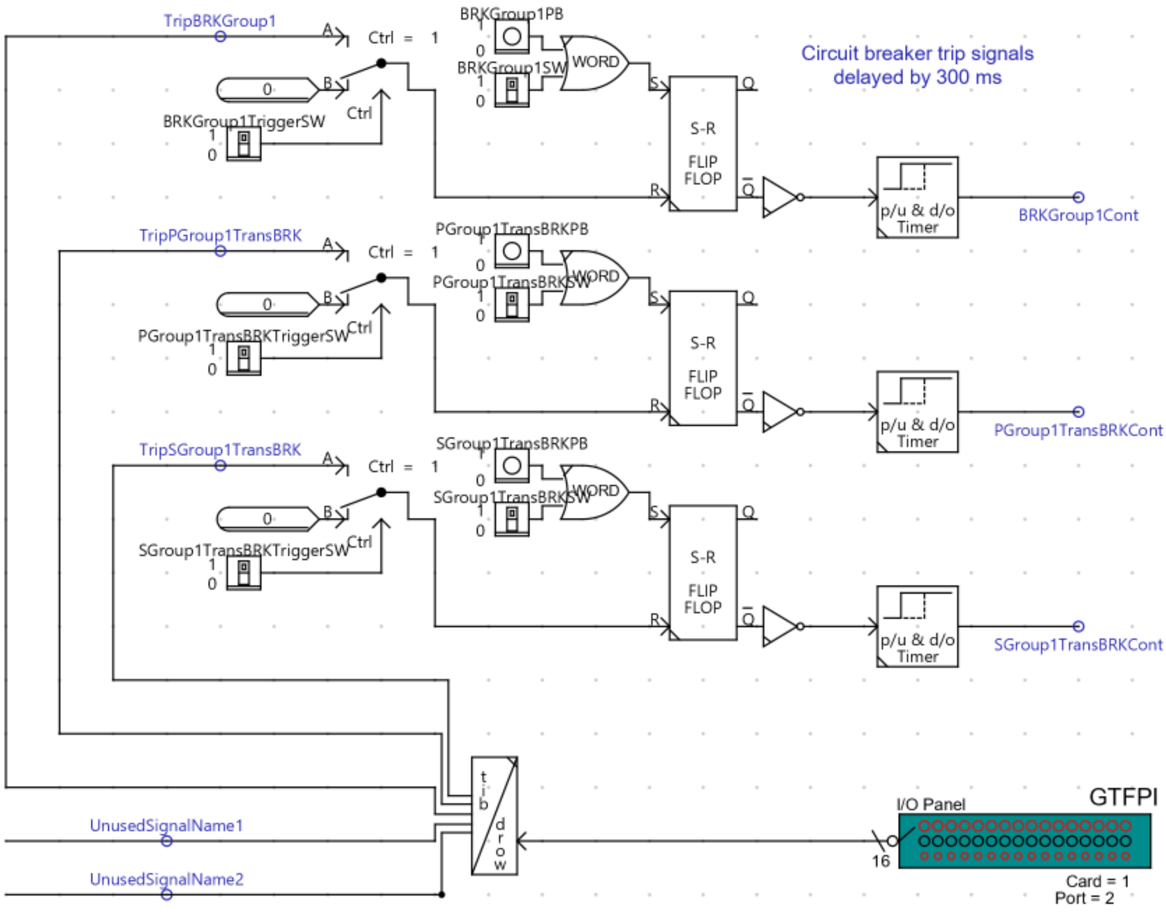

Figure 4.23: **Circuit breaker control logic through the GTFPI**

These digital outputs were connected to the corresponding virtual CB control inputs via the GTFPI interface, enabling real-time actuation within the RSCAD environment. When a fault was simulated and detected by the differential or overcurrent protection logic in the relays, the trip signals activated the breaker controls in RSCAD, opening the circuit breaker and isolating the faulted section.

Figure 4.23 illustrates the circuit breaker control logic and its linkage to the trip outputs from the relays. This figure also demonstrates the use of latching logic, anti-bounce protection, and breaker status feedback mechanisms implemented in RSCAD to mimic realistic circuit breaker behavior and state transitions.

This closed-loop configuration forms a critical part of the hardware-in-the-loop validation process. It ensures that protection decisions made by the relay, based on simulated analog current inputs, result in observable system-level actions (i.e., breaker tripping) within the simulated environment. This allows for a complete evaluation of the timing, accuracy, and selectivity of the protection scheme.

Moreover, it facilitates the verification of coordination logic between the primary (SEL-487E) and backup (SEL-751A) relays. For instance, in scenarios where the SEL-487E successfully trips, the trip logic of the SEL-751A is blocked via GOOSE-based torque control. However, if the SEL-487E fails to act (due to simulated malfunction or deliberate suppression), the SEL-751A executes a delayed trip, providing redundant protection.

In summary, the modeling of the circuit breaker interface in RSCAD and its integration with the SEL protection relays via GTFPI enabled a complete closed-loop simulation. This setup allowed real-time observation and verification of breaker actuation in response to protection logic decisions, ensuring a reliable and robust validation framework for the proposed IEC 61850-based protection scheme.

4.5 IEC 61850 Communication Configuration

The implementation of the IEC 61850 standard was to facilitate high-speed, peer-to-peer communication between the SEL-487E Station Phasor Measurement Unit and the SEL-751A Feeder Protection Relay. This communication ensured the coordinated and selective operation of the protection scheme.

4.5.1 Requirements

Table 4.14 summarizes the logical nodes (LNs) configured on the SEL-487E relay. These LNs were linked to the restrained (87R) and unrestrained (87U) differential protection elements.

Table 4.14: **List of SEL-487E relay word bits and protection logical nodes used**

Data Source	Logical Node	Attribute	Comment
87R[a]	D87RPDIF1	Op.general	Restrained differential element trip
87U[a]	D87UPDIF1	Op.general	Unrestrained differential element trip

The LNs were integrated into the configured IED description (CID) file, which was then used to define the datasets for GOOSE messaging. These datasets, upon trip detection by the SEL-487E, were published to the SEL-751A to block its operation.

4.5.2 SEL-487E and SEL-751A backup protection logic

The logic block implemented in the SEL-751A is shown in Figure 4.24. The SEL-751A receives GOOSE messages via virtual bits VB001 (87R trip) and VB002 (87U trip). If either of these bits is asserted, the torque control logic within the relay prevents unnecessary tripping. In the event that SEL-487E fails to trip due to a circuit breaker (CB) malfunction or auxiliary wiring failure, SEL-751A operates after a set time delay to clear the fault.

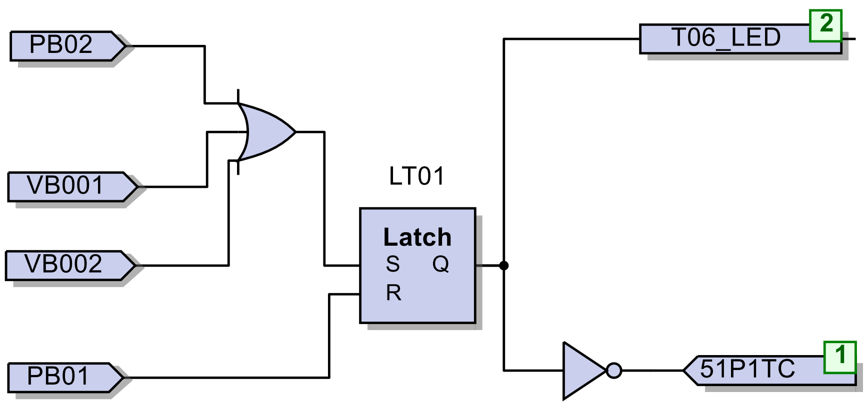

Figure 4.24: **Backup protection logic for blocking SEL-751A operation using GOOSE messages**

The logic also includes manual components: PB01 and PB02 function as pushbuttons for manually controlling the latch and blocking mechanism. Additionally, the front-panel indicator T06_LED lights up when the SEL-751A receives a GOOSE message, signaling that the torque-blocking logic is active and preventing unintended tripping.

4.5.3 Configuration in AcSELerator Architect

The dataset configuration process in the SEL-487E and SEL-751A IEDs is illustrated in the figures listed below:

- Figure 4.25: Dataset definition screen for SEL-487E.
- Figure 4.26: Mapping of GOOSE transmission datasets for SEL-487E.
- Figure 4.27: Mapped datasets received by SEL-751A relay via VB001 and VB002.
- Figure 4.28: Uploading the configured IED description file to SEL-751A.
- Figure 4.29: Confirmation screen of the CID file received by SEL-751A.
- Figure 4.30: GOOSE message status verification on SEL-751A.
- Figure 4.31: Uploading the CID file to SEL-487E.
- Figure 4.32: Confirmation screen of the CID file received by SEL-487E.
- Figure 4.33: GOOSE message server confirmation on SEL-487E.

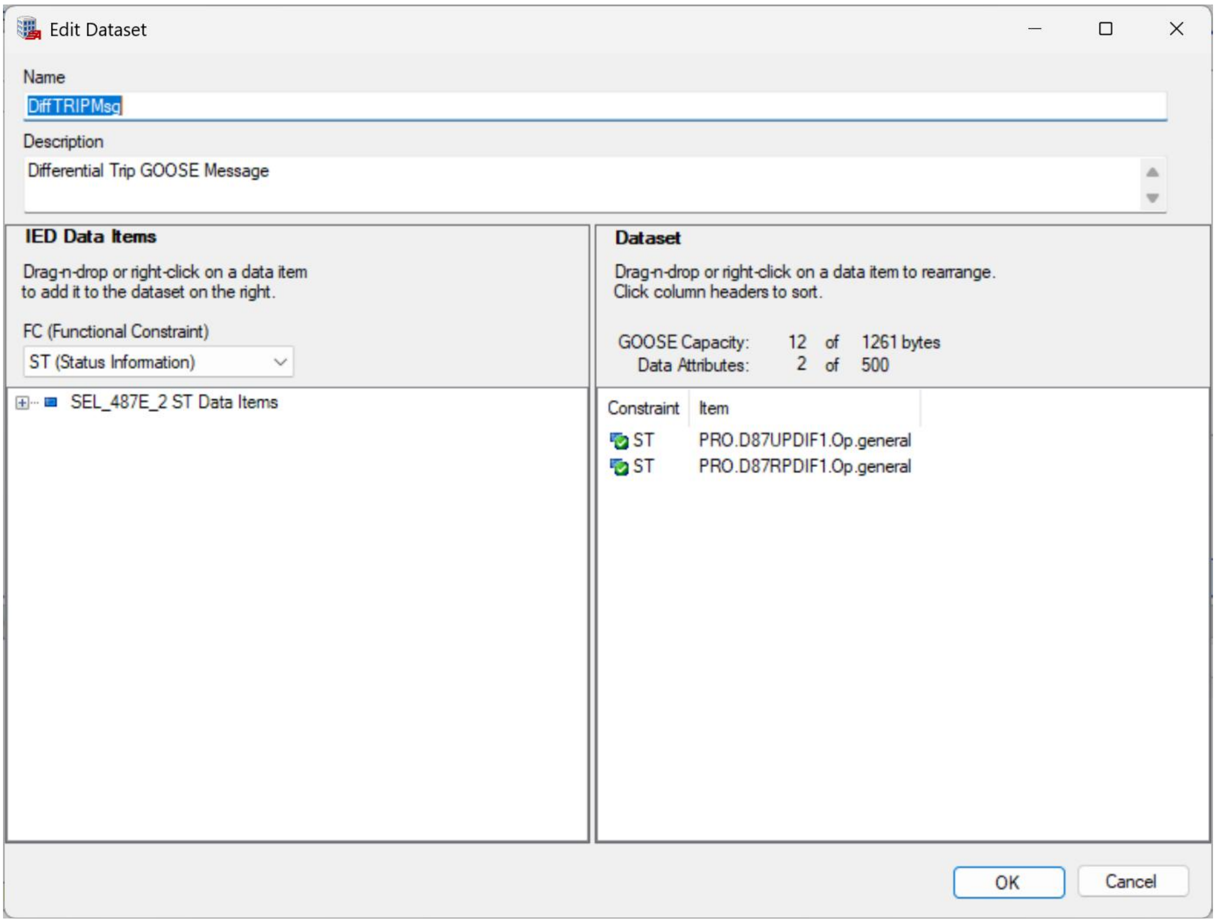

Figure 4.25: Dataset definition screen for SEL-487E

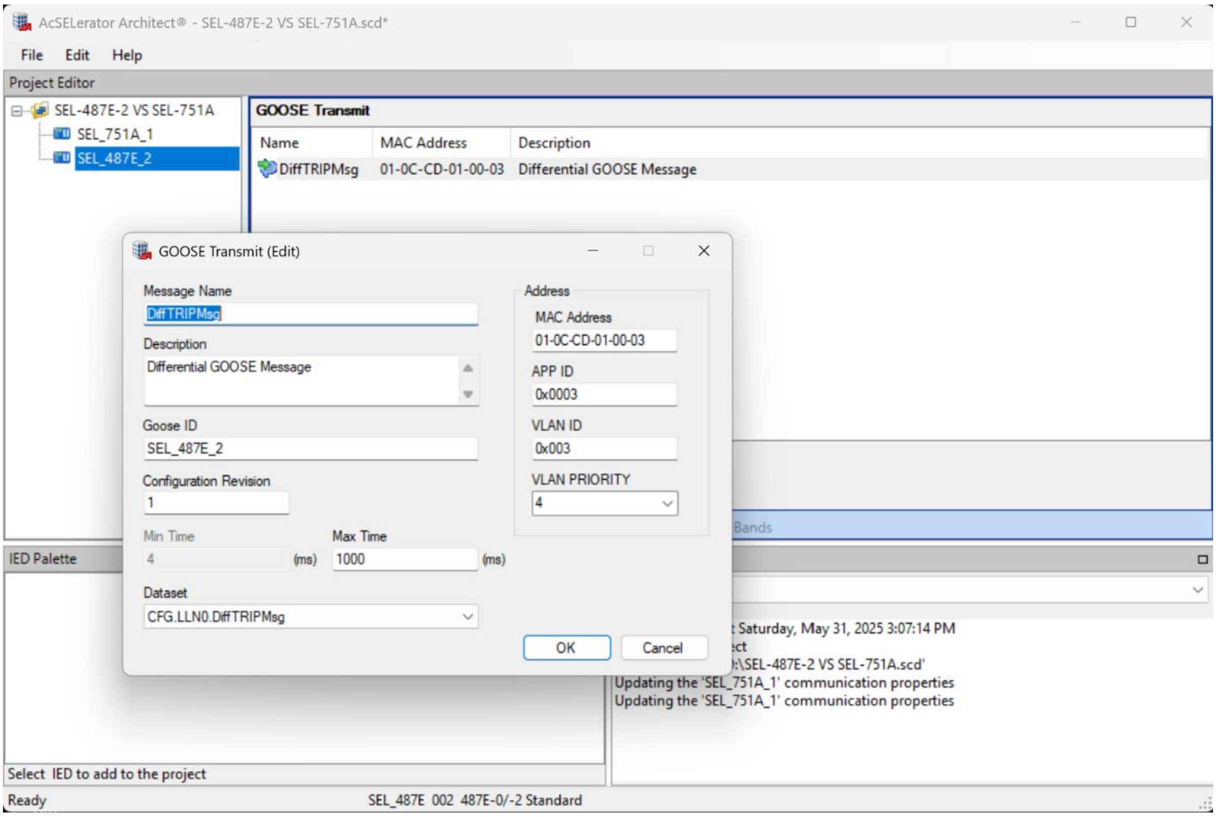

Figure 4.26: Mapping of GOOSE transmission datasets for SEL-487E

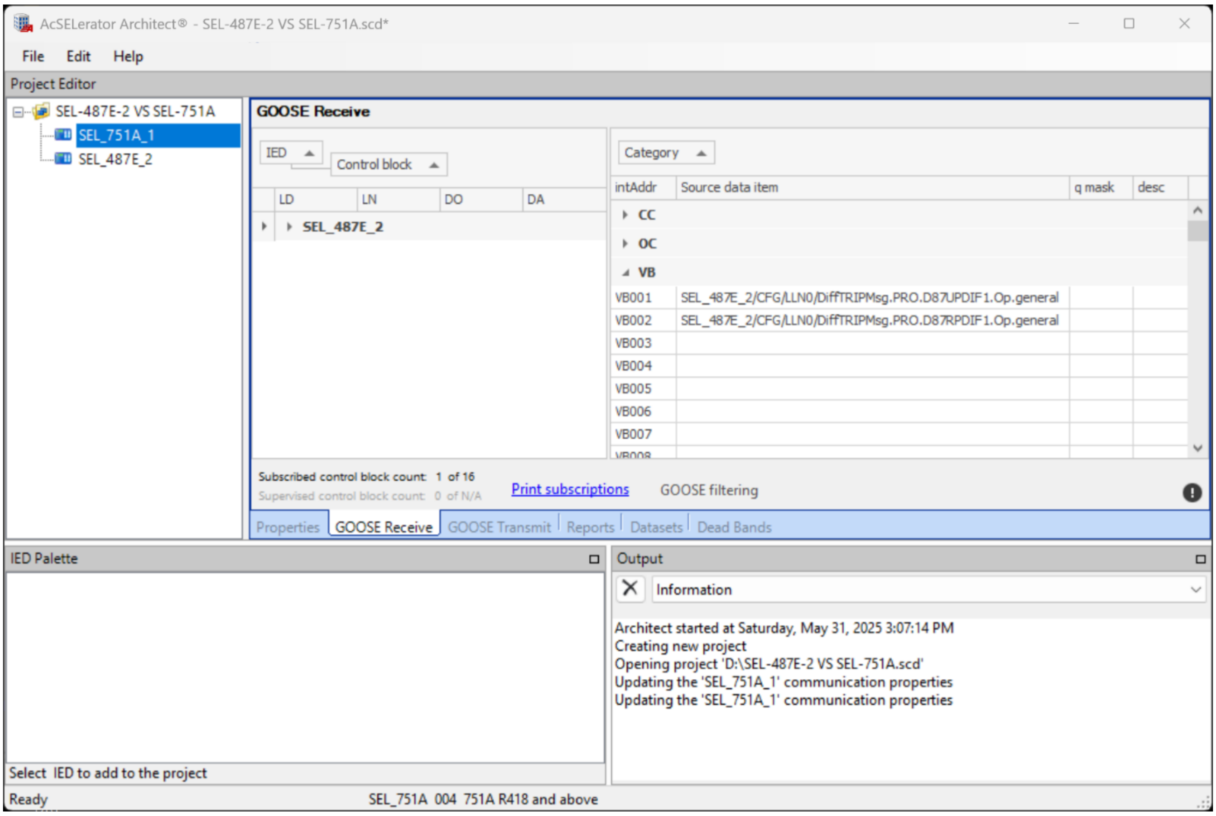

Figure 4.27: Mapped datasets received by SEL-751A relay via VB001 and VB002

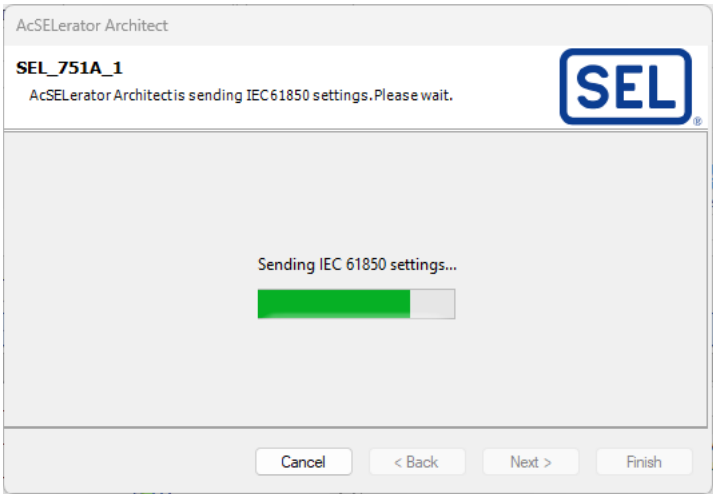

Figure 4.28: **Uploading the configured IED description file to SEL-751A**

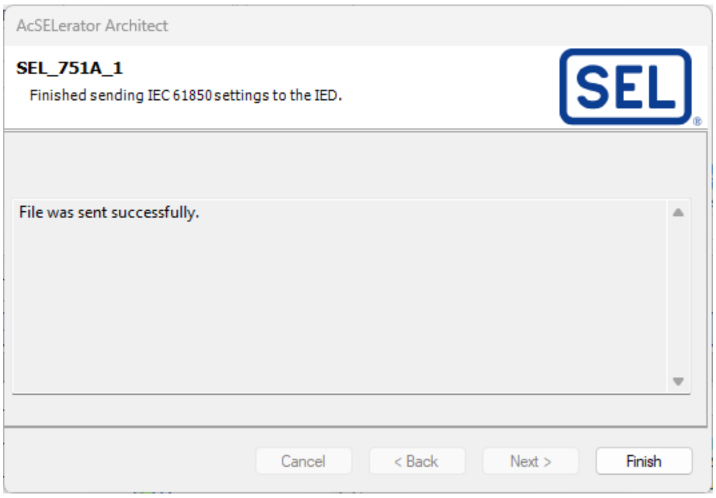

Figure 4.29: **Confirmation screen of the CID file received by SEL-751A**

It is important to highlight that configuring the SEL-751A relay to transmit GOOSE or status messages was not strictly required. However, to verify that its GOOSE functionality was active, messages containing at least one dataset were set up for transmission. This allowed for confirmation of successful online publication. As shown in Figure 4.30, the GOOSE messages observed on the SEL-751A relay served as evidence that its GOOSE capability was functioning correctly.

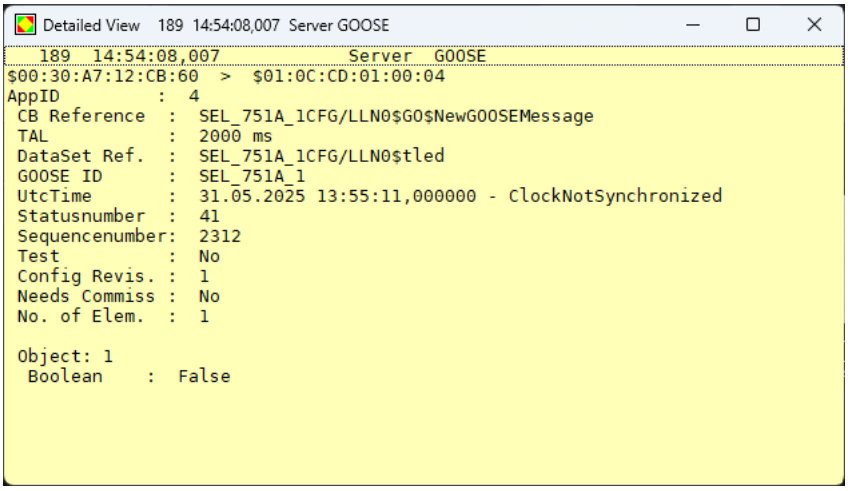

Figure 4.30: GOOSE message status verification on SEL-751A

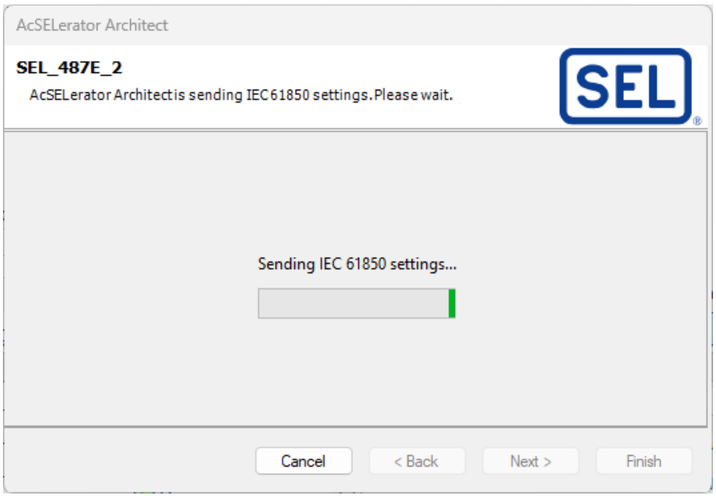

Figure 4.31: Uploading CID file to SEL-487E

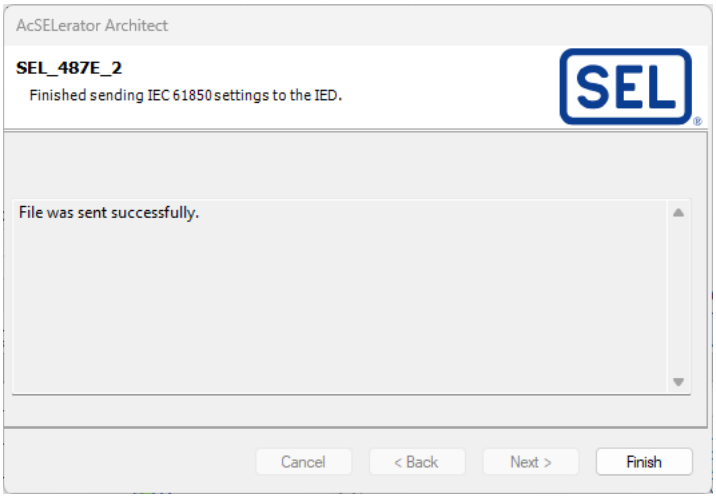

Figure 4.32: Confirmation screen of the CID file received by SEL-487E

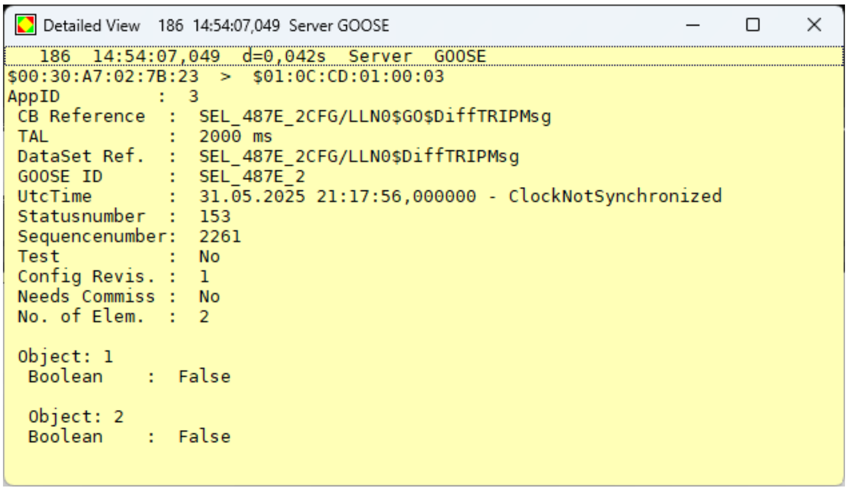

Figure 4.33: **GOOSE message server confirmation on SEL-487E**

These configurations ensured reliable publication and subscription of GOOSE messages, enabling deterministic relay coordination and 3 ms to 4 ms communication latency.

4.6 Functional Testing of SEL-487E and SEL-751A Relays Using Omicron CMC 356

Before proceeding to the case studies in Chapter 5, it was imperative to verify that each protection relay performed as intended under controlled conditions. Functional testing was conducted using the Omicron CMC 356 testing equipment and Test Universe software to simulate fault conditions. These tests aimed to validate the internal logic, element pickup thresholds, and trip response behavior of each relay independently.

This phase ensured that the SEL-487E and SEL-751A relays were correctly configured and operational based on the settings derived in Section 4.3. Importantly, the tests performed here focused on analog signal response and logic operation, while IEC 61850 GOOSE communication was addressed and verified separately in Section 4.5 using GOOSE Inspector.

4.6.1 SEL-487E Station Phasor Measurement Unit

The SEL-487E relay was tested for its differential protection performance. The Omicron CMC 356 was used to inject test currents that mimic both internal and external fault conditions based on transformer full-load values.

Figure 4.34 is the device settings window, and Figure 4.35 is a window showing how the settings for the slope characteristics of the SEL-487E IED from Test Universe.

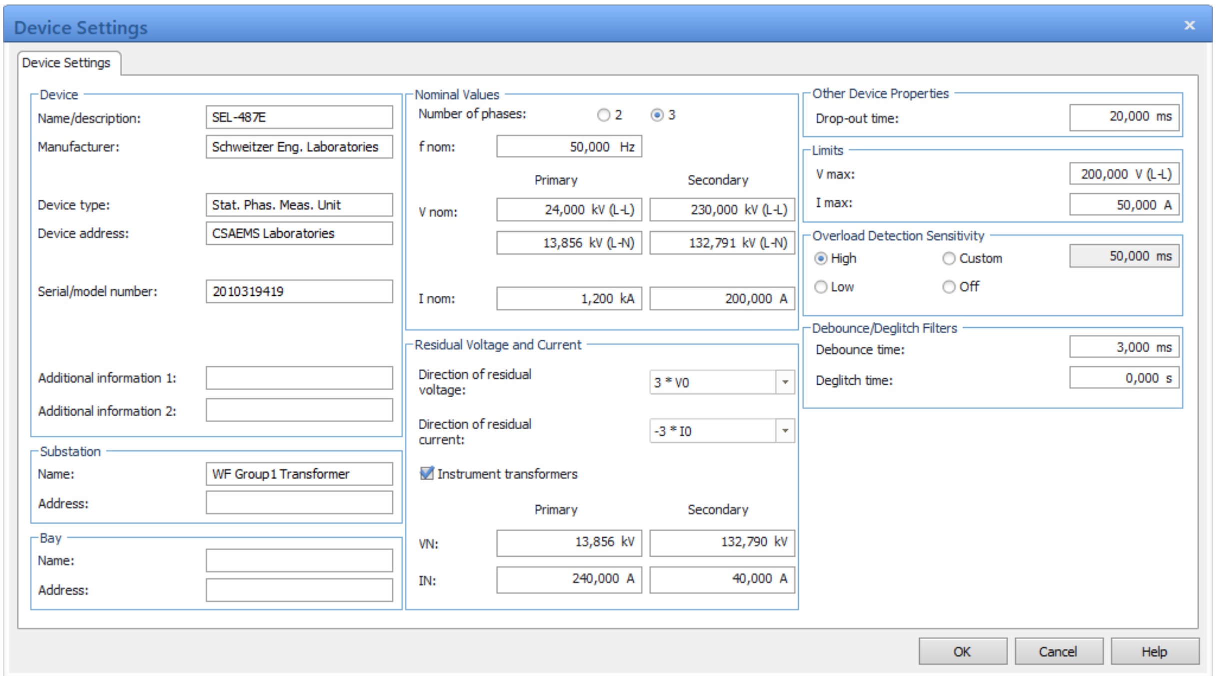

Figure 4.34: **SEL-487E Device settings on Test Universe. Descriptive and numerical data**

Key observations include:

- The relay correctly computed the differential current (I_{Diff}) and restraint current (I_{Rest}).
- It successfully issued trip signals when the differential current exceeded the configured O87P and U87P thresholds.
- The relay remained stable during through-load and external faults, as expected.

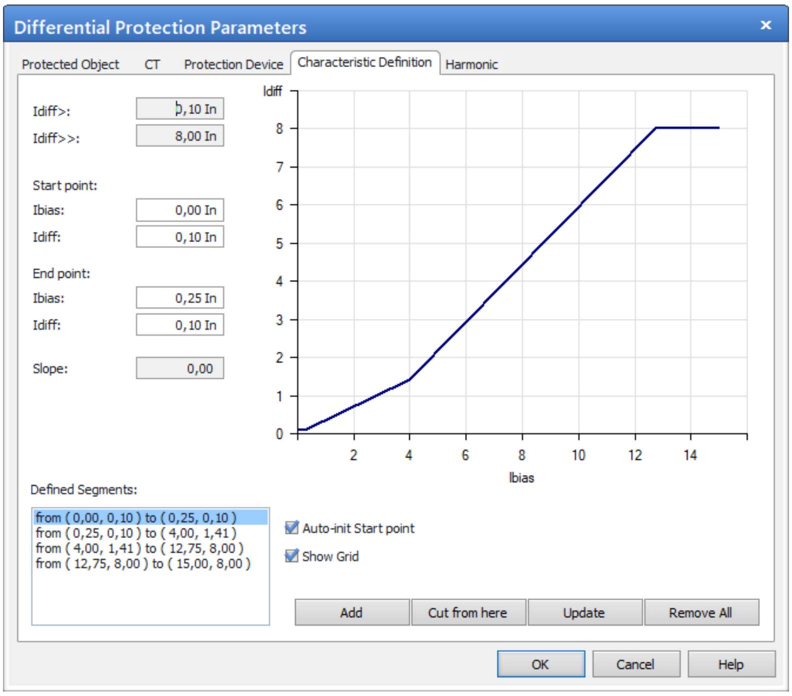

Figure 4.35: **SEL-487E Device settings on Test Universe. Differential protection element configuration and plotting of the coordinates for the characteristic curves**

After the characteristic curves were plotted based on the relay settings, the Test Module was added in Test Universe 5.00 SR, as shown in Figure 4.36. Five testing points were located to test the functionality of the differential elements, as shown in the same figure.

The test was performed for all six points (P1 to P6) as shown in Figure 4.37, and only three points (P1, P2, and P3) caused a relay trip. The other three points (P4, P5, and P6) did not cause any relay trip. P4 was located out of range of the differential pickup settings. P5 and P6 were also put in the restraining region. In the restraining region, the relay is expected not to operate. The results produced from these test points are presented in waveforms in Figures 4.38 to 4.40.

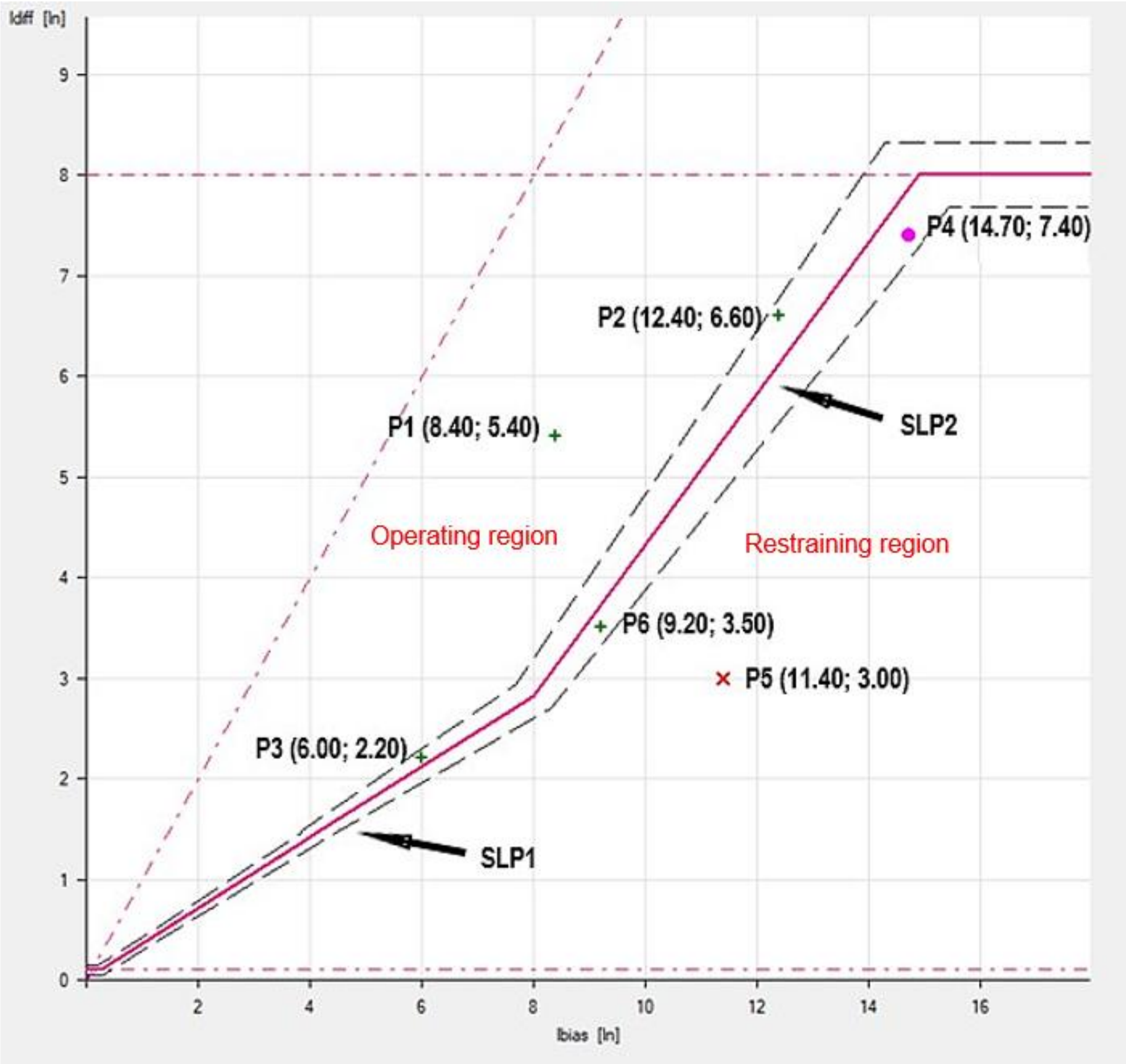

Figure 4.36: **SEL-487E Device resultant characteristic curves on the Test Module**

Test View: Diff Operating Characteristic in Testing of Relays

Shot Test | Search Test | General | Binary Out

Test Points

Idiff	Ibias	tact	tnom	Points
5,40 In	8,40 In	0,025 s	0,03 s	P1
6,60 In	12,40 In	0,027 s	0,03 s	P2
2,20 In	6,00 In	0,025 s	0,03 s	P3
7,40 In	14,70 In	Out of range	N/T	P4
3,00 In	11,40 In	0,025 s	N/T	P5
3,50 In	9,20 In	0,025 s	N/T	P6

Figure 4.37: SEL-487E Device testing. Tested points for operation on the Test Module

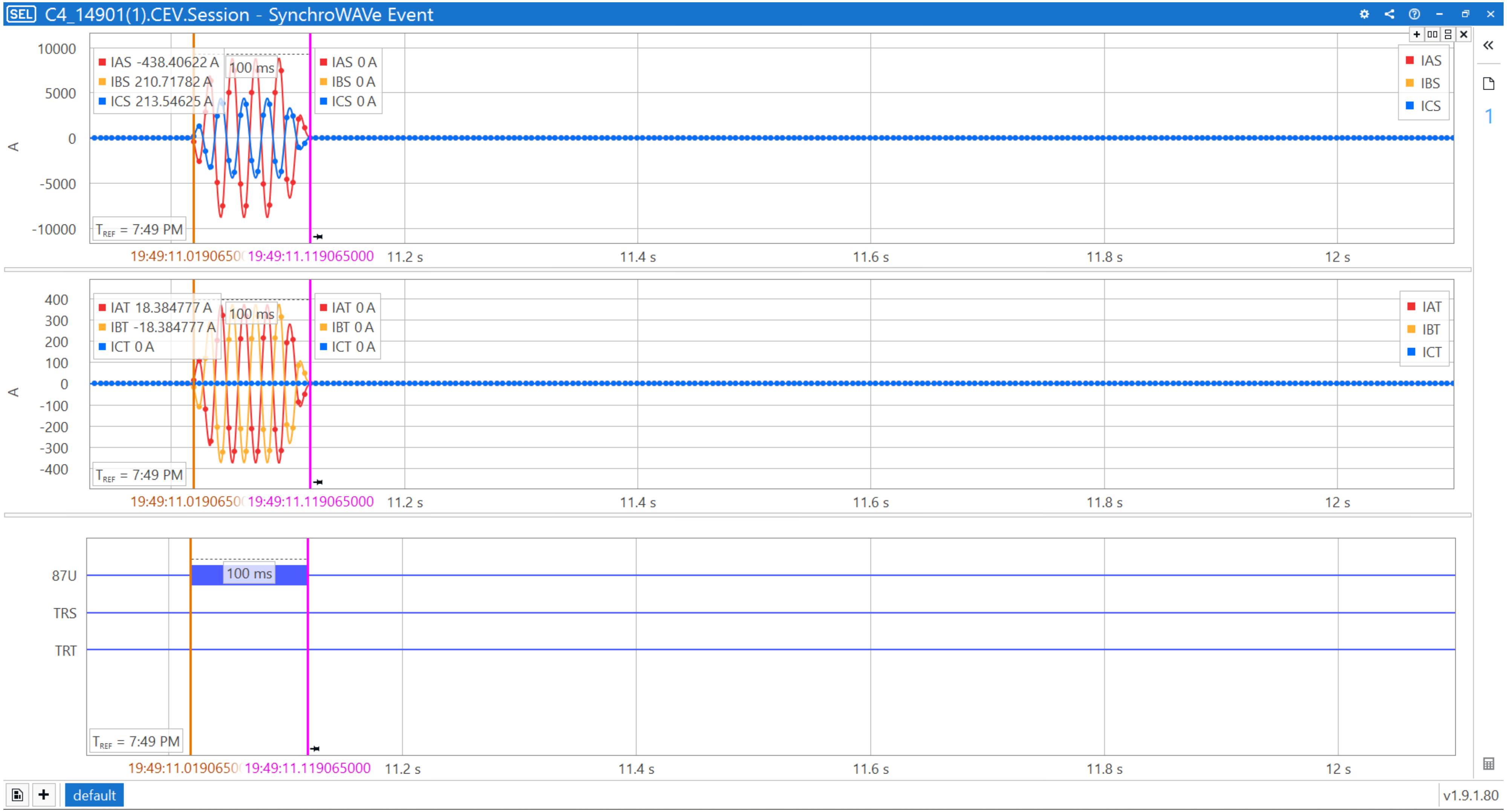

Figure 4.38: Event report waveforms and binary signals extracted from the SEL-487E relay when it tripped for a fault testing point (P1)

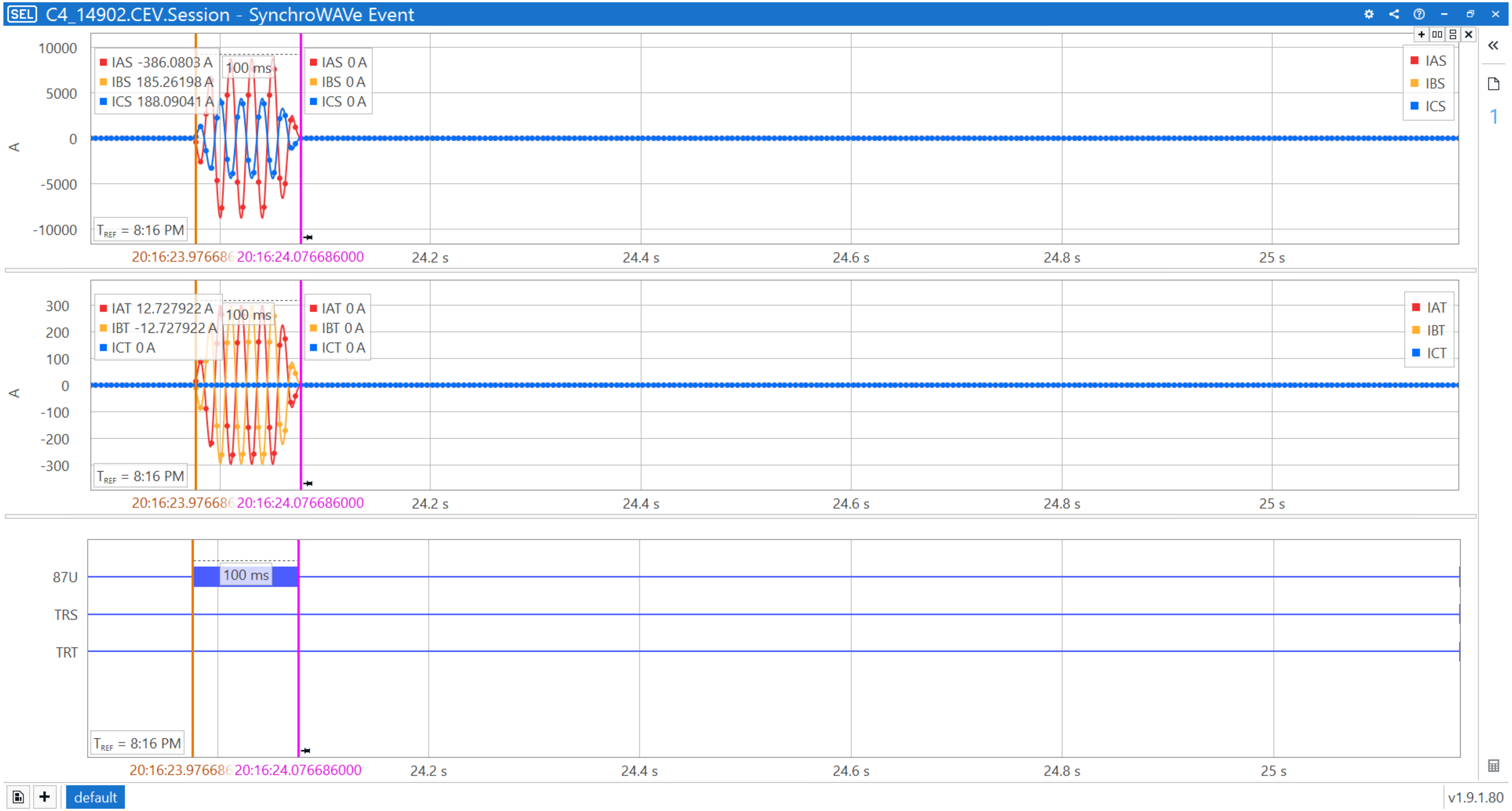

Figure 4.39: Event report waveforms and binary signals extracted from the SEL-487E relay when it tripped for a fault testing point (P2)

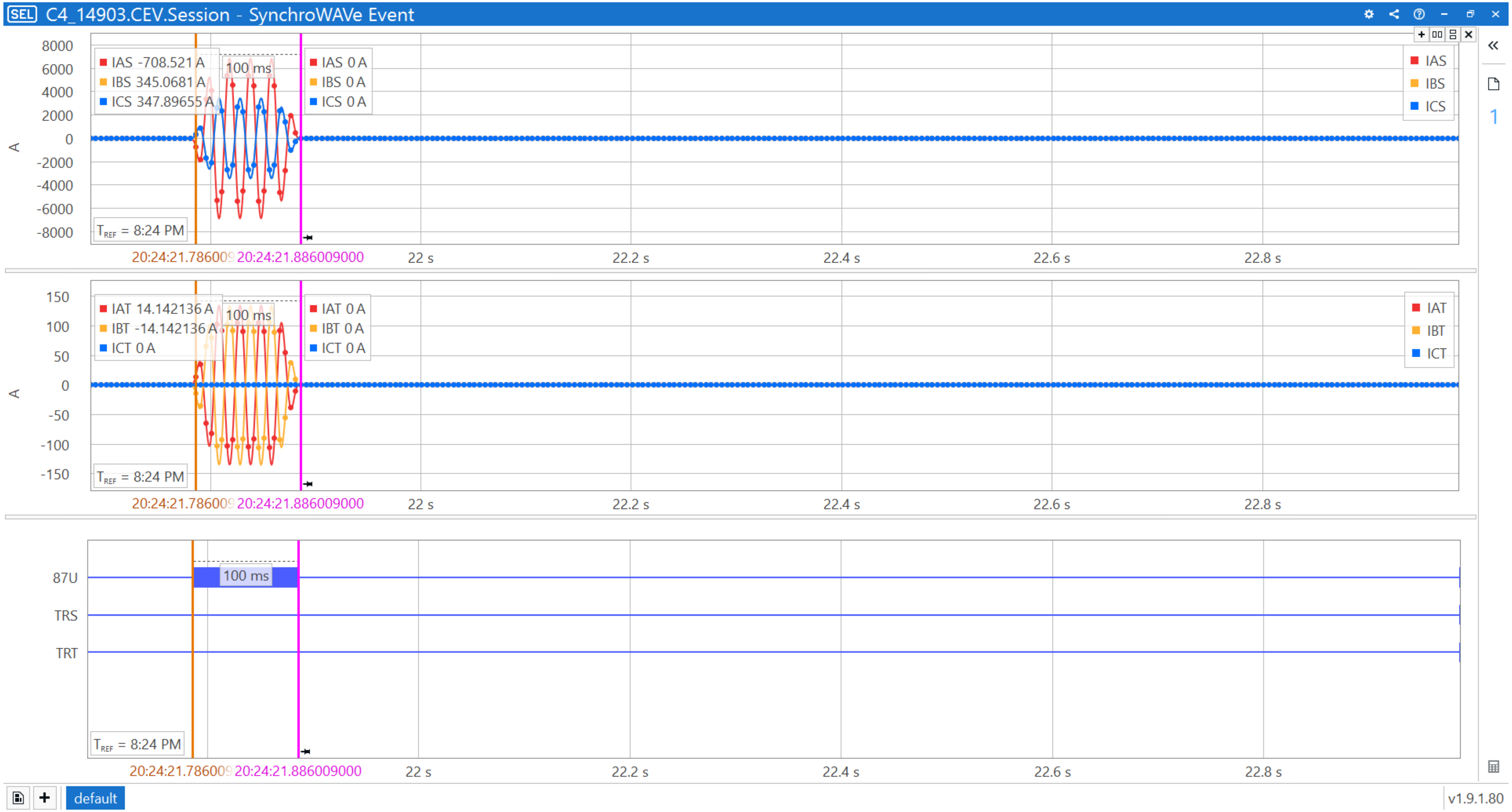

Figure 4.40: Event report waveforms and binary signals extracted from the SEL-487E relay when it tripped for a fault testing point (P3)

4.6.2 SEL-751A Feeder Protection Relay

The SEL-751A feeder protection relay was tested for time-overcurrent protection using the Omicron CMC 356. The tests verified:

- The correct pickup of the 51P1P element at a configured value of 2.5 A.
- The response time of the relay under a standard inverse time characteristic with a Time Multiplier Setting (TMS) of 1.
- Reliable tripping when subjected to fault-level currents exceeding the pickup setting.

The relay operated correctly and issued trip signals based on configured logic, validating the effectiveness of the overcurrent elements as a backup protection.

Figures 4.41 and 4.42 show device settings and the plotted time overcurrent characteristic curve for an SEL-751A IED. The results for this testing are shown in Figures 4.43 and 4.44.

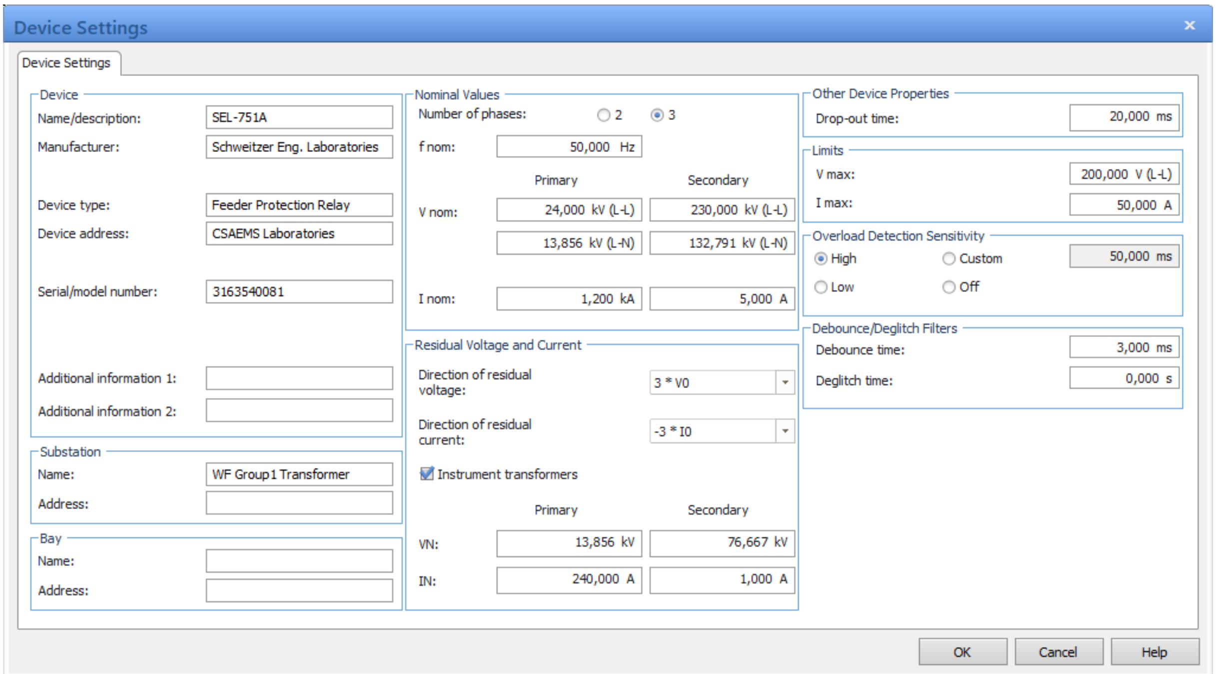

Figure 4.41: SEL-751A Device settings on Test Universe. Descriptive and numerical data

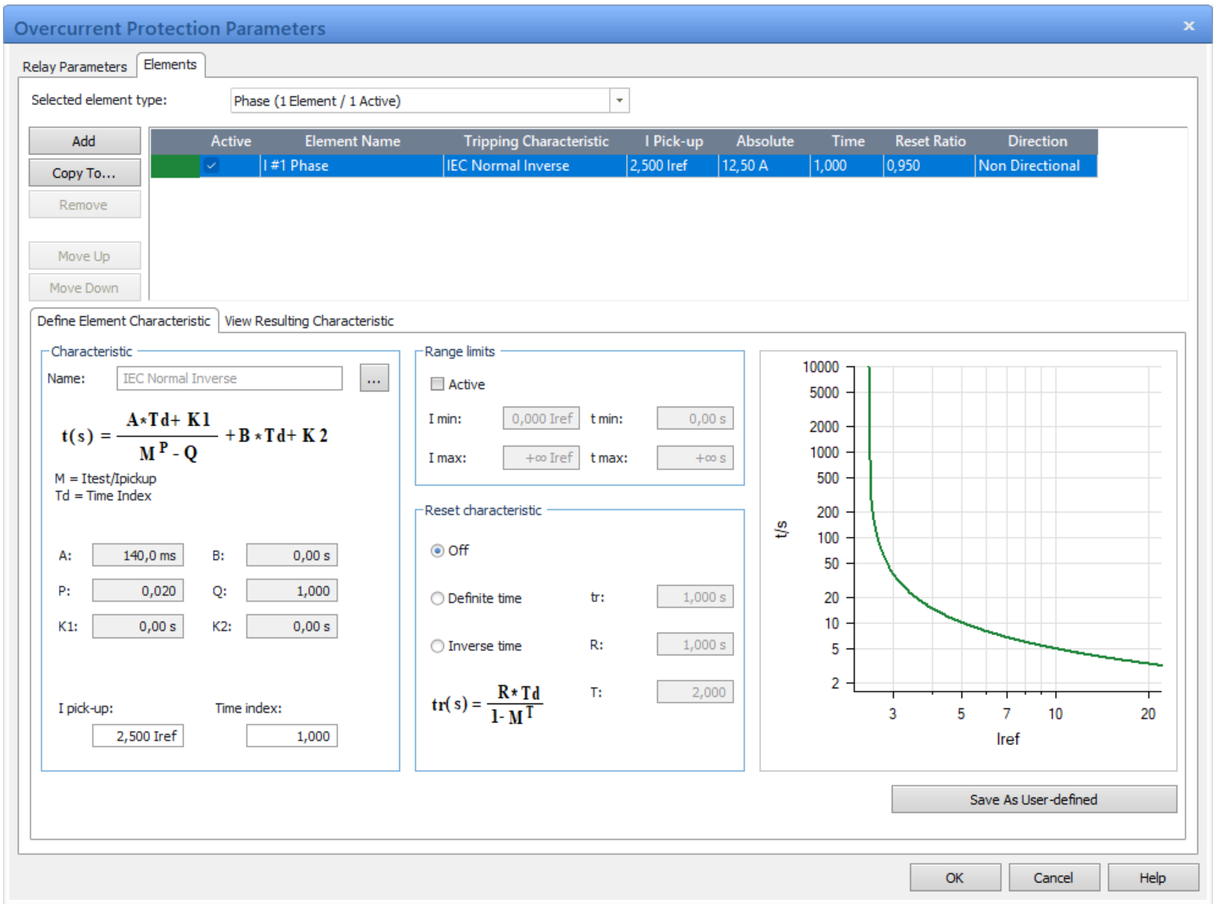

Figure 4.42: SEL-751A Device settings on Test Universe. Overcurrent protection element configuration

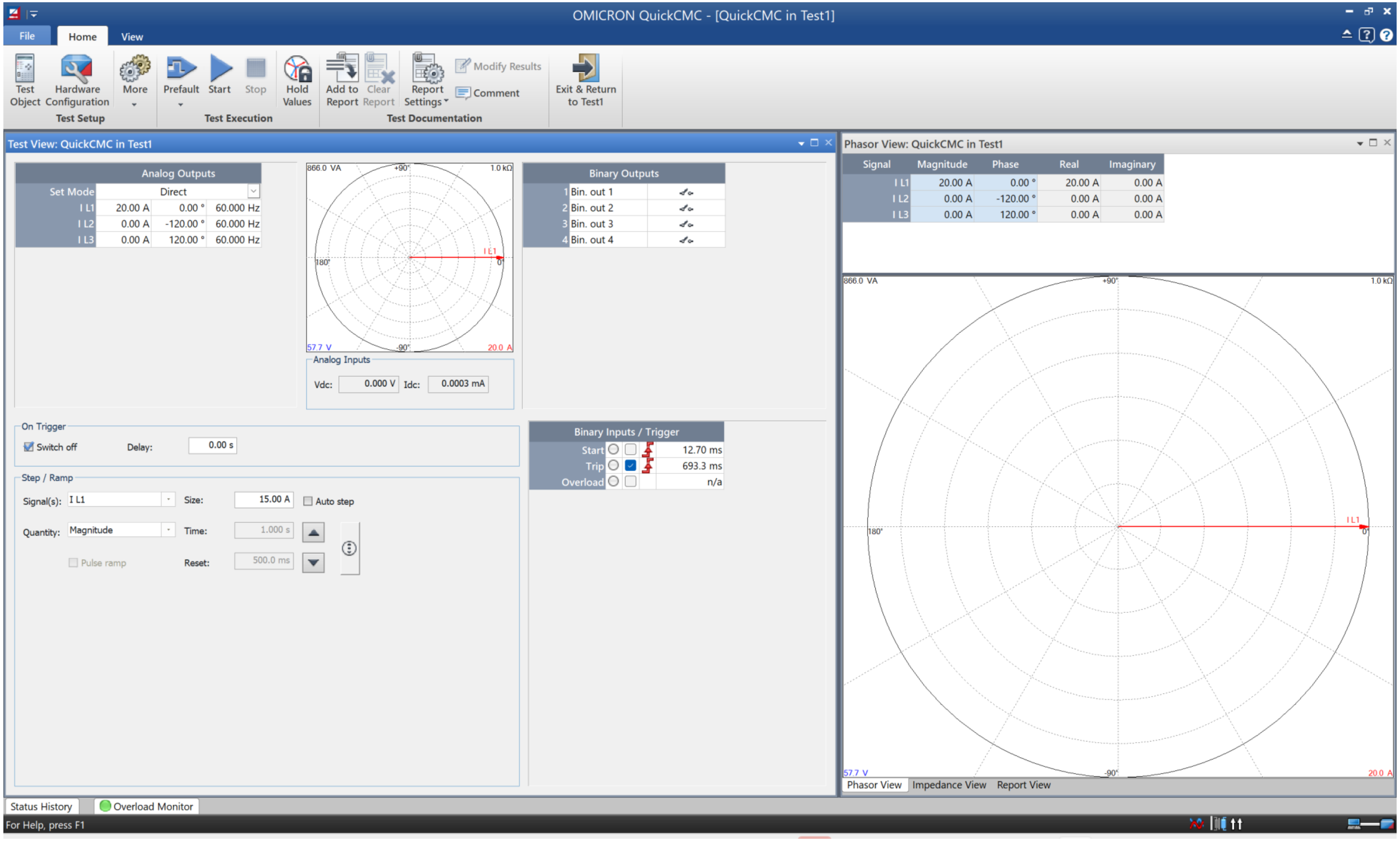

Figure 4.43: SEL-751A Device tuned fault current of 20 amperes on QuickCMC Test Module

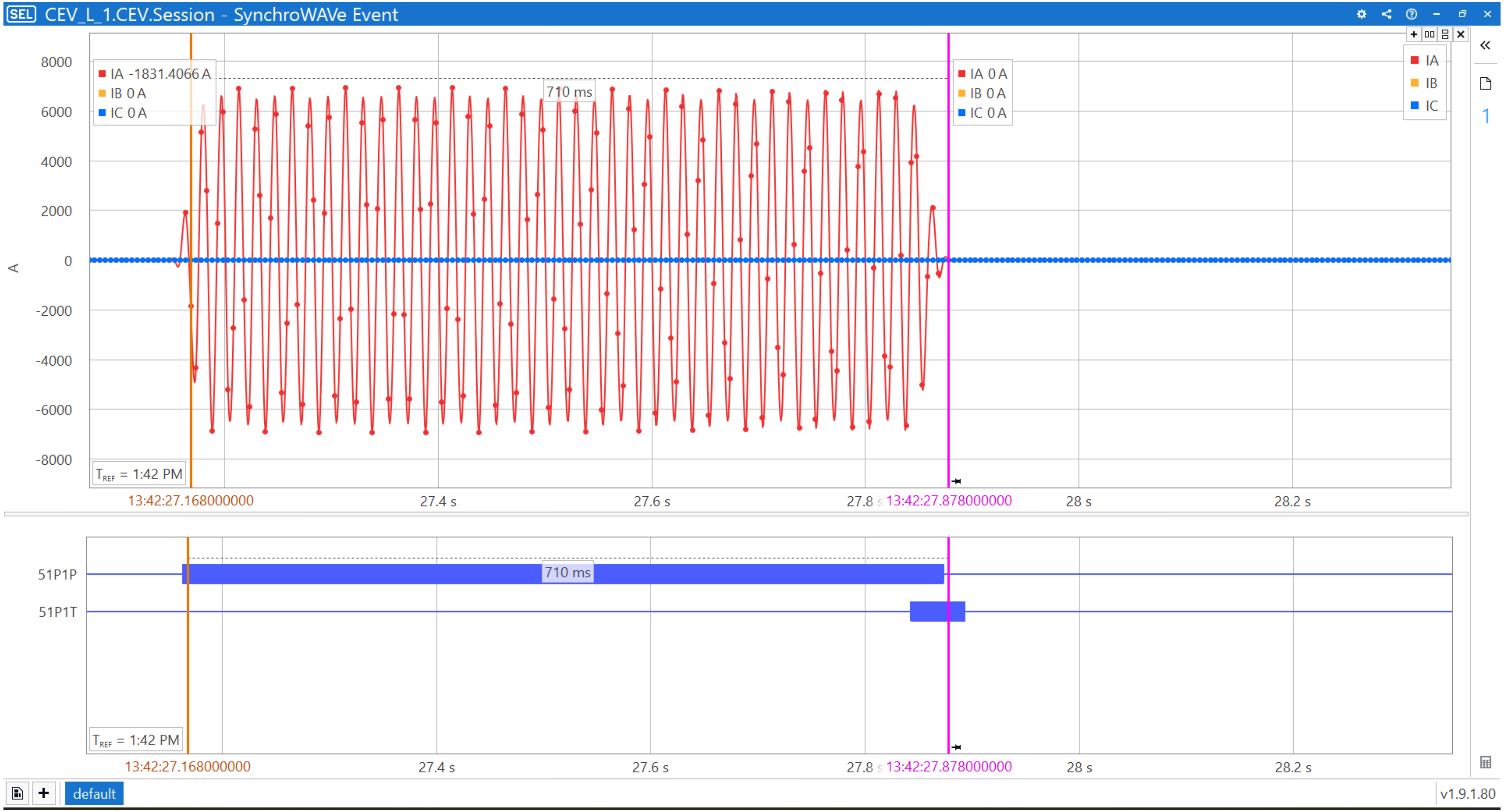

Figure 4.44: Event report waveforms and binary signals extracted from the SEL-751A relay when it tripped for a current magnitude of 15 amperes, exceeding the threshold setting of 2.5 amperes

4.7 Conclusions

The modeling and implementation of a smart grid system integrated with a large-scale wind farm (LSWF), with a focus on protecting the high-voltage (HV) step-up transformer using an IEC 61850-based multi-layered protection scheme, is presented in this chapter.

Key developments and contributions included:

- The integration of the LSWF into the IEEE 9-bus power system, with Bus2 identified as the point of interconnection due to its voltage sensitivity under high load conditions.
- The development of a detailed simulation environment in RSCAD, deployed on the RTDS platform, utilizing five subsystems to represent wind turbine generator clusters and conventional grid zones.
- Implementation of primary protection using the SEL-487E relay, configured for transformer differential protection with harmonic blocking, dual-slope restraint characteristics, and accurately calculated threshold settings.
- Deployment of the SEL-751A relay for backup overcurrent protection, configured with an inverse-time characteristic and coordinated delay to operate only in the event of primary protection failure.
- Modeling of realistic instrument transformers and circuit breakers in the RTDS, with analog signals interfaced to the physical relays via GTAO modules, enabling high-fidelity hardware-in-the-loop (HIL) testing.
- Functional testing of the SEL-487E and SEL-751A relays using the Omicron CMC 356 test set. The SEL-487E was validated under simulated internal and external fault conditions to confirm accurate differential element performance. The SEL-751A was tested for correct operation of its time-overcurrent element, with results confirming proper pickup, delay, and tripping behavior in accordance with configured settings.
- Establishment of IEC 61850 communication between relays using GOOSE messaging, with logical nodes and virtual bits mapped using AcSELerator Architect. While IEC 61850 communication was verified using GOOSE Inspector in Section 4.5, it was not part of the functional testing conducted in Section 4.6.

Overall, the chapter has demonstrated the practical implementation of a coordinated protection framework that combines real-time simulation, digital relays, and standardized communication protocols. The validated protection system offers both reliability and redundancy, which are essential for safeguarding critical assets such as

HV transformers in smart grid environments incorporating variable renewable energy sources.

In the next chapter, simulation and HIL test results will verify the responsiveness, selectivity, and communication performance of the protection scheme under various fault scenarios.

CHAPTER FIVE
TESTING, RESULTS, AND ANALYSIS

This chapter presents and interprets the results obtained from both real-time simulations and hardware-in-the-loop (HIL) testing of the proposed IEC 61850-based multi-layered protection scheme for a high-voltage (HV) step-up transformer in a smart grid integrated with a large-scale wind farm (LSWF). The effectiveness of the SEL-487E (primary) and SEL-751A (backup) relays in detecting and isolating fault conditions is analyzed.

5.1. Simulation and Testing Overview

Two types of fault scenarios were simulated:

- Successful operation of the primary protection relay (SEL-487E).
- Failure of the SEL-487E to trip due to auxiliary malfunction, activating the backup relay (SEL-751A).

These tests validated the fault detection, coordination, and communication capabilities of the implemented scheme under dynamic conditions.

5.2. Fault Scenario 1: Successful Operation of the SEL-487E Relay

Figures 5.1 and 5.2 show the primary (MV) and secondary (HV) current (ampere) waveforms captured from RSCAD Runtime when an internal fault was simulated for the protected transformer (Group1Trans). Figures 5.3 and 5.4 show the event report waveforms and binary signals when an internal fault occurred. This is when the SEL-487E successfully issued a trip signal.

Key observations:

- The differential current exceeded both restrained and unrestrained thresholds.
- The IED issued a trip within milliseconds.
- The virtual circuit breaker in RSCAD FX opened upon receiving the trip signal.
- GOOSE communication between relays was activated to block the backup relay from operating.

Performance Summary:

- Breaker Operation: Successful
- GOOSE Communication: Idle (when backup is not required)
- Detection by SEL-487E: Yes. The fault got cleared at 135 ms after detection.

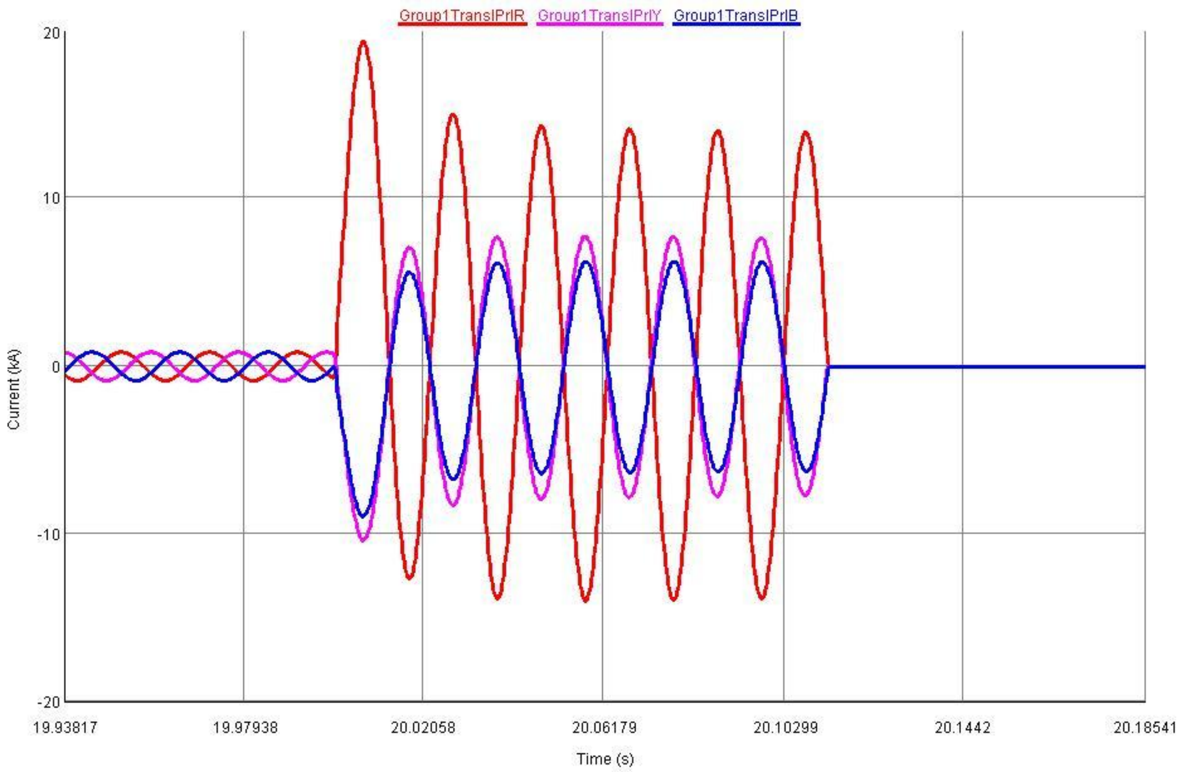

Figure 5.1: **RSCAD Runtime waveforms recorded from the primary side (MV) of the protected transformer (Group1Trans) when the SEL-487E relay successfully issued a trip signal to the circuit breaker for an internal fault**

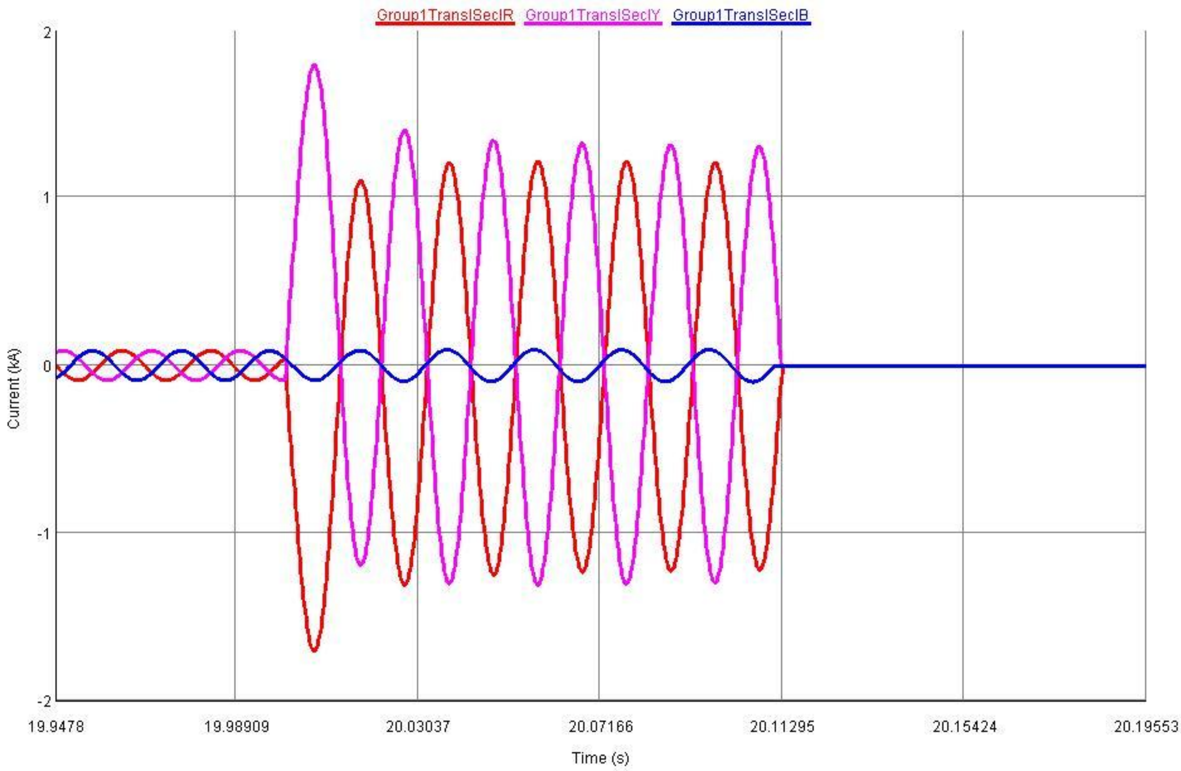

Figure 5.2: **RSCAD Runtime waveforms recorded from the secondary side (HV) of the protected transformer (Group1Trans) when the SEL-487E relay successfully issued a trip signal to the circuit breaker for an internal fault**

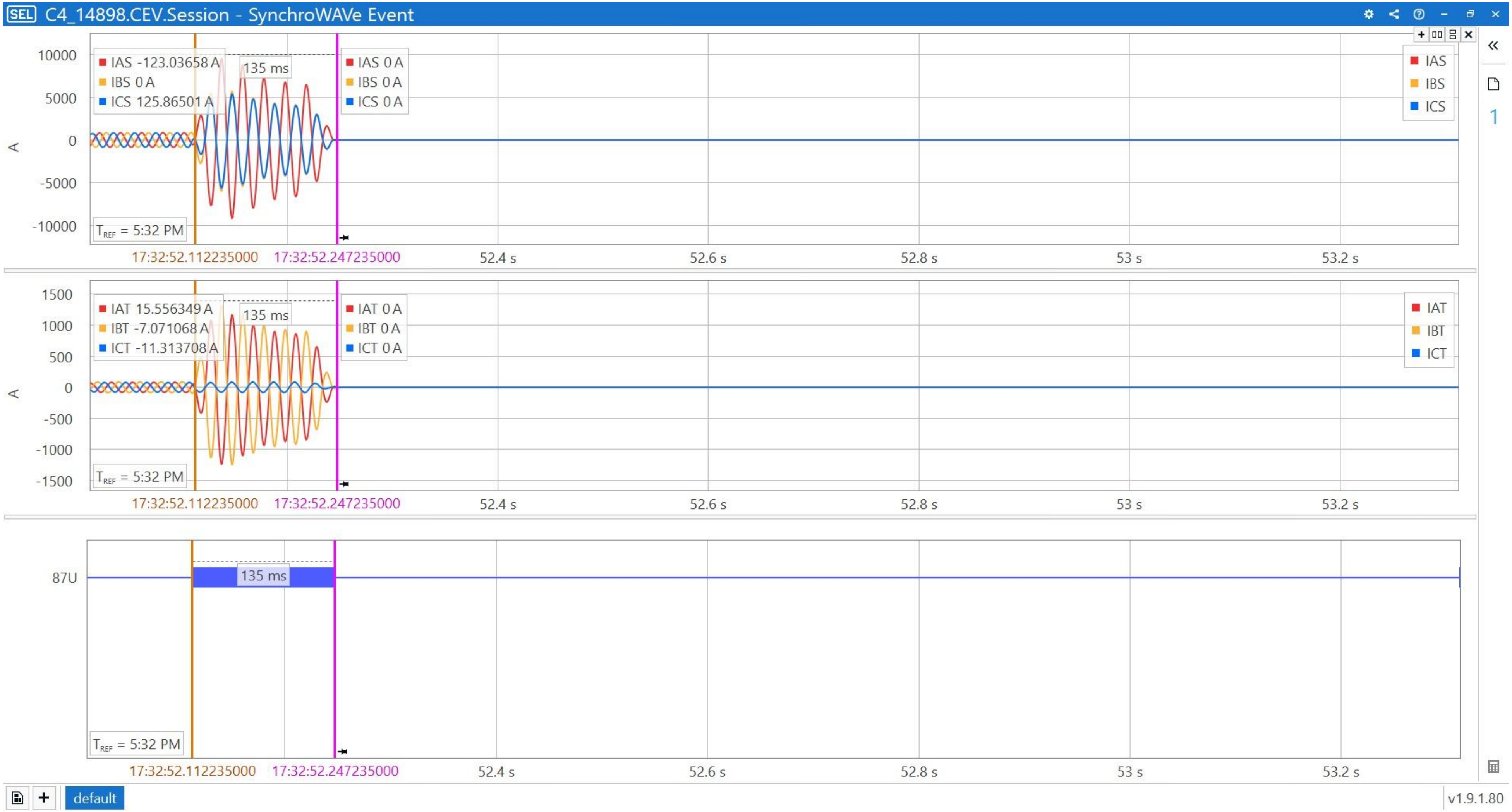

Figure 5.3: Event report waveforms and binary signals extracted from the SEL-487E relay when it successfully issued a trip signal to the circuit breaker for an internal fault

Figure 5.4: **Event report waveforms and binary signals extracted from the SEL-751A relay when the SEL-487E relay successfully issued a trip signal to the circuit breaker for an internal fault**

5.3. Fault Scenario 2: SEL-487E Detects Fault but Fails to Trip

Figures 5.5 and 5.6 show the primary (MV) and secondary (HV) current (ampere) waveforms captured from RSCAD Runtime when an internal fault was simulated for the protected transformer (Group1Trans).

Figures 5.7, 5.8, and 5.9 show the event report waveforms and binary signals when an internal fault occurred, and the SEL-487E failed to issue a trip signal. This is the case when the fault was correctly detected by both the SEL-487E and SEL-751A relays, but the trip command fails to actuate the circuit breaker due to an issue in the auxiliary circuits of the circuit breaker (CB). At this point, the SEL-751A (back-up) waited till the counting time elapsed, and then issued a trip signal to clear the fault.

Key Observations:

- The SEL-487E internally registers a trip event.
- No actual breaker operation occurred due to breaker failure.
- The SEL-751A backup relay is not receiving the GOOSE blocking signal (VB001 or VB002). It, therefore, operates based on its operating settings.
- The fault was cleared by the SEL-751A relay, validating the backup logic.

Performance Summary:

- Detection by SEL-487E: Yes
- Breaker Trip Failure: Confirmed
- Backup Relay Operation: 1.187 s + 243.408 ms = 1.4304 s
- GOOSE Torque Block: Not asserted (due to trip failure)
- Fault Clearance: Successful by SEL-751A

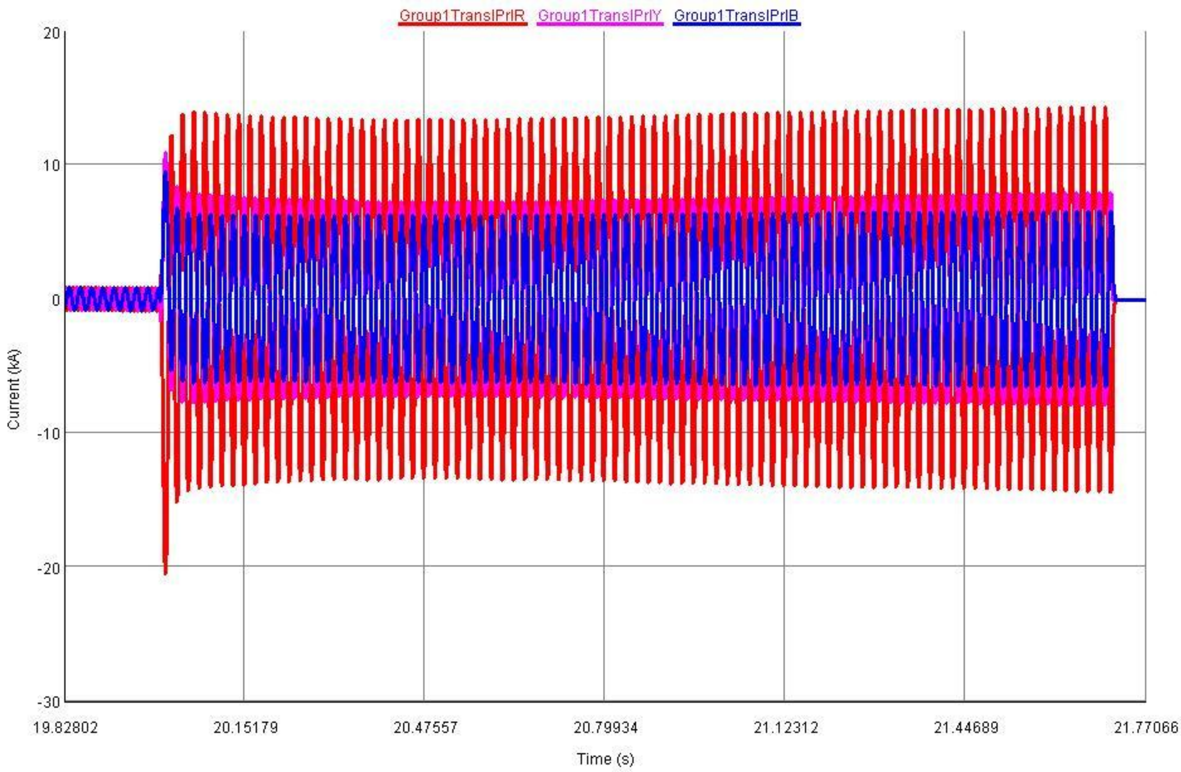

Figure 5.5: **RSCAD Runtime waveforms recorded from the primary side (HV) of the protected transformer (Group1Trans) when the SEL-487E relay failed to issue a trip signal to the circuit breaker for an internal fault**

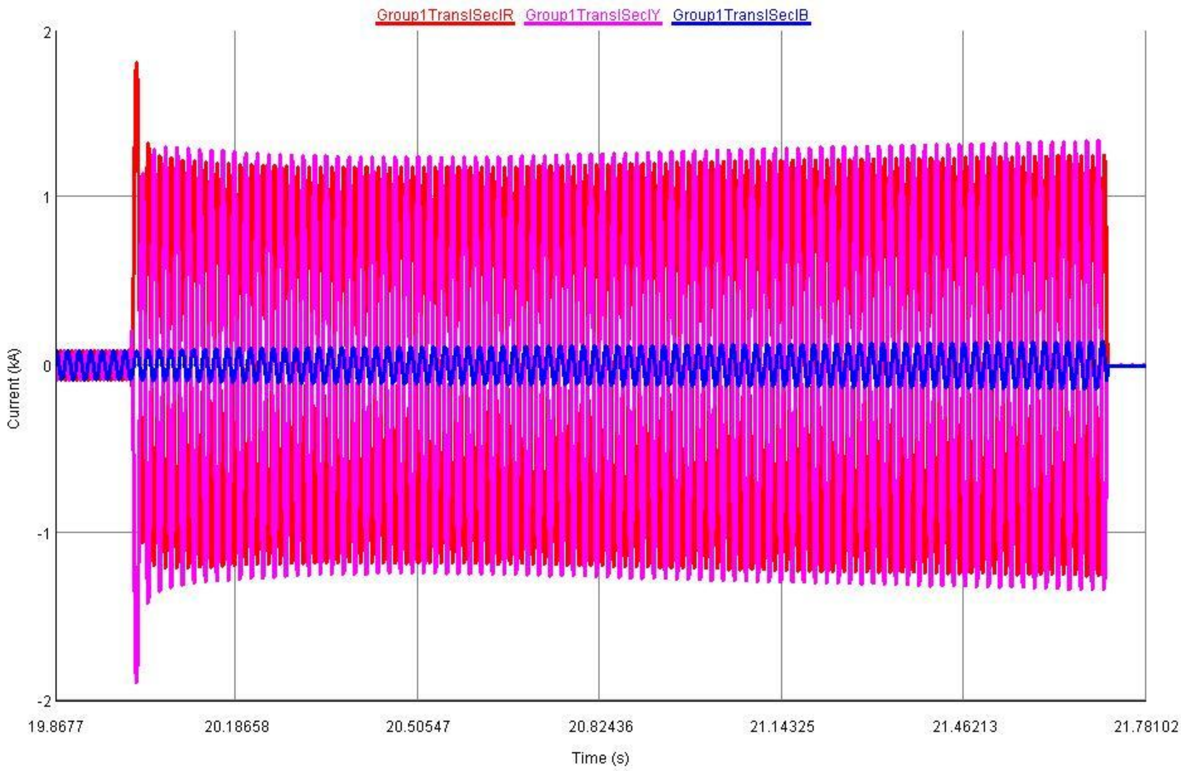

Figure 5.6: **RSCAD Runtime waveforms recorded from the secondary side (HV) of the protected transformer (Group1Trans) when the SEL-487E relay failed to issue a trip signal to the circuit breaker for an internal fault**

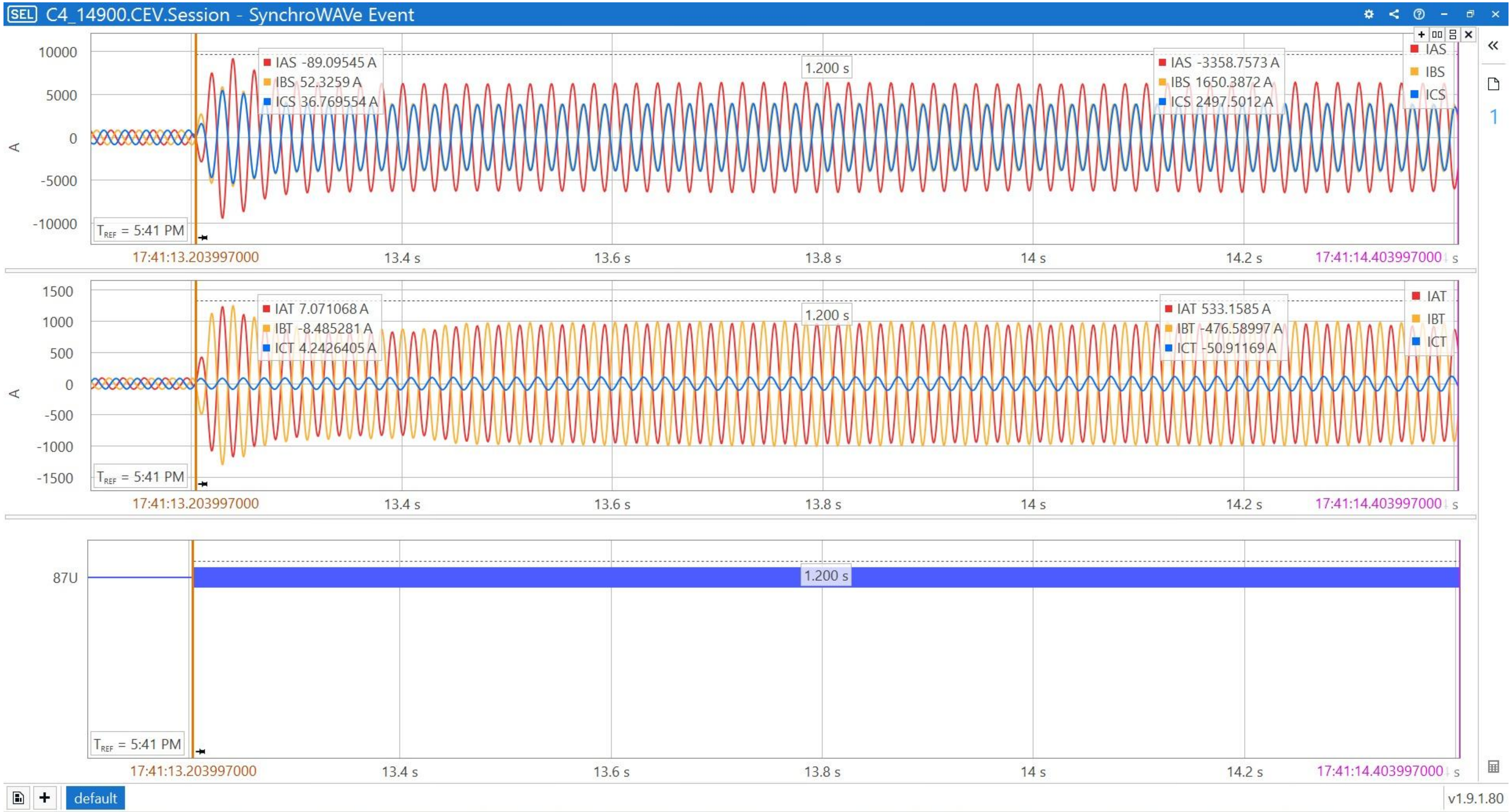

Figure 5.7: Event report waveforms and binary signals extracted from the SEL-487E relay when it failed to issue a trip signal to the circuit breaker for an internal fault

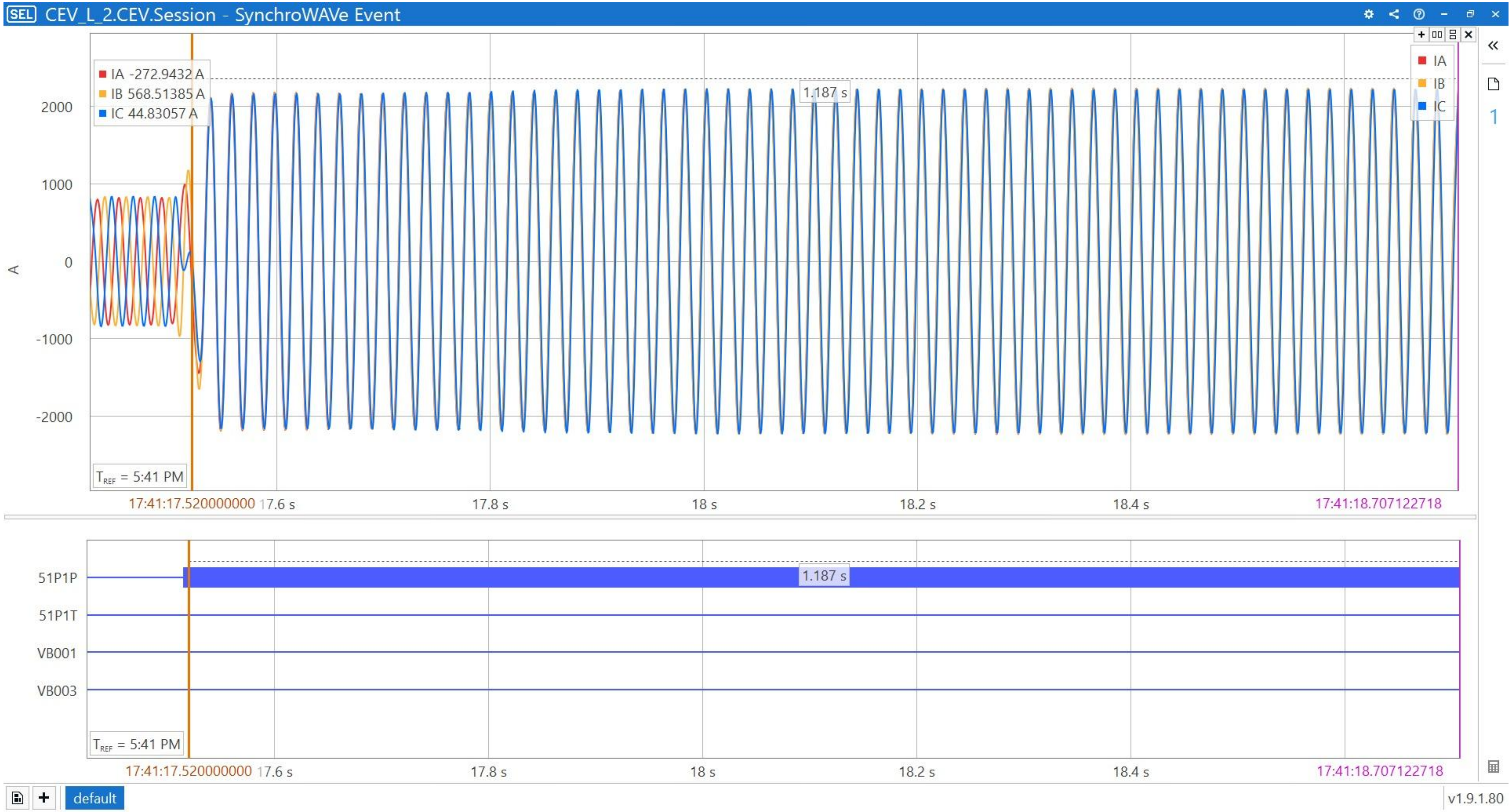

Figure 5.8: Path a). Event report waveforms and binary signals extracted from the SEL-751A relay when the SEL-487E failed to issue a trip signal to the circuit breaker for an internal fault

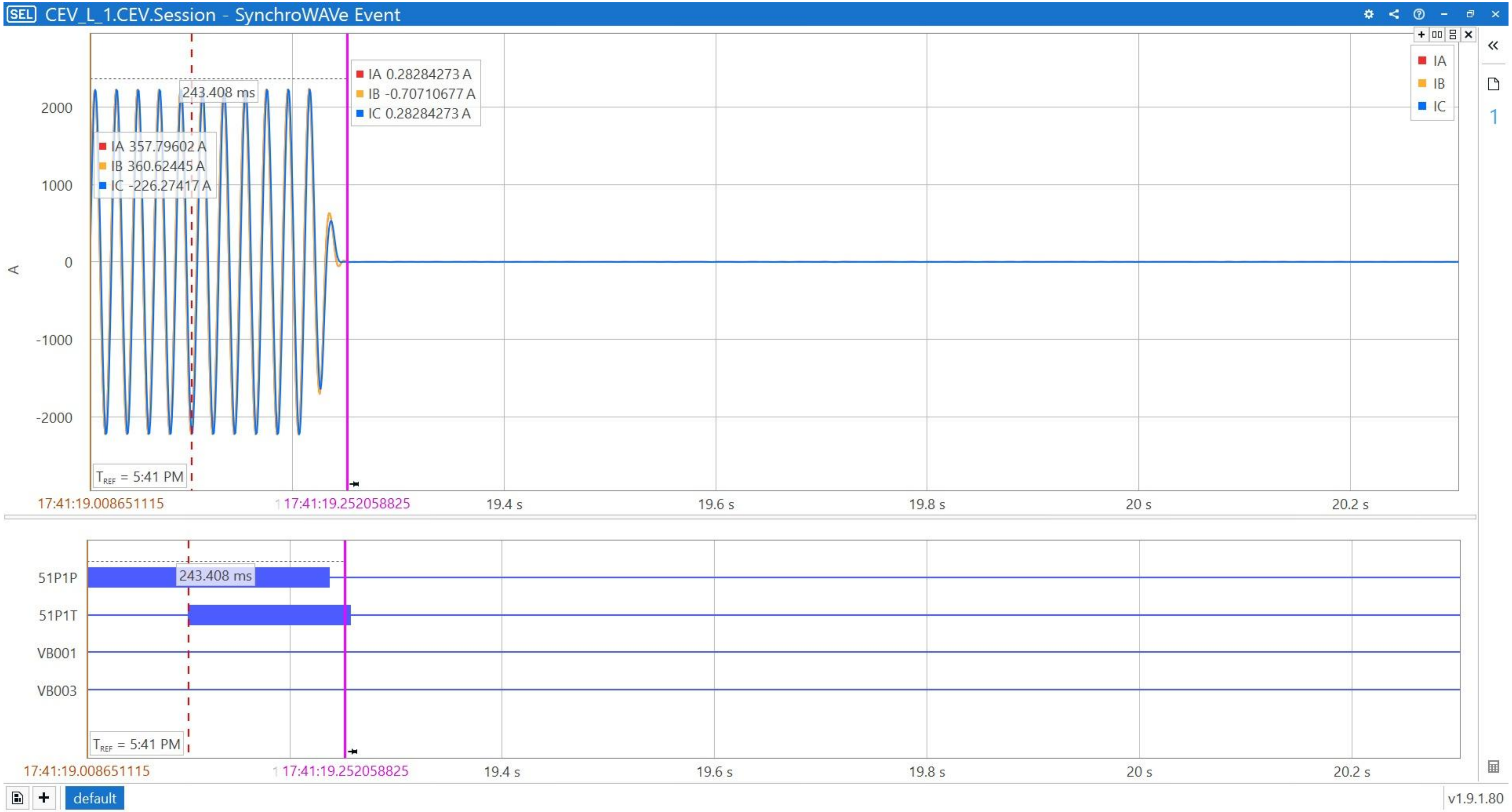

Figure 5.9: Path b). Event report waveforms and binary signals extracted from the SEL-751A relay when the SEL-487E failed to issue a trip signal to the circuit breaker for an internal fault

5.4. Communication and Coordination Performance

Relay Coordination:

- Differential and overcurrent thresholds were set with proper timing offsets to ensure selectivity.
- Torque blocking via GOOSE virtual bits (VB001 and VB002) effectively prevented redundant trips in the backup relay during the primary operation.

IEC 61850 GOOSE Messaging:

- The expected time was maintained within 3 ms – 4 ms.
- The publication and subscription of datasets were successful.
- The backup logic operated as expected.

To evaluate the performance advantage of the proposed IEC 61850-based coordinated protection framework, its quantitative results were benchmarked against conventional protection methods documented in the literature.

Under identical transformer-zone fault conditions, the developed scheme achieved a main differential relay (SEL-487E) fault-clearance time of 135 ms, while the backup overcurrent relay (SEL-751A) operated at 1.4304 s when the main relay failed to trip.

In contrast, conventional transformer protection techniques, such as impedance-based distance protection or standalone differential protection operating without IEC 61850 communication, typically report overall clearing times between 1.2 s and 1.5 s under comparable conditions (George & Ashok, 2018; Ma et al., 2018). When compared numerically, the proposed architecture yields an excellent reduction in clearance time, demonstrating significant improvement in speed and coordination.

The improvement is attributed to (i) the elimination of hard-wired signaling delays by replacing them with GOOSE-based logical communications, (ii) the optimized grading interval of ≈ 100 ms between main and backup protection actions, ensuring proper selectivity, and (iii) the real-time validation through HIL testing that confirmed deterministic relay performance. These quantitative comparisons verify that the proposed IEC 61850-enabled protection framework substantially enhances operating speed, dependability, and coordination relative to conventional protection schemes.

Table 5.1 further summarises the results that were discussed in the previous sections.

Table 5.1: Summarised results

Scenario	Active relay	Trip success	Backup required	Fault cleared	Fault clearance time
SEL-487E Trip Success	SEL-487E	Yes	No	Yes	~135 ms
SEL-487E Trip Failure (Breaker Fault)	SEL-751A	No	Yes	Yes	~1.4304 s

5.5. Conclusions

The effectiveness of the proposed and developed IEC 61850 standard-based multilayered protection scheme is demonstrated in the results presented in this chapter. When the protection scheme was tested under both normal and faulty conditions, the protection system still maintained its reliability in communication, detection of faults, and coordination. Both Intelligent Electronic Devices (IEDs) fulfilled their duties in terms of detecting and isolating the faults when called upon.

The use of the IEC 61850 standard GOOSE messaging enabled fast, effective communication between protection IEDs SEL-487E and SEL-751A. This ensured the reliable coordination through the developed logic. The hardware-in-the-loop (HIL) test using RTDS/RSCAD FX, with the aid of Omicron CMS devices, provided a reliable platform for validating the performance of the protection scheme under realistic electrical power grid conditions. Communication delays observed were minimal and consistent with the requirements of high-speed substation protection standards.

The results obtained during the tests confirm that the integrated protection framework is both robust and responsive, capable of maintaining grid stability and ensuring transformer reliability even under failure scenarios. These findings support the viability of IEC 61850-based architectures for modern protection applications, particularly in systems where renewable energy sources introduce dynamic and complex operational challenges.

CHAPTER SIX
CONCLUSIONS AND RECOMMENDATIONS

6.1. Summary of Findings

The aim of the study presented in this thesis was to design, implement, and validate an IEC 61850 standard-based multi-layered protection scheme for high-voltage (HV) step-up transformers for a smart grid consisting of a large-scale wind farm (LSWF). It has been revealed through the findings that the proposed protection scheme, combining the transformer differential protection relay SEL-487E and its backup overcurrent relay SEL-751A, operates effectively under both ideal and faulted conditions.

The primary protection relay SEL-487E demonstrated some reliability by detecting the internal faults and issuing a response to trigger the circuit breakers connected to it. The protection scheme has also been tested in a failure-to-trip scenario where the auxiliary connections to the circuit breakers (CBs) are faulty. The auxiliary connections were manually made faulty for testing by disconnecting cables that are connected to the RTDS giga-transceiver workstation interface (GTFPI). In this case, after a time delay, the backup relay SEL-751A operated, and this was a clear demonstration of tolerance to faults.

The high-speed communication between the IEDs, SEL-487E and SEL-751A, even when the SEL-751A operated for faults when the SEL-487E did not, was made possible through the application of the IEC 61850 standard. This confirmed the effectiveness and support of the IEC 61850 standard.

Furthermore, validation regarding the operational performance of the proposed and designed protection scheme was done in real time under realistic fault scenarios. This was also made possible by the use of the real-time digital simulator (RTDS) with its software, Real-time Simulation Computer Aided Design (RSCAD) FX, Omicron current signal amplifiers for injection to the relays, and virtual circuit breaker control.

The results obtained in this thesis confirm that the protection schemes made of the IEC 61850 standard provide high-speed response, improved reliability, and coordination for faults occurring in HV power transformers within the wind farm (WF)-based integrated smart grids.

6.2. Contributions of the Study

There are several ways in which the study presented in this thesis contributes to the field of smart grids and power systems in general, as listed below:

- It develops and validates a multi-layered transformer protection scheme combining differential and time-overcurrent elements, specifically tailored for smart grids with high levels of wind energy penetration.
- It demonstrates the practical application of IEC 61850 GOOSE messaging for inter-relay communication, enhancing speed and coordination in fault detection and response.
- It bridges the gap between theoretical protection design and practical implementation through hardware-in-the-loop (HIL) testing, using Intelligent Electronic Devices (IEDs) such as SEL-487E and SEL-751A.
- It establishes a real-time protection validation platform within a realistic smart grid model incorporating a modified IEEE 9-bus system and an 18-unit LSWF.
- These contributions provide a solid framework for future protection designs and real-world deployments that emphasize flexibility, reliability, and standardization.

6.3. Limitations

While the study meets its stated objectives, several limitations should be acknowledged:

- Current transformer (CT) behavior. The study assumed that the CTs used do not saturate and that there is no non-linear behavior.
- Limited fault coverage. The testing scenarios were restricted primarily to internal three-phase short-circuit faults. Other fault types, such as transformer inrush, inter-turn faults, and high-impedance faults, were not considered.
- Partial implementation of IEC 61850. The study implemented GOOSE messaging but did not incorporate IEC 61850-9-2 Sampled Values (SV), which are crucial for full digital substation modeling.
- Hardware constraints. Only the protection IEDs SEL-487E and SEL-751A, and the analogue signal injection testing devices Omicron CMS 156/356 were used in the hardware-in-the-loop (HIL) test setup. The setup may not be the same for other protection scheme testing.
- The cybersecurity was not part of the scope. Cybersecurity is a critical topic in smart grid automation.

The limitations listed and described above explain how the findings were achieved and how the study can be further explored.

6.4. Recommendations for Future Work

The deliverables achieved in this study have lead to the following recommendations and future works:

1) **Consideration of testing using more fault types:** Without deviating from the expected deliverables and proving the concept of the advancement of the developed protection scheme through integration of the IEC 61850 standard, this study tested its developed protection scheme using internal faults. There are other types of faults that may occur, in association with power transformers, some, for example, through faults. Future studies should look at that.
2) **Inclusion of cybersecurity within the developed protection scheme:** The IEC 61850 standard communication network established in this study did not include any confidential passwords for access to IEDs. In real-world cases, this would lead to potential hacks. Therefore, future work will need to extend to the scope of cybersecurity for strengthening the communication network within the protection scheme.

Considering the two items above (and more) will make the protection scheme developed above more relevant to the advancement of smart grids and their operation.

6.5. Publication

The paper titled “Design and Hardware-in-the-Loop Validation of an IEC 61850-Based Coordinated Protection Scheme for Large-Scale Wind Farm Integration in Smart Grids”, by the authors Y. Gcelu, M.E.S. Mnguni, and S. Nomandela, has been submitted for a peer review to the International Journal of Electrical Engineering and Applied Sciences (IJEEAS) on the 21st of October 2025.

BIBLIOGRAPHY

Ahmed, M.A., Kim, C.H., Moness, M., Moustafa, A.M., Ahmed, M.A., Kim, Y.-C.C., Wei, M., Chen, Z., Yu, F.R., Zhang, P., Xiao, W., Choudhury, P., Goraj, M., Epassa, Y., Midence, R., Meadows, D., Ferguson, D., Catterson, V.M., Booth, C., Cruden, A., Tchakoua, P., Wamkeue, R., Ouhrouche, M., Slaoui-Hasnaoui, F., Tameghe, T.A., Ekemb, G., ISO 8573:2010, Wei, M., Chen, Z., Ahmed, M.A., Kang, Y.C., Kim, Y.-C.C., Sidhu, T.S., Yin, Y., Karthikeya, B.R., Schutt, R.J., Thomas, M.S., Ali, I., Pettener, A.L., Golshani, M., Taylor, G.A., Pisica, I., Singh, B.K., Coulter, J., Sayani, M.A.G., Sami, S.M., Khalid, M., Tepe, K.E., Ko, S.-W., Ju, Y.-C., Jang, M.-S., Xqw, D.L.Q.Q., Ri, S., Jhqhudwlqj, W.K.H., Ri, F.F., Prghuq, W.K.H., Julg, X., Ehhq, K.D. V, Vxemhfw, W.K.H., Qxphurxv, R.I., Sdshuv, W., Uhfhqw, R., Ri, F.F., Lqfuhdvh, P., Gallardo-Calles, J.M., Colmenar-Santos, A., Ontañon-Ruiz, J., Castro-Gil, M., Alizadeh, S.M., Ozansoy, C., IEEE Std 286, Society, M., IEEE - Institute of Electrical and Eletronics Engineers, IEEE Power and Energy Society, Coordinating, S., Rating, T., Oh, K.Y., Kim, J.Y., Lee, J.K.J.S., Ryu, M.S. & Lee, J.K.J.S. 2014. Communication Network Architectures for Southwest Offshore Wind Farm. *IET Conference Publications*, 7(4): 1–6. http://dx.doi.org/10.1016/j.energy.2012.07.056.

Ahmed, M.A. & Kim, Y.C. 2014. Communication Network Architectures for Smart-Wind Power Farms. *Energies*, 7(6): 3900–3921.

Alasali, F., Abeid, S., Mustafa, H., Holderbaum, W., Saidi, A.S., El-naily, N., Omran, E. & Saad, S.M. 2024. The Recent Development of Protection Coordination Schemes based on Inverse of AC Microgrid : A Review. , (November 2023): 1–23.

Alizadeh, S.M. & Ozansoy, C. 2016. The Role of Communications and Standardization in Wind Power Applications - A Review. *Renewable and Sustainable Energy Reviews*, 54: 944–958. http://dx.doi.org/10.1016/j.rser.2015.10.061.

Anees, A.S. 2012. Grid Integration of Renewable Energy Sources: Challenges, Issues and Possible Solutions. In *2012 IEEE 5th India International Conference on Power Electronics (IICPE)*. 1–6.

Barra, P.H.A., Lacerda, V.A., Fernandes, R.A.S. & Coury, D. V. 2021. A Hardware-In-the-Loop Testbed for Microgrid Protection Considering Non-standard Curves ☆. *Electric Power Systems Research*, 196(November 2020): 107242. https://doi.org/10.1016/j.epsr.2021.107242.

Cai, R. & Su, B. 2011. Study on protection of large scale wind power integration. *APAP 2011 - Proceedings: 2011 International Conference on Advanced Power System Automation and Protection*, 3: 1718–1722.

Camachi, B.E.M., Chenaru, O., Ichim, L. & Popescu, D. 2017. A Practical Approach to IEC

61850 Standard for Automation, Protection and Control of Substations. In *Proceedings of the 9th International Conference on Electronics, Computers and Artificial Intelligence, ECAI 2017*. 1–6.

Cardenas, J., Muthukrishnan, V., McGinn, D. & Hunt, R. 2010. Wind Farm Protection Using an IEC 61850 Process Bus Architecture. In *10th IET International Conference on Developments in Power System Protection (DPSP 2010), Managing the Change, Manchester, UK, 29 March–1 April 2010*. 1–5.

Gao, B., Wei, W., Zhang, L., Chen, N., Wu, Y. & Tang, Y. 2014. Differential Protection for an Outgoing Transformer of Large-scale Doubly Fed Induction Generator-based Wind Farms. *Energies*, 7(9): 5566–5585.

George, S.P. & Ashok, S. 2018. Modified Differential Protection for Transformers in Wind Farms. *J Electr Eng Technol*, (9): 78–88.

Han, A., Zhang, Z. & Yin, X. 2010. The impacts of distributed doubly-fed induction generators on smart distribution Grid protection. *Modelling, Identification and Control (ICMIC), The 2010 International Conference on*: 71–75.

Ibrahim, H., Ghandour, M., Dimitrova, M., Ilinca, A. & Perron, J. 2011. Integration of Wind Energy into Electricity Systems: Technical Challenges and Actual Solutions. *Energy Procedia*, 6: 815–824. http://dx.doi.org/10.1016/j.egypro.2011.05.092.

Li, B., Sheng, Y., He, J., Li, Y., Xie, Z. & Cao, Y. 2023. Improved Distance Protection for Wind Farm Transmission Line Based on Dynamic Frequency Estimation. *International Journal of Electrical Power and Energy Systems*, 153(July).

Ma, J., Zhang, W., Liu, J. & Thorp, J.S. 2018. A novel adaptive distance protection scheme for DFIG wind farm collector lines. *International Journal of Electrical Power and Energy Systems*, 94: 234–244. http://dx.doi.org/10.1016/j.ijepes.2017.07.008.

Medeiros, R.P., Costa, F.B. & Silva, K.M. 2016. Power Transformer Differential Protection Using the Boundary Discrete Wavelet Transform. *IEEE Transactions on Power Delivery*, 31(5): 2083–2095.

Member, M.B., Berardinis, E. De, Carpini, L.D., Paulon, P., Petroni, P., Sapienza, G., Member, Student, Scrosati, G., Zaninelli, D., Member, Senior & Simulation, A.W.R. 2010. Real Time Simulation of Smart Grids for Interface Protection Test and Analysis. *Proceedings of 14th International Conference on Harmonics and Quality of Power - ICHQP 2010*: 1–6.

Nomandela, S., Mnguni, M.E.S. & Raji, A.K. 2025. A Case Study on the Validation of Renewable Energy Grid Code Compliance for a Large-Scale Wind Power Plant Grid-Connected Mode of Operation in Real-Time Simulation. *Applied Sciences*, 15(5521): 1–38. https://www.mdpi.com/2076-3417/15/10/5521.

Saad, S.M., Elhaffar, A. & El-arroudi, K. 2015. Optimizing Differential Protection Settings for Power Transformers. In *2015 Modern Electric Power Systems (MEPS)*. IEEE: 1–6.

Song, X., Meng, Z., Chang, K., Xue, F. & Zhou, L. 2012. Dynamic Reactive Power Compensation during Fault Conditions for Wind Farms with the Consideration of Wind Turbine Protection Effects. In *IET Conference Publications*. 120.

Ustun, T.S., Ozansoy, C. & Zayegh, A. 2012. Simulation of Communication Infrastructure of a Centralized Microgrid Protection System Based on IEC 61850-7-420. *2012 IEEE Third International Conference on Smart Grid Communications (SmartGridComm)*: 492–497.

Vestas. 2017. 4 MW Wind Platform. *Brocher*. https://www.vestas.com/en/products/4-mw-platform.

Weedy, B.M., Cory, B.J., Jenkins, N., Ekanayake, J.B. & Strback, G. 2012. *Electric Power Systems*. Fifth Edit. Hoboken, NJ, USA: Wiley.

Wu, B., Lang, Y., Zargari, N. & K, S. 2011. Power Conversion and Control of Wind Energy Systems: Appendix B: Generator Parameters. In *Wind Energy*. 319–326.

Zheng, T.Y., Cha, S.T., Crossley, P.A. & Kang, Y.C. 2011. Protection algorithm for a wind turbine generator based on positive- and negative-sequence fault components. *APAP 2011 - Proceedings: 2011 International Conference on Advanced Power System Automation and Protection*, 2: 1115–1120.